Titre: Title:	Assessment of autonomic nervous control of the cardiovascular system by spectral analysis
Auteur: Author:	Zhixing Li
Date:	1994
Type:	Mémoire ou thèse / Dissertation or Thesis
Référence: Citation:	Li, Z. (1994). Assessment of autonomic nervous control of the cardiovascular system by spectral analysis [Thèse de doctorat, École Polytechnique de Montréal]. PolyPublie. https://publications.polymtl.ca/33066/

UNIVERSITE DE MONTREAL

ASSESSMENT OF AUTONOMIC NERVOUS CONTROL OF THE CARDIOVASCULAR SYSTEM BY SPECTRAL ANALYSIS

PAR

Zhixing LI
INSTITUT DE GENIE BIOMEDICAL
ECOLE POLYTECHNIQUE

THESE PRESENTEE EN VUE DE L'OBTENTION DU GRADE DE
PHILOSOPHIAE DOCTOR (Ph.D.)
(GENIE BIOMEDICAL)
mars 1994

ISBN 0-315-93389-5

UNIVERSITE DE MONTREAL

ECOLE POLYTECHNIQUE

Cette thèse intitulée:

ASSESSMENT OF AUTONOMIC NERVOUS CONTROL OF THE CARDIOVASCULAR SYSTEM BY SPECTRAL ANALYSIS

présentée par: Zhixing Li

en vue de l'obtention du grade de: PHILOSOPHIAE DOCTOR (Ph.D.)

a été dûment acceptée par le jury d'examen constitué de:

M. SAVARD Pierre, Ph.D., président

M. LEBLANC A-Robert, D.Sc.A, membre et directeur de recherche

M. NADEAU Réginald, M.D., membre

M. KAPLAN Daniel T., Ph.D., membre externe

SOMMAIRE

La fréquence cardiaque (FC) et la pression artérielle (PA), dans des conditions stables, montrent des fluctuations battement par battement synchronisées avec la respiration (0.25 Hz) (RSA) et avec l'onde de Mayer (0.1 Hz) chez l'homme. Cependant, les variations à court terme des variables cardio-vasculaires sont essentiellement arbitrées par le système nerveux autonome (SNA). En réalité, les caractéristiques du système cardio-vasculaire sont continuellement modifiées et arbitrées par les changements des tonus sympathique et parasympathique. L'étude de variabilité des variables cardio-vasculaires peut donner des indications utiles du fonctionnement du SNA du point de vue de la physiologie et suggérer des applications cliniques possibles. L'analyse spectrale de la variabilité des variables cardiorespiratoires peut être employée comme un outil unique, non-invasif et sensible pour évaluer le fonctionnement du SNA. Cette méthode démontre la présence de rythmes spécifiques dans les variables cardiovasculaires en transformant une série d'événements telle que la FC en composantes fréquencielles. Ces analyses sont réalisées pour fournir des indices quantitatifs importants qui peuvent être utiles dans l'évaluation d'états pathologiques et physiologiques.

Pour caractériser la dynamique du système cardio-vasculaire, nous avons appliqué l'analyse spectrale aux signaux des intervalles RR, au temps de conduction du noeud AV, aux pressions artérielles (systolique=SYS et diastolique=DIAS) et à la respiration. L'estimation spectrale est limitée à la puissance dans la bande de 0.005 Hz à 0.8 Hz. Pour l'analyse, le nombre d'événements a été limité à 512, ceci

correspond à un enregistrement de 6 à 10 minutes chez l'homme. La puissance totale (0.005-0.8 Hz), la puissance VLF (0.005-0.05 Hz), la puissance LF (0.05-0.15 Hz), et la puissance HF (0.15-0.4 Hz, dépendante de la respiration) ainsi que la moyenne et la déviation standard (SD) ont été mesurées pour chaque série. Un algorithme et une procédure d'analyse spectrale normalisée et un système basé sur PC (acquisition de signaux, traitement de signal et estimation spectrale) ont été développés pour exécuter toutes les analyses de façon systématique.

Une première étude fut réalisée chez 41 sujets normaux (29 mâles, 12 femelles) pour construire une base de référence. Les analyses furent basées sur les enregistrements en postures couchées, debout passive et debout active. Les spectres de toutes les variables (sauf la respiration) présentaient trois pics: VLF, LF et HF associé avec la fréquence de la respiration (moyenne=0.24 Hz). Les fluctuations de LF dans les variables cardiovasculaires étaient généralement acceptées comme d'origine sympathique avec contribution parasympathique, tandis que le pic relié avec la respiration était uniquement contrôlé par le système vagal. Les fluctuations dans la VLF pourraient être causées par des propriétés du système thermorégulateur, modulées par le système rénine-angiotensine, ou contrôlées conjointement par les systèmes sympathique et parasympathique. Les variabilités dans la VLF furent observées dans les deux variables, RR et PA dans chaque étape de nos protocoles. Les origines des fluctuations VLF dans les RR et la PA peuvent différer. D'après les données en posture couchée, nous avons observé que la puissance HF dans les variations RR et SYS était dépendante de la fréquence respiratoire. Les corrélations négatives entre les puissances HF dans RR et SYS et la fréquence de respiration peuvent être expliquées comme l'effet de "roll-off" du système parasympathique.

Une réponse typique en posture debout passive est la stimulation de l'activité sympathique et la diminution de l'activité parasympathique. La posture debout

passive a diminué la moyenne de RR (921 à 728 ms, $p < 0.01$), la SD de RR (52 à 46 ms, $p=0.05$); la moyenne de SYS (123 à 117 mmHg, $p < 0.007$); la pression du pouls (58 à 48, $P < 0.001$); l'accroissement de la pression diastolique (64 à 69, $p=0.003$). La pression du pouls est proportionnelle au volume d'éjection. Ici dans la posture debout passive, le volume d'éjection diminue à cause de l'augmentation de la post-charge et de la diminution de la période de remplissage. Nous avons noté une diminution dans la moyenne de la pression du pouls. La puissance HF de RR a diminué (33.2 à 18.6, $p <0.001$), tandis que la puissance LF a augmenté (36.9 à 54.1, $p < 0.001$). Le ratio de LF/HF a augmenté aussi (1.8 à 7.8, $p=0.02$). Les puissances LF des pressions SYS, DIAS et du pouls ont augmenté ($p < 0.05$). Les puissances HF dans SYS et le pouls ont augmenté ($p < 0.005$). La puissance HF dans DIAS n'a pas changée considérablement. La puissance VLF de RR est restée inchangée tandis que la puissance VLF dans toutes les variables de pression ont augmenté ($p < 0.01$). Cela peut être expliqué avec l'hypothèse que la genèse des fluctuations VLF dans RR et PA sont différentes. Les accroissements des fluctuations HF dans la pression SYS et dans la pression de pouls sont dus à l'influence mécanique de la respiration.

En comparant avec la posture debout passive, les sujets ($N=27$) ont respiré plus rapidement (0.28 Hz vs 0.23 Hz, $p=0.04$) que dans la posture debout active. Les moyennes des variables cardiovasculaires étaient similaires dans les deux postures ($p > 0.2$), mais la variation de RR était considérablement plus grande en posture debout passive (SD: 46 vs 39, $p < 0.05$). Les variations de pressions dans les HF étaient plus larges en posture debout passive ($p < 0.05$). La fluctuation des HF dans les RR a une tendance à être plus importante en posture debout passive ($p=0.06$). Cela implique qu'il y a un retrait plus important de l'activité parasympathique en posture debout active.

La variation battement par battement du temps de conduction du noeud AV a été analysée chez 27 volontaires normaux et 10 patients avec pacing pour évaluer les influences du SNA sur le noeud AV. Il est démontré que la durée AR peut être déterminée battement par battement avec une bonne précision avec notre méthode. Une faible variation a été observée dans la série AR et le spectre de AR a démontré aussi clairement trois pics. Nos données montrent qu'il existe une corrélation positive entre AR et RR ($r=0.6$, $p < 0.05$) au repos. En réponse à la posture debout passive, la puissance HF de AR s'est accrue (23.6 à 33.9 $p=0.015$) par rapport à RR, le ratio de LF/HF de AR a diminué considérablement de 2.7 à 1.3 ($p=0.029$). Nos données confirment que le noeud AV est aussi influencé par le SNA, et l'analyse spectrale de la variabilité du temps de conduction du noeud AV paraît être utile à l'évaluation de l'influence du SNA. Nos résultats montrent aussi que les "patterns" de fluctuation dans le temps de conduction du noeud AV et RR sont différents et que le noeud AV est plus influencé par le système parasympathique que le noeud sinusal.

Des analyses furent exécutées chez 14 patients hypertendus (10 mâles) et 24 patients syncopaux (18 mâles) pour évaluer la fonction autonome chez ces patients. Au repos, l'hypertendu peut être caractérisé par la perte de la variabilité des RR, de plus grandes variabilités (SD) dans la PA, de plus grandes puissances VLF et de basses puissances HF dans toutes les variables. Avec la stimulation sympathique (debout actif), nous avons trouvé une réponse déprimée du système parasympathique chez les patients hypertendus. Ceci se caractérisait par une légère diminution de la puissance HF dans les RR et aucun changement de la puissance HF dans toutes les PA dû à la basse activité parasympathique au repos. Pour le groupe syncopale au repos, la puissance VLF des RR était plus élevée ($p=0.011$), tandis que la puissance HF des RR était plus basse ($p=0.019$). Les autres paramètres spectraux n'étaient pas considérablement différents. Nos résultats montraient une plus haute variabilité VLF

dans les RR dans les deux postures chez les sujets syncopaux, tandis que les fluctuations VLF de la PA étaient similaires à celles du groupe de normaux. Cette instabilité sur le contrôle de la FC dans la bande VLF peut contribuer à l'évanouissement chez les patients syncopaux.

Les enregistrements de 8 chiens bâtard (18-30 kg) furent aussi analysés. Nos mesures dans les domaines du temps et de la fréquence concordaient avec les données pharmacologiques pour démontrer les effets des manipulations différentes sur SNA, telles que stimulation, désactivation ou activation des récepteurs présynaptiques et du blocage parasympathique. Avec la perfusion d'épinephrine (EPI), la moyenne de RR a diminué et la puissance LF des RR a augmenté. Ces données suggèrent que l'EPI circulante et libérée localement peut activer les autorécepteurs présynaptiques et accroître ainsi la libération du neurotransmetteur (NE). En comparant les résultats avant et après l'administration de yohimbine (YHMB), on a constaté que la moyenne des intervalles RR n'a pas diminué considérablement, que la puissance HF est restée inchangée tandis que la puissance LF de RR s'est accrue ($p < 0.05$) de 23.6 à 38.0. Ce bloqueur de α_2 spécifique désactive le mécanisme de rétroaction du contrôle de la concentration de NE (arbitré par l'adrénocepteur présynaptique du α_2 dans les terminaisons sympathiques) conduisant à une diminution de l'inhibition de la libération du neurotransmetteur et à une facilitation de la libération de NE. Après l'administration de fénoterol ($ß_2$ agoniste), la FC a augmenté significativement ($p < 0.05$) par rapport au contrôle mais n'était pas différente de celle constaté après YHMB; la puissance HF était plus élevée que dans les deux enregistrements précédents. Il se pourrait que l'accroissement de la puissance HF ne soit pas nécessairement dû à une augmentation du tonus parasympathique, mais qu'elle soit le résultat d'une réponse vagale accrue. Ceci peut s'expliquer par un mécanisme désigné par l'appellation antagonisme accentué. Avec une stimulation du ganglion

stellaire gauche, l'intervalle RR raccourcissait considérablement ($p < 0.05$). La puissance LF s'accroissait de 25.6 à 36.9 ($p < 0.05$). Cela confirme l'hypothèse que le tonus sympathique se reflète sur la puissance LF. La dernière phase du protocole testait l'effet du blocage de l'activité du système parasympathique. Le blocage vagal diminuait la moyenne des intervalles RR (415.5 à 317.0 ms, $p < 0.02$) et dans le même temps la variabilité RR (SD) diminuait (9.0 à 4.4 ms, $p<0.05$). Les deux composantes LF et HF diminuaient considérablement après l'administration d'atropine. L'abolition des composantes LF et HF des RR après atropine fournit l'évidence que le système parasympathique est responsable des fluctuations LF et HF de RR.

Enfin, nous proposons un modèle conceptuel pour mieux comprendre l'interaction entre les variables cardiovasculaires.

L'analyse spectrale des variables cardiovasculaires, telles que la FC, et la pression artérielle, s'avère être un outil non-invasif valable pour évaluer à court terme le contrôle nerveux autonome du système cardiovasculaire. Il peut être employé pour évaluer les variations physiologiques de tonus sympathovagal chez les individus. Les mesures quantitatives des puissances spectrales dans chaque bande de fréquence peuvent être utiles pour évaluer le fonctionnement du contrôle autonome. Chez des patients avec dysfonctions du système autonome, l'analyse spectrale de la variabilité de la FC et de la PA sera utile pour évaluer l'efficacité des traitements ou pour déterminer le pronostic.

ABSTRACT

Oscillations in heart rate and arterial blood pressure (BP) reflect autonomic modulation of cardiovascular activity. To assess the autonomic control of the cardiovascular system, spectral analysis of RR intervals, BP and respiratory signals were applied to human and canine subjects. Spectral powers in VLF (.005-.05 Hz), LF (.05-.15 Hz), HF (.15-0.4 Hz) bands were measured for each time series. A systematic procedure consisting of a normalized spectral analysis algorithm implemented on a PC-based bedside system was developed to perform all analyses.

A study was first performed on 41 normal subjects in resting supine, passive head-up tilt and active standing positions. Principal results may be summarized as follows: 1) in response to tilt, HR and diastolic blood pressure increased and systolic and pulse pressures decreased. For RR intervals, HF power decreased; LF power increased; consequently LF/HF ratio increased. For BP, LF and HF powers increased significantly except for HF power in diastolic pressure. These are due to the activation of sympathetic and decrease of vagal activities. 2) High frequency variations in BP and RR were higher in the passive tilt than those in the active standing (N=27). This implies that there is a more important withdrawal of the vagal activity in active standing. 3) Spectra of AV conduction time clearly showed 3 peaks. In response to tilt, HF power increased significantly and in contrast to RR, the LF/HF ratio of AR decreased. Data indicated that the AV node is also influenced by the autonomic nervous system and the AV conduction time is mediated mainly by the vagal system.

Secondly, analyses were performed on 14 essential hypertension subjects and 24 syncope-prone subjects to assess abnormality of autonomic function. In supine rest, the hypertensive may be characterized by loss of RR variability, larger

variabilities in BP, larger VLF power and lower HF power in all variables. In response to active standing, depressed response of the vagal system in hypertensives was noted. This was characterized by a smaller decrease of HF power in RR and no change of HF power in all BP variables due to a lower vagal activity at baseline. In the syncope group, VLF power of RR was higher, while HF power of RR was lower at resting supine. The data showed a higher VLF variability in RR at both supine and tilt in the syncope group, while the VLF powers in BP were similar to those of the normal group. This instability of the HR control in the VLF band may contribute to the fainting in syncope prone patients.

The third stage of the study consisted in the evaluation of the power spectrum of RR in 8 mongrel dogs. With perfusion of epinephrine (EPI), RR decreased and LF power increased, suggesting that EPI activates presynaptic β_2 adrenoceptor leading to an increase in neurotransmitter release. With yohimbine, HF power did not change, while LF power increased significantly due to a facilitation of the NE release. With fenoterol, LF power was significantly higher than that at baseline while the HF power was higher than those in both baseline and after yohimbine. The increased HF power could be the result of an increased vagal response. Stimulation of left stellate ganglion resulted in a decrease of mean RR and an increase of LF power. This confirms that the LF power reflects the sympathetic tone. Vagal blockade decreased the mean RR and SD as well as the LF and HF powers. This provides evidence that the vagal system is responsible for the LF and HF fluctuations in RR.

Finally, a conceptual model to explain interactions among the different cardiovascular variables has been proposed. Spectral analysis of HR and BP is a valuable non-invasive tool to assess short term autonomic control of the cardiovascular system. Studies of oscillations in HR and BP may give useful indications of the functioning of the ANS and to suggest possible clinical applications.

ACKNOWLEDGEMENT

I would like to express my great gratitude to my advisor, Prof. Robert LeBlanc of the Institute of Biomedical Engineering, for his constant guidance, encouragement, understanding and continuous support of the work represented in this thesis.

I wish to express my sincere gratitude to Dr. R. Nadeau, Director of the Research Center of Sacré-Coeur Hospital of Montreal, for his encouragement and support in many ways.

Many thanks are due to Dr. Amine Yacine for his helpful discussion and cooperation and to Dr. Ghislain Boudreau for recordings from his experiments.

I would also like to express my great gratitude to my wife, Ping Chen, for her full understanding and patient encouragement.

In addition, I would also like to acknowledge the help from my friends and members of the personnel of the Research Center of Sacré-Coeur Hospital.

TABLE OF CONTENTS

LIST OF FIGURES

LIST OF TABLES

Chapter 1 Introduction

The heart rate and consequently the blood pressure, is the most constant sign of life in humans. The existence, under steady conditions, of rhythmic beat-to-beat fluctuations in these cardiovascular variables has been recognized for a long time [39,60]. Both blood pressure and heart rate show oscillations synchronized with respiration in man. At rest, the heart rate increases on inspiration and decreases on expiration. This variation in beat-to-beat interval, which occurs during a respiratory cycle, has been of interest to cardiopulmonary physiologists for a long time. This phenomenon is called the respiratory sinus arrhythmia (RSA). As early as 1876, Mayer described, in a classical paper [61], waves (now referred to as Mayer waves) which were slower than the respiration in animals with normal respiratory movements. These oscillations are due to complex cardiovascular regulations, such as autoregulative, neural and humoral regulations. However, the short term variations of the cardiovascular variables are mainly mediated by the autonomic nervous system (ANS).

1.1 Short term regulation of the cardiovascular system

The ANS comprises two subsystems: sympathetic nervous system and parasympathetic (or vagal) nervous system. The neural regulation of circulatory function is mainly effected through the interplay of the sympathetic and vagal outflows. In general, it is believed that rhythmical beat-to-beat oscillations of one cardiovascular controlled variable might provide some criteria to interpret the

complex interplay among neural regulatory outflows.

The sympathetic and parasympathetic nerves innervate the heart (the sinus node, the conducting tissue, the muscle of both the atria and ventricles, and the coronary vessels) and the vessels [58]. The effect of an increased activity in efferent sympathetic nerves is observed as an increase in heart rate, an increased rate of change in the force of contraction of cardiac muscle, increases in blood pressure and in vascular resistances (through the increased vascular tone). On the other hand, an increase in activity in the parasympathetic nerves causes a decrease in heart rate, a decrease in the contraction force of the atrial muscle, and a decrease in the peripheral resistance. The cardiovascular regulation through the efferent sympathetic and vagal nerve fibres represent the efferent limb of many reflexes which involve receptors in the cardiovascular system, as well as somatic, pulmonary and visceral receptors. There are different levels of integration of the cardiovascular function: spinal, bulbar, subcortical and cortical [58]. The operation of the autonomic control system is complex and nonlinear. The vagal and sympathetic pathways have a definite tonus and their activities are modulated through the neurotransmitters. Combinations of the inhibitory and facilitatory mechanisms are found in both systems. Sympathovagal balance is tonically and phasically modulated by the interaction of the central neural integration, peripheral inhibitory reflex mechanisms (with negative feedback characteristics), and peripheral excitatory reflex mechanisms (with positive feedback characteristics) [62].

A simplified control system model (ref. Figure 1.1) of the cardioregulatory system includes: (1) a controlled subsystem comprising the heart functions (heart rate, stroke and wall tension), blood pressure, peripheral resistances and blood volume;

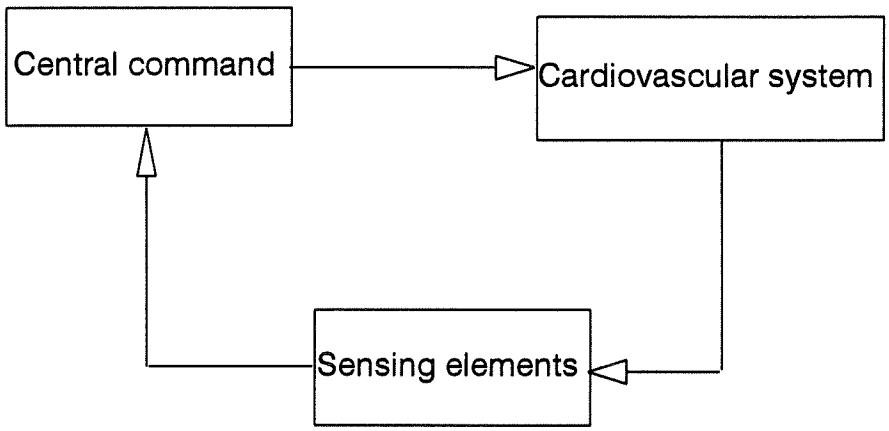

Figure 1.1. A simplified control model of the cardiovascular system

(2) the sensing elements, namely the baroreceptors; and (3) the controlling subsystem or "central command", comprising afferent neural traffic from the baroreceptors, the central cardioregulatory centers in the mid-brain, and the efferent nerve traffic to the heart and blood vessels.

The heart, in connection with the vessels, transforms intermittent blood flow into a constant flow. The periodicity of the heart rate has different qualitative and quantitative aspects. The rhythmicity of the heart action is the basis of the cardiovascular controlling activity. The heart and vessels have a common regulation. Requirements for an increased action are distributed to both components of the system. The adaptation to new environmental conditions depends on the efficiency of the regulatory system.

Fluctuations of these cardiovascular variables reflect the presence of a variety of physiological perturbations which take place naturally in the cardiovascular system and the dynamic response of the control system to those perturbations. For example, perturbations may be: variations of the intrathoracic pressure due to the respiration which mechanically perturbs the venous return and the arterial blood pressure; variations of the arterial pressure which influence the heart rate through the baroreceptor reflex; variations of the vascular resistance due to the regulation of regional blood flows. The ANS plays an important role in the control of the cardiovascular system. Actually, the characteristics of the cardiovascular system are continuously modified and mediated by the changes of sympathetic and parasympathetic tones. Several authors have hypothesized that studies of variabilities in hemodynamic parameters may give useful indications of the functioning of the ANS.

Abnormal autonomic control of cardiovascular function may contribute importantly to the pathophysiology of patients with chronic congestive heart failure, [70], diabetic [64,65], coronary artery disease [66], acute atrial fibrillation [67], myocardial infarction [27,68,69,71], syncope [56,72-77], and hypertension [31,78,79]. Potentially, quantification of parasympathetic and sympathetic nervous system activities may contribute to understanding the pathophysiologic basis, and may be useful clinically in establishing the diagnosis, prognosis and management of patients with these diseases.

1.2 Power spectral analysis in evaluation of ANS function

It is difficult to investigate clinically the functioning of the ANS, since methods generally used are based on pharmacologic manipulations or on direct neural recordings. This affects the system to be studied. Non-invasive diagnostic cardiology has suffered from a lack of intrinsic indices and sensitive methods for quantitative analysis of the cardiac regulatory system. Some researchers proposed that spectral analysis of the variability of cardio-respiratory variables, such as heart rate, arterial blood pressure and respiration may be used as a unique non-invasive and sensitive method to evaluate the functioning of the ANS [18,31]. This method shows presence of specific rhythms in the cardiovascular variables by transforming a time event series such as heart rate into its frequency components. The pharmacologic blockade as well as spectral analysis showed that the heart rate variability represent the activities of both sympathetic and parasympathetic nervous systems [1,2,107]. Spectral analysis of cardiovascular variables is based on the hypothesis that variabilities of these variables result from cardiovascular and respiratory regulations, which are mediated by the ANS.

Spectral analysis methods were introduced in technical sciences and even in neurophysiology almost 50 years ago. Their application to slow variations in the circulation did not appear before the mid-sixties. In 1966, several researchers independently published the first results obtained by means of spectral analysis methods. Zatsiorsky and Saraniya [80] demonstrated the first autocorrelograms of the heart rate. Taylor [81] used spectral analysis in combination with random stimulation of cardiac nerves to estimate the impedance of the vascular system in the ultra-low frequency range. Penaz and Fisher [82] published, in the same period, results of a frequency analysis of fluctuations of the heart rate and the finger plethysmogram performed by analog filtering; one year later, the same analysis was repeated using digital computation. Penaz *et al.* [83] probably showed for the first time the spectrum of the heart rate in relation to the peripheral vasomotricity.

In the last decade, the power spectral analysis technique has been widely used to quantify non random components of RR intervals, arterial pressures and respiration variabilities in the evaluation of the ANS on the control of the cardiovascular system [1-9,12-14,16-25,33,88,91,93,95-97,99-102,106-109]. These analysis are claimed to provide important quantitative indices which can be helpful in the evaluation of physiological and pathological states. For example, the main frequency components of different signals have been correlated to understand various physiological mechanisms: respiration, arterial blood pressure control and the effect of temperature [5-8,23].

Spectral analysis was also used by some pioneer researchers, such as Sayer [42], Hyndman [40], Kitney et Rompelman [23] in studies of the heart rate variability. They found that short time variations (from seconds to minutes) in cardiovascular variables were concentrated in three peaks: 1) a peak concentrated at the respiratory

frequency (high frequency) which is displaced with the respiration rate; 2) a peak found between 0.1 Hz and 0.15 Hz, so called Mayer waves, which is probably related to vasomotor activities, and 3) a peak at the frequency between DC and 0.1 Hz (very low frequency). Hyndman [40] and Kitney [23] related this very low frequency peak to thermoregulatory fluctuations of the vasomotor tone.

Studies to test influences of the ANS on hemodynamic variables by analysis of rhythmic oscillations have been conducted in animals and human subjects. In dogs and humans, Akselrod *et al.* [1,2], Pagani *et al.* [31] and Pomeranz [32] showed that the respiratory rhythm is modulated mainly by the parasympathetic system and the low frequency peak (0.1 Hz) is modulated by the sympathetic system, but that both of their amplitudes are affected by the vagal activity.

de Boer [13], Zwiener [37] and Baselli [7] used cospectral and cross spectral methods to study the relationship between variabilities of heart rate, arterial blood pressure and respiration. They demonstrated that the 10-second rhythm (0.1 Hz) and the respiratory peak are present simultaneously and coherently in variabilities of the heart rate and blood pressure. These two peaks exist clearly in both variables and the coherences are higher in both bands. They also indicated that the arterial blood pressure leads the heart rate by a phase of 60° (i.e. about 2 heart beats delay) in the low frequency band (LF) and a null phase difference between blood pressure and heart rate in the respiratory band (HF). Also, the power in the low frequency and high frequency bands as well as the ratio LF/HF have been used to give indications of the sympato-vagal balance in different physiological conditions.

The spectral analysis method has been used also by some researchers to

evaluated autonomic control in some pathological conditions. For example, it has been shown that in the patients recovering from a myocardial infarction, a decrease of the heart rate variability showed an increased mortality [12,27]. Cerutti *et al.* used cross spectra to evaluate autonomic diabetic neuropathy [43].

The control mechanisms of the cardiovascular system are complex with many parallel sub-systems. Oscillations in cardiovascular variables result from the effects of feedback mechanisms related to physiological control. In principle, the cardiovascular control system consists of negative feedback loops with delays. From the point of view of system analysis, the cardiovascular control system is a black box with closed loops and oscillations in heart rate and blood pressure as system variables, which may be thought of as outputs of a feedback network that is continuously monitored and regulated by the ANS. The analysis of the oscillations and their relationship among cardiovascular variables, such as heart rate, blood pressure, may give some useful criteria to interpret complex effects of the control mechanism and the system behaviour. Akselrod *et al.* [2] used a model (ref. Figure 1.2) of closed feedback loop to couple fluctuations in heart rate and arterial blood pressure with noise sources. They explained their results with this simple model. Kitney *et al.* studied the interaction of cardiovascular variables with a non-linear model [23] and they found some similarities between the simulated signal from their non-linear model and the recorded signal with an autoregressive method. Kalli *et al.* [21,22] proposed a method with parametric representation to study the autonomic control of the cardiovascular system. This method uses a multivariable autoregressive model to characterize recorded signals which are coupled in a closed loop system. They found the method useful to study complex interactions between heart rate, blood pressure and respiration in neonatal lamb. Appel [38] used a transfer function method to

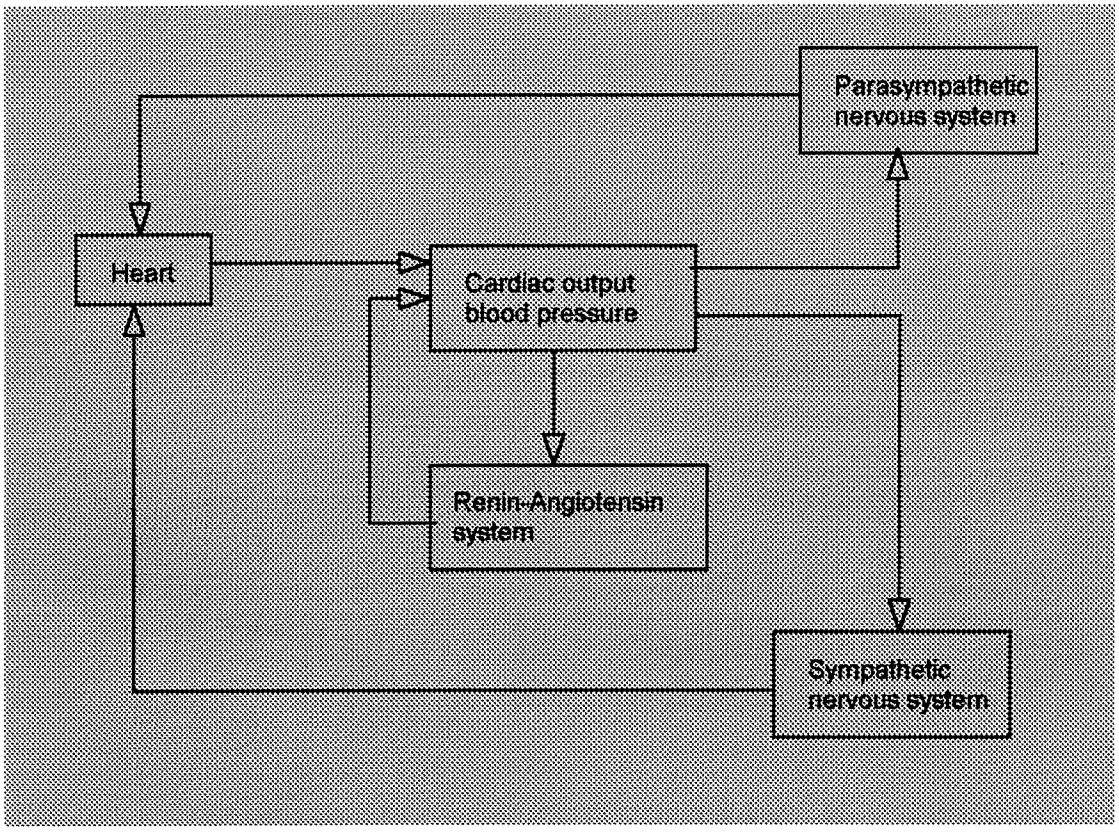

Figure 1.2. Simplified model of cardiovascular control showing modulation of heart rate by parasympathetic and sympathetic nervous systems (adapted from ref. [2]).

study autonomic control of cardiovascular system. Berger, Saul and Cohen [10,11,15,94] also computed the transfer function to characterize the frequency response of the system by proposing broadband respiration as a measurable input excitation and monitoring the resulting fluctuations in the output signals. They indicated that results obtained with this method were comparable with those obtained using traditional methods. They also indicated that by combining the broadband respiration and the system identification method, it is possible to evaluate the transfer function of the baroreceptors without influencing the normal closed loop functioning of the cardiovascular system.

Baselli *et al.* [4-8] inspired by Akselrod's model [1,2], proposed a more elaborate closed loop model (ref. Figure 1.3), considering the respiration like an external input and adding a loop of action of the pressure to pressure, a direct feedback from s to s (mediated by non measured variables such as peripheral resistances, contractility. etc.). They tried to give a global evaluation of certain regulatory activities of the ANS. Results of their model shed some light on certain physiologic characteristics. Some interesting hypotheses were proposed according to simulation of this model as respiration appeared to affect the arterial pressure more than the heart rate and the pressure to pressure loop seemed to be responsible for the 10-second waves.

Other methods have also been used to study the autonomic control of the cardiovascular system. For example, Kaplan *et al* [46] recently applied chaos theory to quantify the complexity (entropy and dimension) of the heart rate and blood pressure. They showed that the complexity is reduced with age. They indicated that the complexity may be a useful physiological marker of the autonomic function.

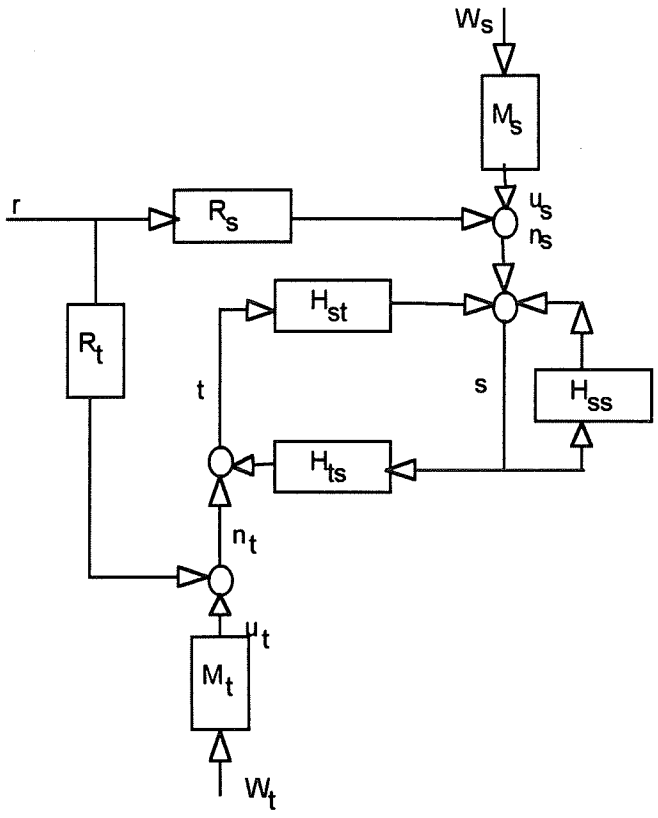

Figure 1.3. s-t-r interaction model.

This model contains a double loop structure : a) s-t-s loop (s: variability of systolic blood pressure; t: variability of RR intervals and r: variation of respiration), with a forward pathway from t to s (H_{st}) and a feedback one from s to t; b) s-s loop. Respiration r is considered as exogenous signal which is input both to s and t. Non measured inputs on s and t are described as to uncorrelated noises (u_s and u_t) (adapted from ref. [8]).

1.3 Objectives

Studies of variabilities of cardiovascular variables in time and/or frequency domains may shed light on the influences of the ANS on the regulation of the cardiovascular system. The present work was performed by using spectral analysis of variabilities of cardiovascular variables as a non-invasive method so as:

1) to construct a reference base of basic characteristics of cardiovascular regulation (in basal condition and responses to different stimulations or posture changes) mediated by ANS in normal subjects.

2) to assess different autonomic responses to passive head-up tilt and active standing.

3) to assess influences of the ANS on atrioventricular conduction time.

4) to assess abnormalities in autonomic function in patients with neurally mediated syncope and in patients with essential hypertension.

5) to expand the study in dogs with ANS manipulations.

6) to evaluate spectral analysis for the assessment of ANS control of the cardiovascular system.

7) to establish a conceptual model to explain interplays among cardiovascular variables.

To achieve these aims two developments were realized:

a) A PC-based bedside system to perform the data acquisition, signal processing and spectral analysis.

b) A normalized spectral analysis algorithm and procedure in order to conduct the evaluation of the ANS in a systematic way.

Chapter 2 Methods

Evaluation of the ANS functions will be based on the analyses of times series of cardiovascular variables, such as: RR (from ECG), AA (from oesophageal electrogram, OEG), AR (from both ECG and OEG), arterial blood pressures variables and the respiration signals. To perform the spectral analysis of cardiovascular variability, the time series should be extracted from the raw data. This chapter describes steps and methods to conduct the analysis, including the equipment, laboratory installation and software (i.e., extraction of events, construction of time series, spectral analysis, presentation of the results).

2.1 Instrumentation:

A) *Human subjects:*

Most of the investigations in human subjects were conducted in the ANS Laboratory (ANSL) and some recordings were conducted in the human electrophysiology laboratory (EPlab). The recording configuration and connections are shown in Figure 2.1.

1) The lead II ECG was recorded with a VR-12 amplifier (Electronics for Medicine);
2) The oesophageal electrogram (OEG) was recorded from an oesophageal pill electrode placed at the level of the right atrium to record the atrial electrical activity [44]. This signal was amplified and then connected to the VR-12. The amplifier is a locally made amplifier;

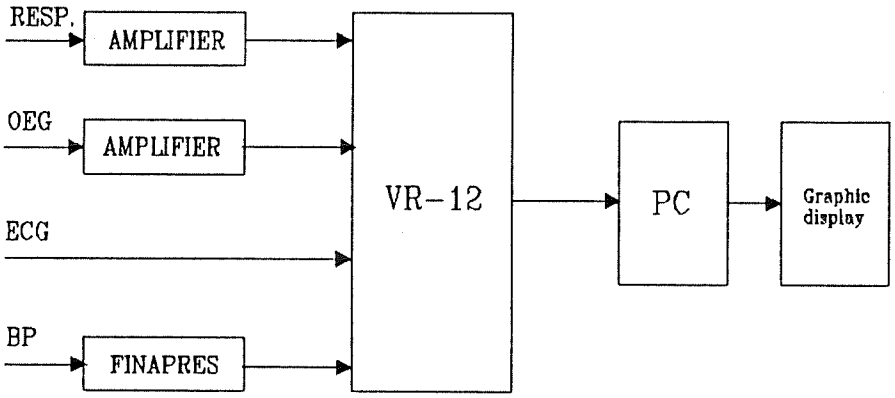

(a)

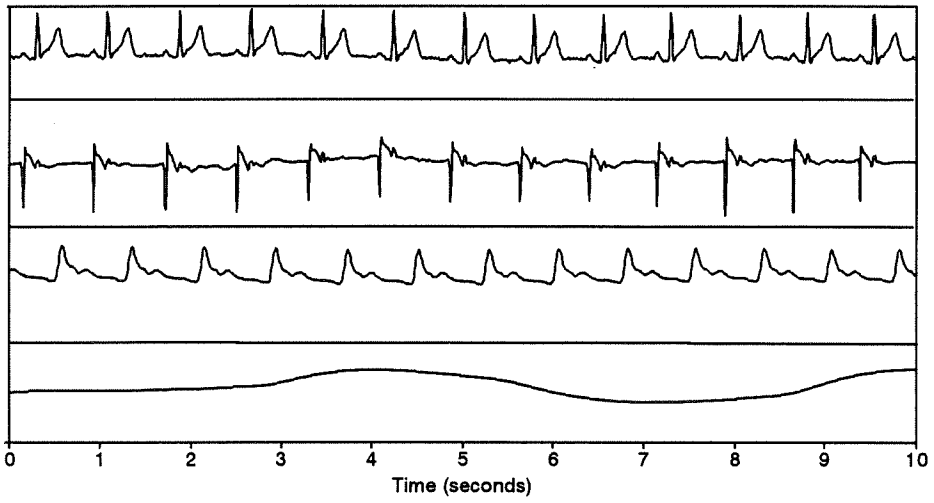

(b)

Figure 2.1 (a) Recording configuration in ANSL. Four signals (ECG, OEG, BP and Respiration) are connected to the VR-12. The signals are conditioned and connected to the data acquisition PC. Signals are monitored both on the VR-12 and the PC to allow quality control of the recorded signals. (b) Display of signals: ECG, OEG, BP, respiration (from top to bottom).

3) The systemic arterial blood pressure (BP) was measured non invasively from the output of a plethysmographic finger transducer (FINAPRES, OHMEDA) attached to the left middle finger;
4) The respiration signal (RESP) was obtained from a nasal thermistor. The signal was amplified by a locally made amplifier and then connected to the VR-12.

All four channels were filtered. The ECG and OEG were filtered with a bandwidth of 0.5-250 Hz, blood pressure was filtered from DC to 100 Hz, and the respiration was filtered from 0.05 to 50 Hz. The four signals from the output of the VR-12 were connected to a bedside data acquisition system based on a standard IBM compatible PC. This system is equipped with 16-channel A/D data acquisition card (Data Translation model DT2801) with a sampling capacity of up to 1000 samples/sec with 12 bits/sample. The data acquisition program ACQ (developed for this project and described in Appendix A) controls the data acquisition. It allows the operator to:

-- record the patient identification and comments,
-- choose channels, the gain of the card, the sampling rate and the duration of the acquisition.

On-line signal display (with or without data storage) allows the operator to adjust the gain from the VR-12 for maximising the usage of the dynamic range of the data acquisition card, for quality control and to choose the starting moment. During the protocol, on-line display is used for quality control. When data are stored, a disk file is used with a header identifying the patient and conditions of the recording (i.e. patient name; patient identification; a brief description of the patient; a brief description of the experiment; number of channels; description of the each channel;

recording gain and sampling rate).

Investigations conducted in the EPLab were recorded on a 16 channel analog cassette recorder (RTP-800, DATA RECORDER, Kyowa). Signals were digitized off-line by the acquisition system from tape playback. Equipments of the EPLab of Sacré-Coeur Hospital are: an integrated 16 channel system of amplification, filtering, and visualization of ECG and intracardiac signals (VR-16 SIMULTRACE, Honeywell), a stimulator (DTU-101, Bloom Associates, Ltd.) and a paper recorder (MINGOGRAF T16, Siemens).

Assessment of the ANS control on the cardiovascular system will be based on the study of the variabilities of seven time series of cardiovascular variables which are extracted from the four recorded signals. The time series are

1) RR interval (RR), time interval between two consecutive QRS complexes measured from the ECG;
2) AA interval (AA), time interval between two consecutive A waves measured from the OEG;
3) AR interval (AR), time interval between A wave in OEG and the following QRS complex in ECG;
4) systolic blood pressure (SYS), maximum value of the arterial blood pressure between two consecutive QRS complexes;
5) diastolic blood pressure (DIAS), minimum value of the arterial blood pressure between two consecutive QRS complexes;
6) pulse blood pressure (PULSE), difference of SYS and DIAS and
7) respiration (RESP), sample of respiration signal at the QRS occurrence time.

B) *Animals*:

Lead II ECG was recorded from a Nihon-Kohden amplifier with a bandwidth of 0.05-250 Hz; the systemic arterial blood pressure was measured by a catheter; the respiration movements were recorded with a belt transducer. Part of the data were collected directly by the PC data acquisition system, others were recorded first on a 4 channel FM analog tape recorder (HP 3960) and then digitized off-line from tape playback. Finally, all raw data (for human subjects and animals) are stored on a 700 Mbyte magneto-optic disk for off-line signal processing, spectral analysis and archive. Sampling rates used in different laboratories and protocols are given in the following table.

Sampling rate (samples/second) used in different protocols (12 bits/sample)

Laboratory	ANSL	EPLAB	Animal Lab
Human subjects	250	500	
Dogs			500

2.2 Signal processing:

Regardless of the kind of analysis (heart rate variability, AV conduction time variability, BP variability, Respiration, etc.), the first step is to measure RR intervals from the ECG, AA intervals from OEG, AR intervals from ECG and OEG (time

interval between A wave and QRS complex), systolic and diastolic blood pressures from continuously recorded blood waveforms and the sampling of the respiration signal. Each time series is composed of real physiological variability signal plus noise. Noise originates from many sources: noise of the signals, amplifiers, A/D converter, or measurement algorithm. Once the converter system and sampling rate are chosen, the accuracy of the time series to be analyzed depends mainly on the computer detection and measurement algorithm. Thus the degree of accuracy of measurements and the jitter in the fiducial marking of each waveform determine the confidence of the analysis. The design of the detection procedure was based on the objective of minimizing measurement errors in order to generate accurate time series for later analysis.

An interactive program, DETECT, was developed to detect different events (ref.: user's manual in Appendix A). The detection can be performed automatically or under user's supervision. If needed, this program displays signals and event markers. It allows operator to edit, to validate, or to modify the fiducial point location of waveforms presented in the data window. With our good quality recordings, modification of fiducial point locations has been rarely used.

2.2.1 QRS detection and fiducial marking

QRS detection plays a key role in the detection of the other events (A waves, systolic blood pressure (SYS), diastolic blood pressure (DIAS), pulse pressure (PULSE) and respiration (RESP)) and the analysis. The algorithm used for QRS detection in the ECG and the A wave in the OEG signal is a modified version of the algorithm proposed by Tremblay and LeBlanc [44]. This algorithm is composed of

a preprocessor, decision rules and fiducial marking (Fig. 2.2).

a) Preprocessor:

The preprocessor is a linear filter followed by a nonlinear transformation. A simple linear filter (high pass) is used.

$$y(n) = x(n) - x(n+3) \qquad (2.1)$$

where x(n) is the sampled signal, y(n) is the output of the filter, n is the sample number.

Fig 2.3 shows the ECG signal before and after filtering. The linear filter removes slow trends due to respiration or baseline drift. A higher order filter can be applied at the expense of computing time. Since we are dealing with good quality signal (i.e. patients at rest), the chosen filter is adequate.

The nonlinear transform has for its objective to obtain a single positive peak for each QRS wave and a high S/N ratio, which then allows the use of a peak detector or a one-sided threshold. The nonlinear transform is constructed so that it can obtain a signal in which QRS complexes are enhanced from the background of P-waves, T-waves, noise and artifacts. The following transformation has been used:

$$z(n) = \sum_{k=n-W/2}^{n+W/2} y^2(k)\, h(n-k) \qquad (2.2)$$

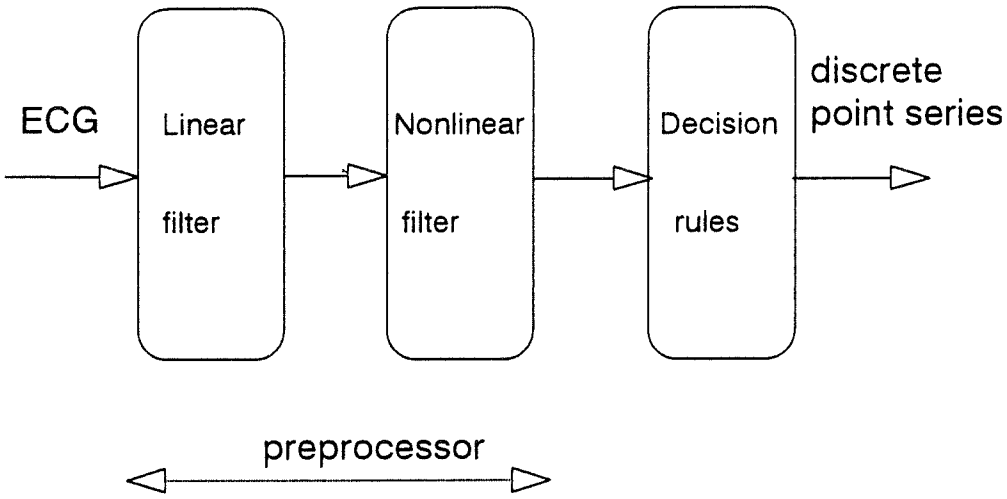

Figure 2.2 Flowchart of event detection

The detection of QRS event has three phases. First, the ECG signal is filtered by a linear filter. Second, the filtered ECG is converted to the local energy function by a nonlinear transformation. Third, the QRS waves are detected from the energy function according to decision rules.

This transform corresponds to the short-time energy. The squared signal is then fed to a filter with a finite impulse response, h(k), which is an averaging filter:

$$h(k) = \begin{cases} 1 & k=-W/2,\ldots,W/2 \\ 0 & otherwise \end{cases}$$

W was determined experimentally. This parameter is sensitive. A value of half of the approximate duration of the event to be detected is used. For a QRS complex, it represents a data window of approximately 40 ms, i.e., W=10 for a sampling frequency of 250 samples/sec. This nonlinear transformation provides the necessary smoothing of the signal so that only large-amplitude events of sufficient energy, i.e. QRS complexes are preserved in z(n). The bottom panel of Fig. 2.3 shows the output of the nonlinear filter. It is also noted that the short-term energy produces a signal with a high SNR, i.e., one in which the background noise is suppressed.

The choice of the data window size depends on the quality of the signal and available memory. The longer the data window, the faster the processing. The detection program gives a default window duration of 5000 samples, i.e., 20 seconds for human subjects with a sampling rate of 250 samples/sec, 10 seconds for dogs with sampling rate of 500 samples/sec. If the signal has a high SNR, a longer data window can be used (related to available memory) to accelerate the processing. In case of a noisy signal or with the presence of baseline drifts, a short window size has to be used because of the difficulty in choosing a suitable threshold TH(f). The window duration can be chosen at the beginning of the detection session (ref. Appendix A). Event detection in most recordings has been done in the default window duration, i.e. 20 seconds for human subjects and 10 seconds for dogs.

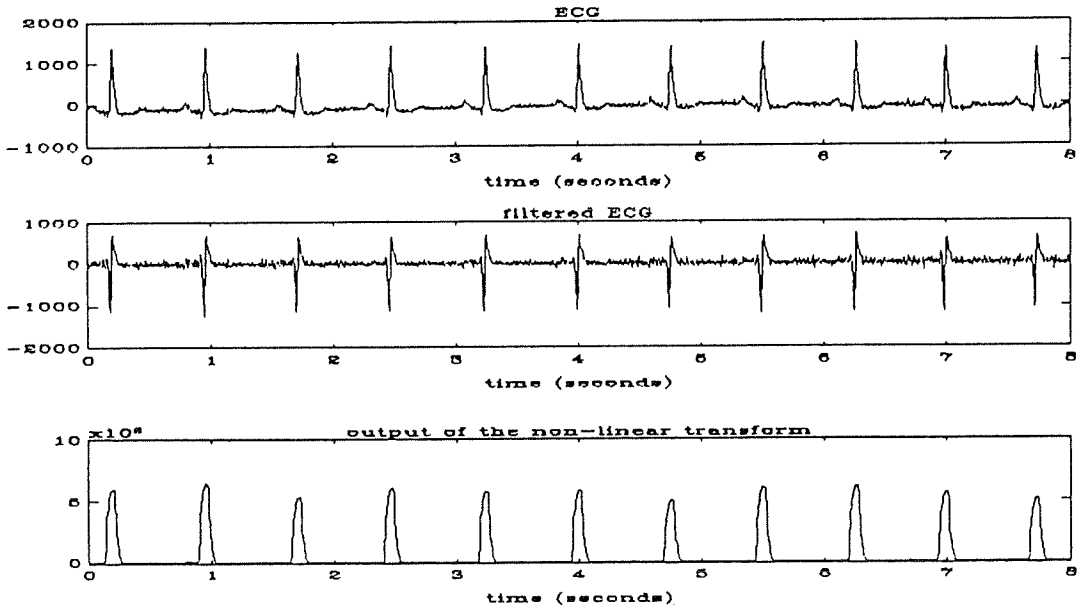

Figure 2.3 Example of ECG signal processing (ordinate: A/D conversion units):

top panel: original ECG

middle panel: output of the linear filter

bottom panel: output of the nonlinear transformation

b) Decision rules:

Decision rules are applied on z(n) at the output of the preprocessor to determine whether or not a QRS complex occurred. The rules and algorithm are based on amplitude thresholding and time adaptativity. The steps to be followed are:

Step I) initial threshold TH(f):

The appropriate starting detection threshold TH(f) of the non-linear transformed signal is evaluated in each time window f (D = 20 seconds and N = 5000 for human subjects recorded with sampling rate of 250 samples/sec) as follows:

1) TH1(f): average of the energy function over the data window f;

$$TH1(f) = \frac{1}{N}\sum_{n=1}^{N} z(n)$$

2) TH2(f): average of the M values of Z(n) over the TH1(f);

$$TH2(f) = \frac{1}{M}\sum_{n=1}^{N} (z(n) \,|\, z(n) > TH1(f))$$

3) TH3(f): average of the maximum values in each second;

$$TH3(f) = \frac{1}{D}\sum_{k=1}^{D} Vmax(k)$$

where Vmax(k) is the maximum z(n) in second k.

4) TH4(f): threshold calculated from this data window:

5) TH(f): threshold to be used is the weighted sum of the threshold used in the

$$TH4(f) = (TH2 + TH3)/2 \qquad (2.3)$$

preceding time window TH(f-1) and TH4(f) calculated from the current frame f

$$TH(f) = \alpha\, TH(f-1) + \beta\, TH4(f) \qquad (2.4)$$

α and ß were chosen as 0.4 and 0.6 respectively according to experimental trials.

Step II) detection of QRS complexes in the time window:

Search for a QRS complex occurrence time R_i: starts at the preceding detected QRS location R_{i-1} followed by T_{ref} samples. (T_{ref} is a constant refractory period after the QRS. It is used to reduce the computational load as well as the risk of tall T wave detection).

When a QRS occurs at or near a frame boundary, continuity needs to be kept, for example:

1) to decide if this QRS belongs to frame f or f-1?
2) to detect an A wave on the OEG between two R waves in ECG when this interval bridges a frame boundary;
3) to measure SYS and DIAS pressures between two R waves in ECG.

Window boundary and time continuity for QRS detection are overcome by keeping an overlapping buffer (ref. Fig. 2.4). Two consecutive data windows overlap by two seconds or less, depending on the heart rate (this overlapping interval must

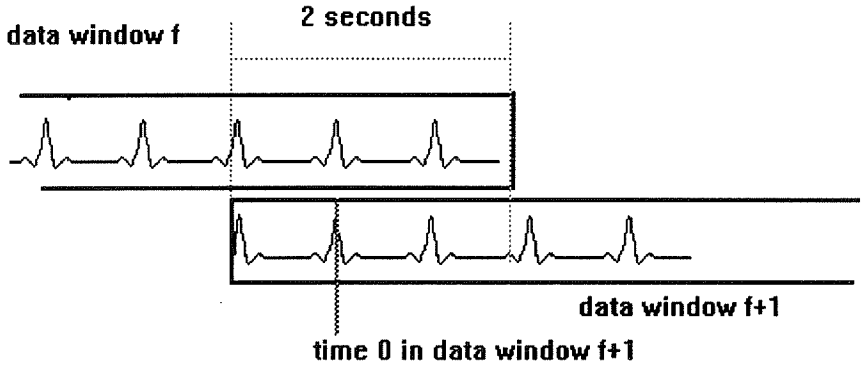

Figure 2.4 Overlapping of data windows. It is chosen to guarantee that there are at least two complete QRS in this overlapping window.

contain at least two complete QRS). After searching for QRS complexes in window f, QRS complexes following the first complete QRS in the overlapping period are discarded from the sequence. This last QRS of window f will be the first event in the next data window, f+1. The search for QRS in data window f+1 will start from this common QRS, i.e. this QRS serves as a time zero for each window. To initiate the detection, the very first window is processed twice. The first process serves to define the reference point (time zero) and the mean RR interval, which are needed for the following detection.

If the duration during which the energy function z(n) has values above the threshold TH(f) is found but is too short (<20 ms in human), the QRS complex is rejected and the search continues. Such a situation may be due to an artefact or noise.

If the duration during which the energy function z(n) has values above the threshold TH(f) is found but is too large (>400 ms in human). The threshold TH(f) is raised by TH(f)/2 and step II is repeated.

This search is repeated until the end of the data window f. The QRS complex location time is decided according to the fiducial marker definition which will be given in the section discussing fiducial marking.

Step III) adaptation of the threshold

The QRS detection process II) results in a sequence of QRS wave occurrence times $\{R_0,R_1,\ldots R_i,\ldots\}$. The properties of this sequence can be used to control a

"look-back" mode in the algorithm to adapt threshold TH(f) with a few physiological considerations. TH(f) was adapted with the following rules:

1) Too many QRS detected in the data window (>200 bpm in human), the threshold is raised with TH(f) = TH(f) + TH(f)/2;
2) Too few QRS detected in the data window (<30 bpm in human), the threshold is lowered with TH(f) = TH(f) - TH(f)/2;
3) Occurrence of a RR of 1.65 times the length of the global mean RR ($mean_{RR}$). Such a situation may be due to the occurrence of a low-amplitude ectopic beat in an otherwise stable sinus rhythm. A local TH(f) is used to locate a QRS in this interval. The same algorithm as in rule 1 and rule 2 is used to adapt the local threshold to find a peak in the given period. This does not affect the global threshold.

   The $mean_{RR}$ is adapted after each data window as a weighted sum of the average RR (RR_{mean}) in this data window and $mean_{RR}$:

$$mean_{RR}(f) = 0.6 \times mean_{RR}(f-1) + 0.4 \times RR_{mean}(f) \qquad (2.5)$$

4) Interval between last QRS and the end of the data window > 1.65 $mean_{RR}$. A local TH(f) will be used to locate a QRS between the two boundaries as in rule 3 and the global threshold remains unchanged.
5) Occurrence of RR < 0.4 $mean_{RR}$, possibly due to an artefact or an important T-wave. TH(f) is raised with TH(f) = TH(f) + 0.2 * TH(f).

If none of the above cases occurs, the search for QRS terminates. Otherwise

repeat the process from step II. The data window is re-detected with a newly adapted threshold. If the detection in the data window does not succeed after more than 20 trials, a short text is displayed to explain the reason and the program switches to the graphic display. It allows the operator to correct false detections by visually positioning cursors in the data window.

c) Fiducial marking:

It is important to define a stable fiducial point for each detected QRS complex for construction of RR time series. The definition is critical to maintain the accuracy of interval measurements, particularly for short intervals such as AR intervals [44]. A stable fiducial reference minimizes jitter. For spectral analysis, the jitter results in a wideband noise which is named measurement noise. Commonly used definitions are the peak of the R-wave, the maximum negative slope, the central point of the energy function, the onset of the waveform, [47,48] etc... Tremblay and LeBlanc [44] defined the midpoint of the number of samples over the detection threshold in the energy function. The resolution is the quanta of the sampling interval (4 ms for a sampling rate of 250 Hz). The central point of the QRS energy function is defined here as the midpoint between points A and B (Fig. 2.5). Both A and B are determined at points defined by the intersection of the line which connects the consecutive samples below and above the threshold. The centre of the local energy, T_{mid}, is the mean value of the timing for points A and B, represented by a floating point number. With this technique, the central point is interpolated and gives a finer definition of the event occurrence time.

Since the morphology of the QRS complex changes slightly during recording, this may cause the fiducial point to jitter. The location T_{max}, defined as the maximum

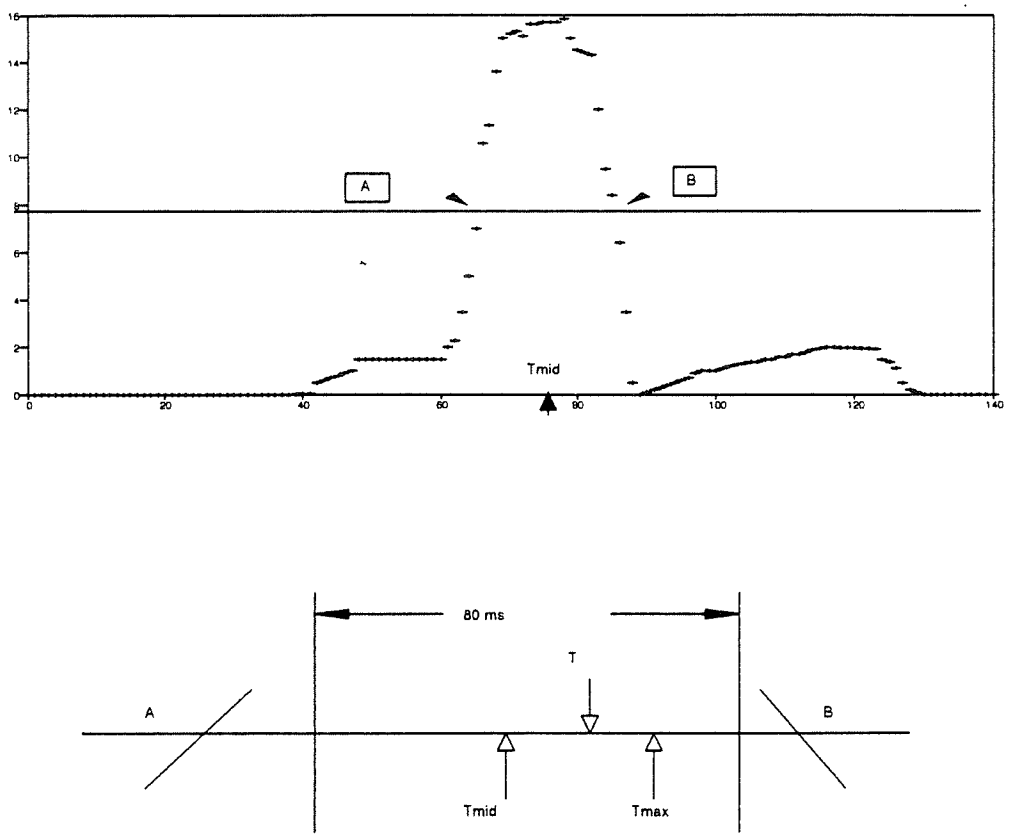

Figure 2.5 Definition of fiducial marker corresponding to the QRS complex.
top: definition of mid-point of the energy function T_{mid}
bottom: Maximum negative slope is searched in a window of 80 ms centred at T_{mid}. The fiducial marker, T, is the average of T_{mid} and the time of maximum negative slope, T_{max}

negative slope in the QRS complex is introduced. This value is obtained from a local window of 80 ms which centers at T_{mid}. The final fiducial point, T, is the average of the two time locations, i.e., $T = (T_{max} + T_{mid})/2$. Application of this algorithm to all normal subjects in our study showed that such defined T was not very sensitive to QRS morphology changes.

2.2.2 Detection of A wave:

The A wave detection takes place when the RR time series and the RR wave timings are available. Each A wave is searched in an interval limited by two QRS complexes instead of the whole data window. A waves are searched for from the OEG signal in a window of $[t(R_{i-1})+RR_i/2, t(R_i)-RR_i/10]$, where t is the QRS complex occurrence time and RR_i is the interval between the two R waves. The preprocessing and the fiducial point definitions are identical to those used for QRS detection. This strategy is used because a stable recording for OEG for long periods is often difficult.

2.2.3 Measurement of the systolic and diastolic blood pressure

The systolic and diastolic blood pressures were measured as follows: the ABP signal was filtered by a five point average filter (cut off frequency is 50 Hz at a sampling date of 250 samples/second).

$$ABP^f(i) = \frac{1}{5}\sum_{n=-2}^{2} ABP(i+n)$$

The maximum and the minimum points were searched for in the interval between two consecutive R waves. It gives the systolic (SYS) and diastolic (DIAS) pressures for

this heart beat. The pulse pressure (PULSE) is simply SYS-DIAS.

2.2.4 Sampling of the respiration signal:

The respiration signal was sampled at the QRS complex occurrence time. It provides a relative measurement of the respiration rate and relative change in tidal volume.

2.3 Time series

From the signal processing, seven or less (depending on the recorded signals) non uniformly sampled simultaneous time series are obtained (RR, AA, AR, SYS, DIAS, PULSE and RESP). Each time series is limited to a maximum of 532 consecutive events and is stored for further processing (i.e., time domain analysis and spectral analysis). There is no limit to the number of events detected by the detection program. However, our analysis has been normalized to a 512 point time series. If less points are available, mean values are added to complete the series (i.e., zero padding).

Time series are filtered to contain 512 points. The purpose of this filtering is:

1) to eliminate premature extrasystolic intervals and the corresponding post-extrasystolic pauses (ventricular or supraventricular). A premature beat is detected when the absolute values of the differences between the premature interval and the mean of RR, and between the post extrasystolic pause and the mean of RR are greater than 3.6 times the SD of RR. The two corresponding points of a premature beat for each series are removed. The rest of the points

in the series are shifted in time by adjusting their occurrence time accordingly;

2) to eliminate outlier intervals, based on the hypothesis that the physiologic mechanisms controlling the sinus rhythm do not induce a sudden change in heart rate in a stable condition as established in our recording protocols (ref. chapter 3). These values may also contaminate the spectra which is known as "Gibbs phenomenon". Fig. 2.6 shows the effect of a single value far from the average in a time series. The spectrum is contaminated because the spike introduces a significant high frequency components.

In summary, if more than 20 points need to be eliminated, the detection procedure must be repeated or the recording has to be rejected since there are too many outlier beats or the signal is too noisy. Finally, the blood pressure time series is calibrated to mmHg units (ref.: Appendix A for the utility program used to visualize the recorded signal and allow the operator to calibrate the blood pressure signal from a recorded calibration square waves generated by the Finapres OHMEDA).

2.4 Time domain analysis:

Common statistics such as mean and standard deviation are given for each time series. Tachograms (value of each point vs its occurrence time) and histograms (distribution of values) can be displayed and printed to visualize the variabilities of the series and to verify the stationarity and some statistical information (coefficient of variation and skewness). Fig. 2.7 shows an example of a tachogram of RR and its histogram in a normal subject.

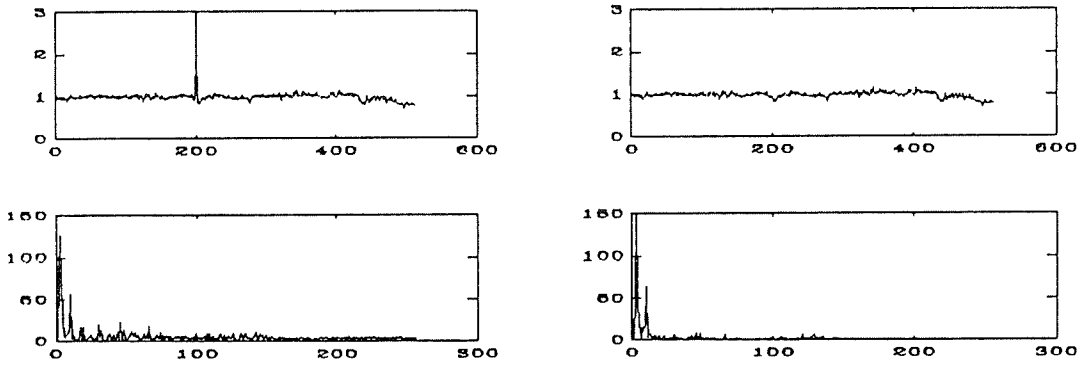

Figure 2.6 Effect of an artefact or an extrasystole in a RR interval series from a normal subject. High frequency components are apparent.

A) top: a signal with an outlier, bottom: the corresponding power spectrum.

B) top: the same signal but the outlier was removed.

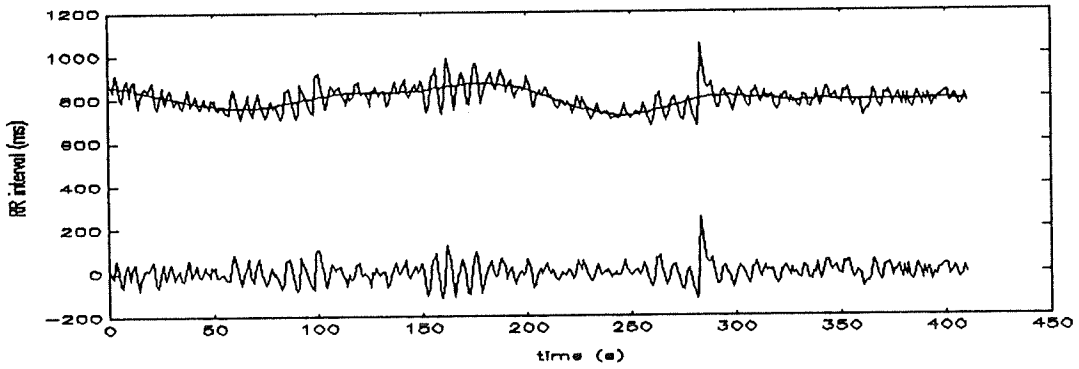

(a)

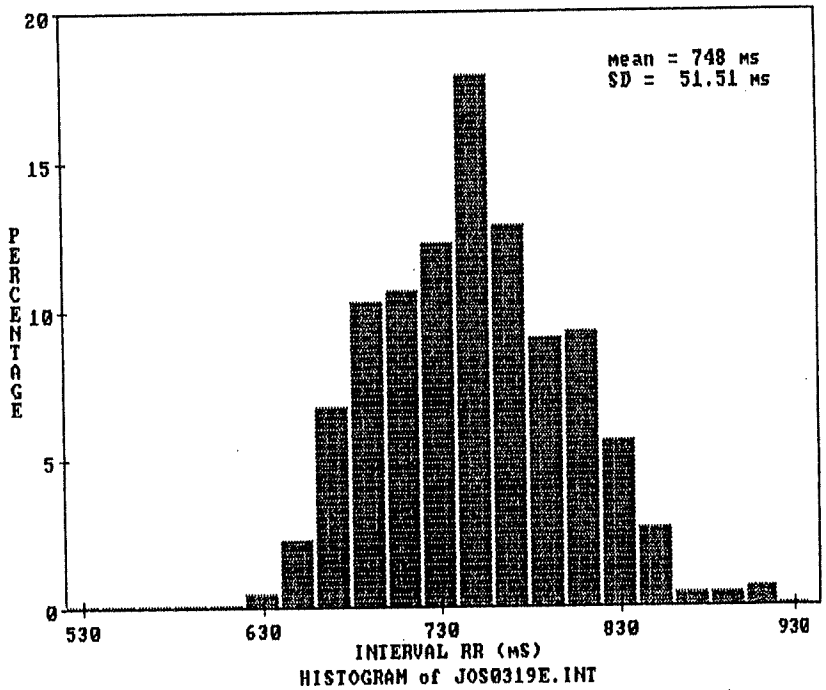

(b)

Figure 2.7 Recording of a normal subject at rest in supine position. a) RR interval tachogram. upper curves: raw RR and its trend, lower part: RR after detrending and average removal. b) Histogram of raw RR intervals.

2.5 Spectral estimation:

a) Preprocessing:

A detrend process is applied on each time series in order to remove frequencies < 0.005 Hz. This band usually shows noisy content or non-stationarity. It is not subject to analysis since it does not involve short term autonomic control of cardiovascular variables. The trend is approximated by a polynomial of order 4, defined as:

$$T_i = a_0 + a_1 x_i + a_2 x_i^2 + a_3 x_i^3 + a_4 x_i^4 \qquad (2.6)$$

where x is the occurrence time (relative to the first QRS wave, time zero) of an event point in the time series. The coefficients are calculated by solving the following linear system:

$$\sum_{j=0}^{M} \alpha_{kj} a_j = \beta_k \qquad k = 0, 1, 2, \ldots, M \qquad (2.7)$$

where

$$\alpha_{kj} = \sum_{i=1}^{L} x_i^j x_i^k$$

$$\beta_k = \sum_{i=1}^{L} y_i x_i^k$$

M is the order of the polynomial, i.e. M = 4, a_i are the parameters to be fitted, L is the length of the window where the detrend procedure is applied and was chosen as L = 70 RR intervals, i.e. approximately 60 seconds. Curve fitting of 4th order polynomial in the chosen window of RR time series preserves approximately the

frequency components in the band of less than 0.005 Hz. Fig. 2.7a shows the effect of the detrend process. The top traces are the original RR interval time series (solid line) and the slow trend (dashed line) estimated by the detrend process. The bottom shows the time series after removing the trend and the average RR.

The power spectrum estimation requires evenly sampled time domain data. A linear interpolation technique (resampling) is applied to each time series to generate evenly spaced points (sampling rate $>$ 4 samples/sec, varying according to the HR). Since our study is based on a uniform time series length corresponding to 512 RR intervals, (instead of a uniform time duration) and the Fast Fourier Transform (FFT) algorithm used is based on a number of points in the time series which is a power of 2, the resampling rate is chosen to form a record length of 2048 evenly spaced sample points (four times the number of points of the original time series).

b) Normalized auto-spectra:

In the literature, different approaches to spectral estimation have been used to study the ANS response to physiologic perturbations. Results differ from one method to another and the reproducibility is questionable. This situation makes spectra comparison for different manoeuvres and different groups hardly possible. Spectral differences may be due to highly random and dynamic perturbations of physiological origin, lack of identical recording conditions or use of different signal processing methodologies [18]. A normalization and standardization process would be useful in order to reduce differences and to improve the reproducibility of observations. Several attempts at normalization have been published, but each method gave different quantities and did not significantly reduce the interspectral differences [18,31,43].

A systematic approach to standardize spectral estimation is used. Spectral analysis is applied on the standardized variable,

$$z_i = \frac{x_i - \mu_{x_i}}{\sigma_{x_i}} \qquad (2.8)$$

where μ_{xi} is the mean value of the variable x_i, σ_{xi} is the standard deviation of variable x_i, i represents the sequence number of the time series for analysis. Thus, variable z_i has zero mean and unit variance.

A data record of finite duration is equivalent to multiplying a theoretically infinite stretch of data with a rectangular window. Direct application of the FFT on the data is equivalent to convoluting the Fourier transform of the data by the Fourier transform of the rectangular window. Windows with a shape different from a rectangular shape have been proposed to reduce energy leakage in the side lobes. Here, the Hanning window is always applied to the time series in order to reduce the power leakage in the main peaks.

For a stationary and ergodic signal with finite energy, its power spectral density defined by the FFT can be obtained as follows:

$$G_f = \frac{T}{N}|X_f|^2 \qquad (2.9)$$

where T is the sampling period, N is the number of points and X_f is the DFT of the normalized time series z. The total power over the whole band gives the variance of the time series, i.e.,

$$\sigma^2 = \int_0^\infty G_f \, df = 1 \qquad (2.10)$$

In our analysis of time series, all the spectra were normalized to give total unit power. Non-normalized spectra were obtained for comparison. Fig. 2.8 shows spectra of two subjects at rest. A much larger difference is observed between the non-normalized spectra than between the normalized ones.

With normalization, the spectra of the group is easily plotted on the same scale, which is very difficult to realize for the non-normalized ones. Non-normalized spectra give a large variance which causes difficulty in power comparisons between the two manoeuvres. On the one hand, normalized spectra are considered of value for group comparison while on the other, absolute spectra may be necessary to evaluate autonomic tones. The absolute spectra may be recovered from the normalized power by multiplying the normalized spectra by the variance of the time series.

c) Spectral parameters

The spectral estimation is limited to the power in the band from 0.005 Hz to 0.8 Hz. The number of events for analysis being fixed at 512, the duration used for different recordings ranges from 6 to 10 minutes. For FFT, the frequency resolution is roughly the reciprocal of the period T, i.e. 1/T. Variable duration, T, between time series gives a variable frequency resolution. A linear interpolation is used in each spectrum from 0 to 0.8 Hz to get 512 values. The total power (P_t: 0.005-0.8 Hz), the VLF band power (P_{vl}:0.005-0.05 Hz), the LF band power (P_l: 0.05-0.15 Hz), and the HF band power (P_h) were measured. P_h is calculated with the estimation

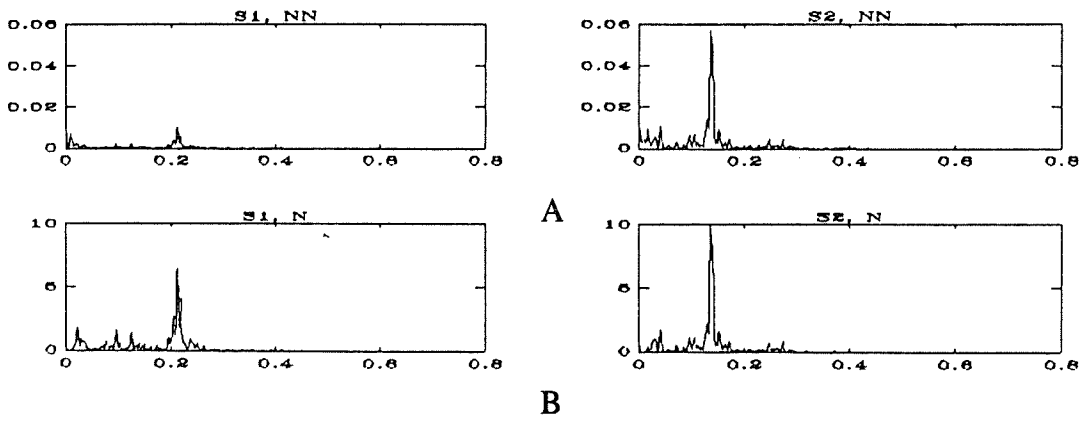

Figure 2.8 Computation of Non normalized (NN) and Normalized (N) power spectra of RR intervals.

A) NN spectra for subjects S1 and S2.

B) N spectra for S1 and S2.

of the respiration frequency band obtained from the spectrum of the respiration signal. The HF bandwidth is defined with the help of the spectrum of the respiration signals with the following procedure:

i) calculate the respiratory energy spectrum from the respiratory power spectrum. The energy for a given frequency is defined as the area in the power spectrum in a window of ± 0.0125 Hz centred at this frequency point. The energy spectrum is generally much smoother than the power spectrum.

ii) define HF band by the window for which the energy is greater than a threshold. The threshold equals to 3 x average power over the 0.03--0.8 Hz band;

iii) HF peak position is defined as the position of the maximum power value in the HF band defined in ii). Note that this will be specific and probably different for each recording.

iv) apply this bandwidth to all other spectra, such as RR, AA, AR, SYS, DIAS, and PULSE to measure HF power.

To define the LF band, we first calculate the energy spectra for each of the six variables from their corresponding power spectra in the same way as the respiration energy spectrum. In each energy spectrum, we search for the maximum value position in the band 0.05--0.15 Hz. The average of the six peak positions will be defined as the LF peak position for all the six spectra (but not for the respiration spectrum). The LF band will be defined as a band of 0.1 Hz centered at the LF peak

position.

Note: for difficult cases, graphical interaction is available to edit marker locations of spectral peaks and bandwidth limits.

A total of 16 parameters are extracted from each time series:

1) 4 time domain measurements: mean value, standard deviation, coefficient of variation, and skewness;
2) 12 spectral parameters (VLF, LF and HF): peak positions (Hz), maximum peak values, powers associated with the peak, percentages of the peak power over P_t.

This information for each recording and for each subject is stored in a file, which has a format compatible with Quattro Pro and a statistical package (SYSTAT), for group analysis.

2.6 Statistics

The results are expressed as means $\pm$ SE. The Student T test has been used to test the significance of variables between different manoeuvres. Student's paired *t* test was used for individual changes and the unpaired *t* test used for group data or unpaired observations. Differences were considered significant with a p value less than 0.05. The statistics were conducted by the software package SYSTAT version 5.01 (SYSTAT, Inc. Evanston).

Chapter 3 Results

The aim of this chapter is: a) to validate our spectral analysis method with simulated signals; b) to relate quantitatively the spectral components and the autonomic responses to various stimuli in healthy volunteers, hypertensive patients and syncope prone patients. Analyses have also been conducted in dogs to study the effects of manipulations on the ANS by drugs and electrical stimulation.

3.1 Validation

1) **Simulated signals:**

To validate the method, a simulated 512 points RR interval time series has been used. It oscillates around a mean interval of 800 ms with two known frequencies (f_1 = 0.1 Hz, f_2 = 0.25 Hz) and amplitudes (50 ms and 30 ms) and added white noise with a range of ± 2 ms. The time series is defined by the following equation:

$$X(t_i) = 50\sin(2\pi f_1 t_i) + 30\cos(2\pi f_2 t_i) + 800 + 2\,rand(t_i) \qquad (3.1)$$

where t_i = i*dt (i=0..511, dt = 0.8 sec.). The function *rand* generates values uniformly distributed between 1 and -1. This 512 events simulated time series is equivalent to a data collection run of 6.9 minutes. The frequencies were chosen to approximate human spectrum of RR intervals where two peaks around 0.1 and 0.25

Hz are found. Amplitudes were imposed to insure that the RR interval series had a standard deviation (SD) of 41 ms which correspond to the average SD values of the group of normal volunteers included in the study. Figure 3.1A illustrates the tachogram of the simulated RR interval time series.

This simulated time series passed analysis steps outlined in chapter 2 (interpolation, normalization, Hanning windowing, FFT). The resulting spectral estimate of this time series is shown in Figure 3.1B. Two peaks at 0.1 and 0.25 Hz are easily located. By this simple test, the spectral estimation algorithm is shown to behave as predicted.

2) **Advantage of normalized spectra**

As mentioned in chapter 2, the normalization procedure was applied to obtain a zero mean and unit variance random process. In spite of the large inter-subject variability of cardiovascular variables, measurements of power spectral parameters are realized on a normalized random process; i.e. the power spectrum corresponds to the relative power and the power is non-dimensional. This makes possible spectral comparisons between different cardiovascular variables, for example, blood pressure and RR intervals.

Table 3.1 presents two parameters (LF and HF) extracted from both normalized and non-normalized spectra of RR time series each recorded in rest and passive head up tilt positions. These data were obtained on 20 normal subjects. Non-normalized spectra failed to prove the significant difference in parameters for the group between the two conditions ($p>0.2$), even though for each individual, the

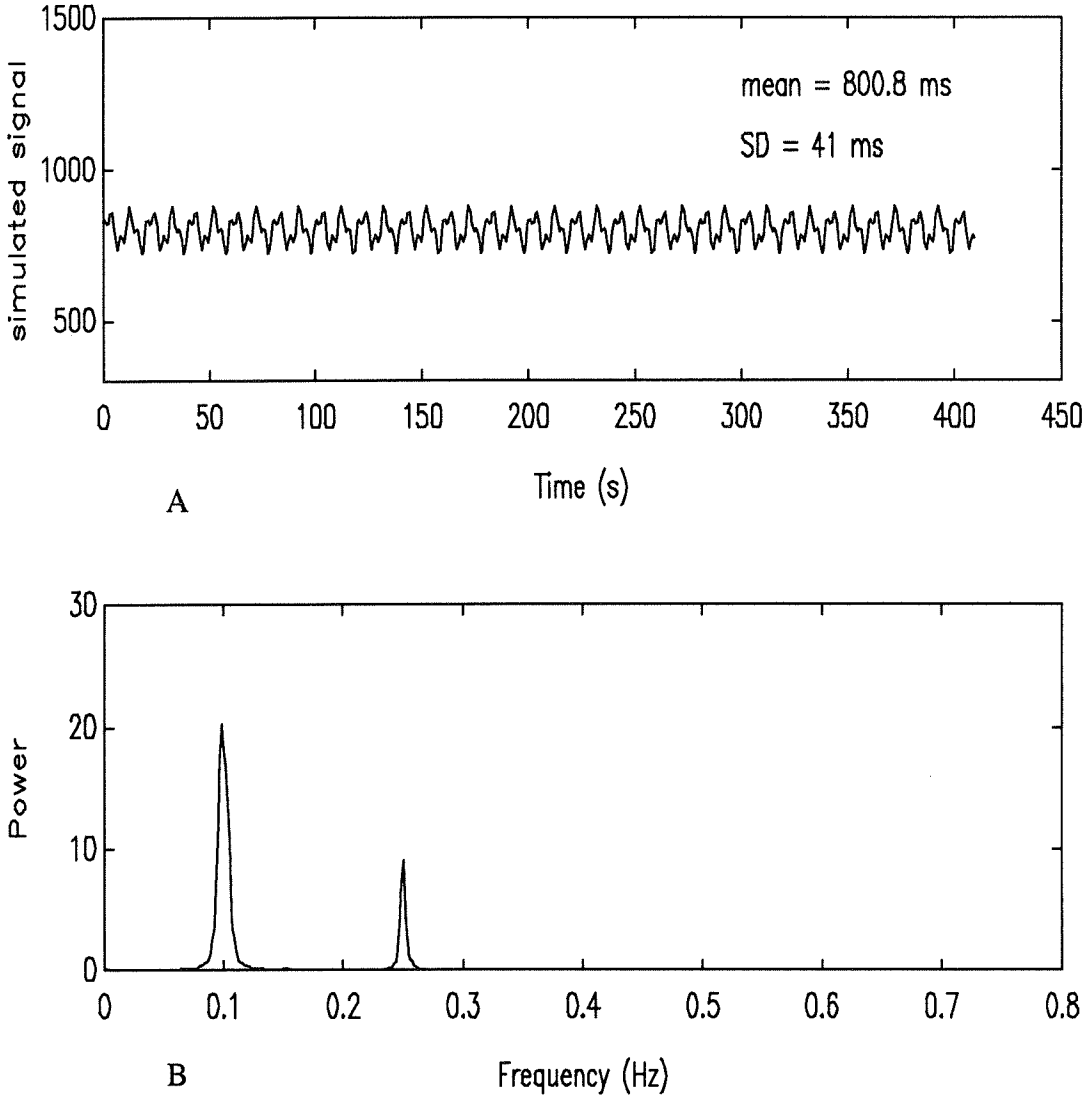

Figure 3.1: Validation of the analyses with a simulated signal
A) simulated signal, B) normalized spectrum

difference is evident. The normalized method clearly demonstrates a significant difference ($p < 0.001$).

The drawback of the normalized spectrum is the loss of the absolute values of the power. In this type of group analysis, the absolute power was not used because of large inter-subject variabilities of the power spectra of the cardiovascular variables.

Table 3.1 Normalized and non-normalized spectral parameters in RR interval (N = 20)

	supine (RR=894 ms)		tilt (RR=723 ms)	
	LF	HF	LF	HF
Normalized*	31.88±12.90	35.18±19.10	63.15±23.39	19.52±15.74
Non normalized* ($x10^{-4}$)	65.33±64.66	115.3 ±157.0	74.63±79.59	67.07±160.0

* this number without multiplying by df = 0.8/512 Hz

3.2 Human studies

3.2.1 Normal volunteers

Subjects

Forty one subjects (29 males, 12 females; 20-50 years old) without any clinically evident diseases participated in this study. None was receiving medication. The protocol was approved by the Human Subjects Review Committee ("Comité d'éthique de la recherche") of Sacré-Coeur Hospital. Ninety percent of the recordings were obtained between 9:00 and 13:00. The subjects were instructed to avoid taking

coffee and cigarettes 2 hours before signal recordings and to eat a light breakfast. They were all well informed about the studies.

Protocol and materials

The patients were placed on an electrically driven tilt table in the ANSL. Four signals were recorded: lead II ECG, OEG, arterial blood pressure (ABP) and respiration. All the protocols began with a 15 to 30 minute explicative session. The experimental room was quiet and with dimmed lights. The test was conducted at a comfortable room temperature (18°C-20°C). Care was taken to avoid repetitive external auditory or visual stimuli. The recording in each position started after a certain period (3 to 10 minutes) to permit cardiovascular baroreflex mechanisms to achieve steady state. The study consists of three protocols (Fig. 3.2):

I) Protocol I (Fig. 3.2A): *7* subjects (6 males, 1 female)

A given session has four recordings.

a) Each subject was asked to rest supine on the table, to remain awake and to breath spontaneously and regularly. Following the explicative session, at least 10 minutes have to pass before starting the recording to meet stabilization requirements. Then, all four signals were recorded for 10 minutes. This duration was selected as a good compromise for adequate frequency resolution and the stationarity of each recording.

b) The subjects had been passively moved to an upright position (85° head up) by the electrically driven tilt table. At least 5 minutes were elapsed between

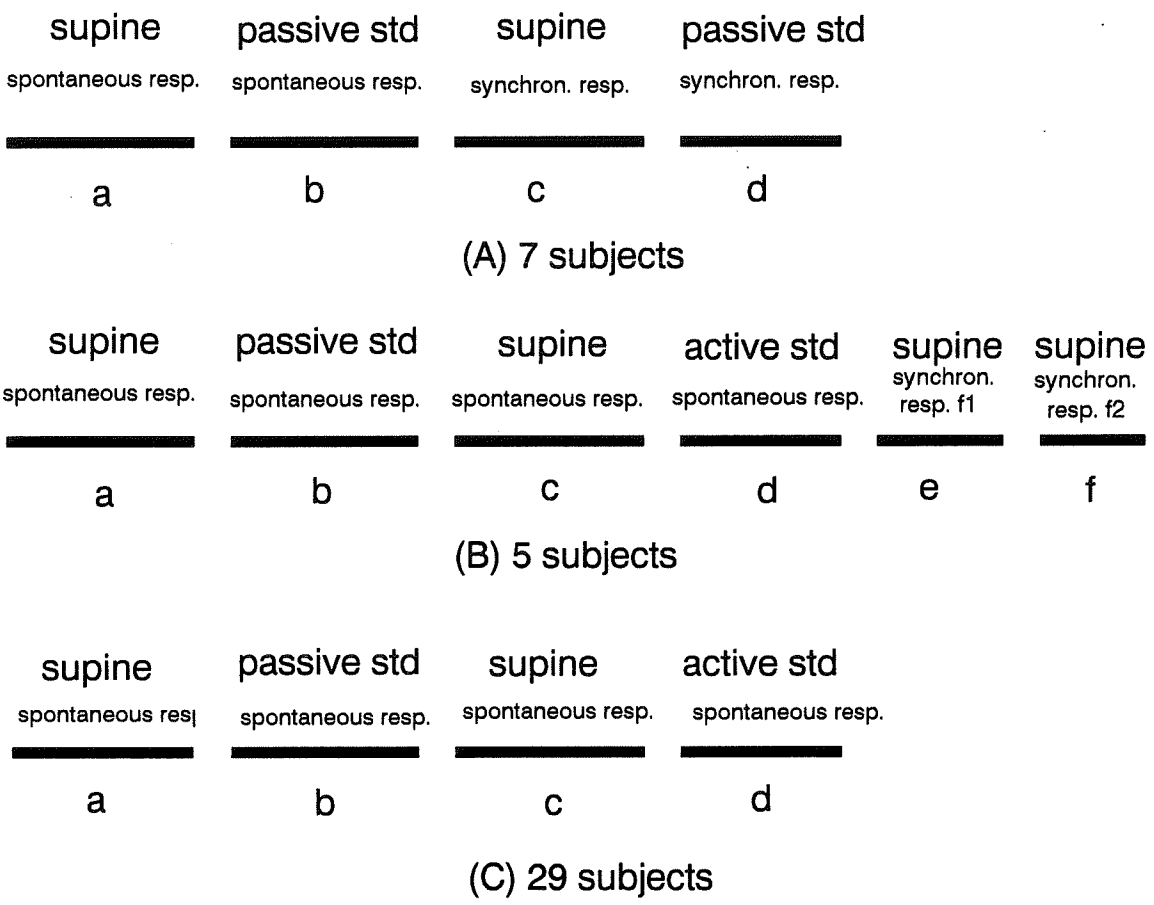

Figure 3.2: Protocols for normal subjects.

The duration of each recording is 10 minutes, 3 to 5 minutes elapsed between consecutive recordings to insure stationary recordings

A) protocol I,

B) protocol II,

C) protocol III

recordings to avoid the transient period. The same signals were recorded for 10 minutes under spontaneous respiration. The subjects rested on their feet and were allowed to move their feet occasionally when they felt uncomfortable.

c) The subjects were returned to the supine position by rotation of the tilt table. An interval of at least 10 minutes was used before starting synchronized respiration. The subjects were asked to breath at a fixed respiration rate following a metronome. The signals during the last 10 minutes were recorded. The imposed breath rate was selected according to one's spontaneous respiration rate and had approximately 1.8 times the natural breath rate. This imposed breath rate ranged from 20 to 30 breaths/min.

d) The subjects were brought back to their upright position and asked to breath in synchrony with the metronome at the same rate as in session c). Also signals were recorded for 10 minutes after a waiting period of 3-5 minutes.

II) Protocol II (Fig. 3.2B): *5* subjects (all males)

Six recordings were done for each subject. The first two recordings were identical to a) and b) of protocol I. In recording c), the subjects were replaced to the supine position and rested for 20 minutes. The subjects breathed spontaneously. The signals for the last 10 minutes were recorded to compare with the first rest and to verify the reproducibility. In recording d), the subjects were asked to get off the table and stand on their feet actively for fifteen minutes. The signals of the last 10 minutes were recorded under spontaneous respiration. The subject was placed back in the supine position for 20 minutes and breathed in synchrony with a metronome adjusted at two different frequencies for 10 minutes each and signals of each 10

minutes were recorded (recording e) and f)). Frequencies were chosen based on the comfort of patient and a little higher than his (or her) spontaneous breath rate (f1 ≈ 1.5 and f2 ≈ 1.8 times the natural breath rate respectively). Signals for the 10 minutes controlled respiration were recorded in both e) and f).

III) Protocol III (Fig. 3.2C): *29* subjects (18 males, 11 females)

This protocol was the same as the second protocol limited to the first four recordings, no controlled respiration. Fourteen of these subjects did not have OEG recording and fifteen with OEG recording.

In summary, 41 subjects were recorded during rest and passive standing under spontaneous respiration; 27 recorded with OEG. A total of 27 subjects were recorded during active standing, 18 with the oesophageal electrode.

Results

Results of the normal group with spontaneous respiration (basic statistics of cardiovascular variables and their spectral parameters) will be given in three groups: 1) characteristic profile in supine position, 2) parameter changes in responses to head-up tilt and 3) the comparison between the response to head-up tilt (passive standing) and the response to standing alone (active standing).

3.2.1.1 Baseline characteristics of the normal group (supine):

In this section, the profile of the normal group in supine position is given in Table 3.2. It includes basic statistical parameters (average RR interval and blood

Table 3.2 Basal (phase A of protocol I, II and III) characteristics in 41 volunteers in supine position and spontaneous respiration

RR (ms)	921±18
SD (ms)	52±2
VLF	23.8±2.1
LF	36.9±2.3
HF	33.2±2.8
SYS (mmHg)	123±3
SD (mmHg)	5±0.4
VLF	41.8±2.6
LF	40.1±2.1
HF	15.6±2.1
DIAS (mmHg)	64±2
SD (mmHg)	2±0.12
VLF	32.3±2.8
LF	54.1±2.6
HF	10.3±1.6
PULSE (mmHg)	58±2
SD (mmHg)	5±0.3
VLF	48.0±3.0
LF	28.8±2.2
HF	19.8±2.6

***Values are mean ± standard error.**

pressures) and spectral parameters. Correlations of spectral parameters with respiratory frequency and with mean RR interval are presented as well. The group (N=41) has a mean heart rate (HR) of 65 beat/min. The variational ranges of the mean values for each variable in the group are summarized as the following: RR from 751 ms to 1240 ms, standard derivation of the RR interval from 20 ms to 143 ms, systolic blood pressure from 91 mmHg to 170 mmHg, diastolic pressure from 46 mmHg to 94 mmHg and pulse pressure from 22 mmHg to 90 mmHg). The variational ranges of the spectral parameters are:

	VLF	LF	HF
RR:	4.1 to 56.0	11.9 to 71.2	7.0 to 73.9
SYS:	15.5 to 78.1	15.7 to 71.7	1.4 to 66.9
DIAS:	6.3 to 79.6	16.7 to 87.5	1.0 to 56.2
PULSE:	11.3 to 85.6	9.2 to 72.0	1.6 to 68.3

Spectra of all variables (except respiration) presented three peaks: VLF below 0.05 Hz, LF between 0.05 and 0.15 Hz and HF associated with respiration frequency. The average location of the respiration peaks for the group is 0.24 Hz (i.e. 15 breaths/min), ranging from 0.1 to 0.4 Hz (6 to 24 breaths/min).

Figure 3.3 is an example of tachograms of seven signals (left column) and their corresponding normalized power spectra (right column). The respiration spectrum shows a main peak around 0.35 Hz in Figure 3.3g (21 breaths/minute). Three peaks at VLF ($\approx$ 0.04 Hz), LF ($\approx$ 0.12 Hz) and HF ($\approx$ 0.35 Hz, respiratory frequency), are clearly visible in all intervals (RR, AR and AA) spectra (Fig 3.3a-c). In the systolic pressure spectrum (Fig 3.3d), three peaks are clearly visible too. In

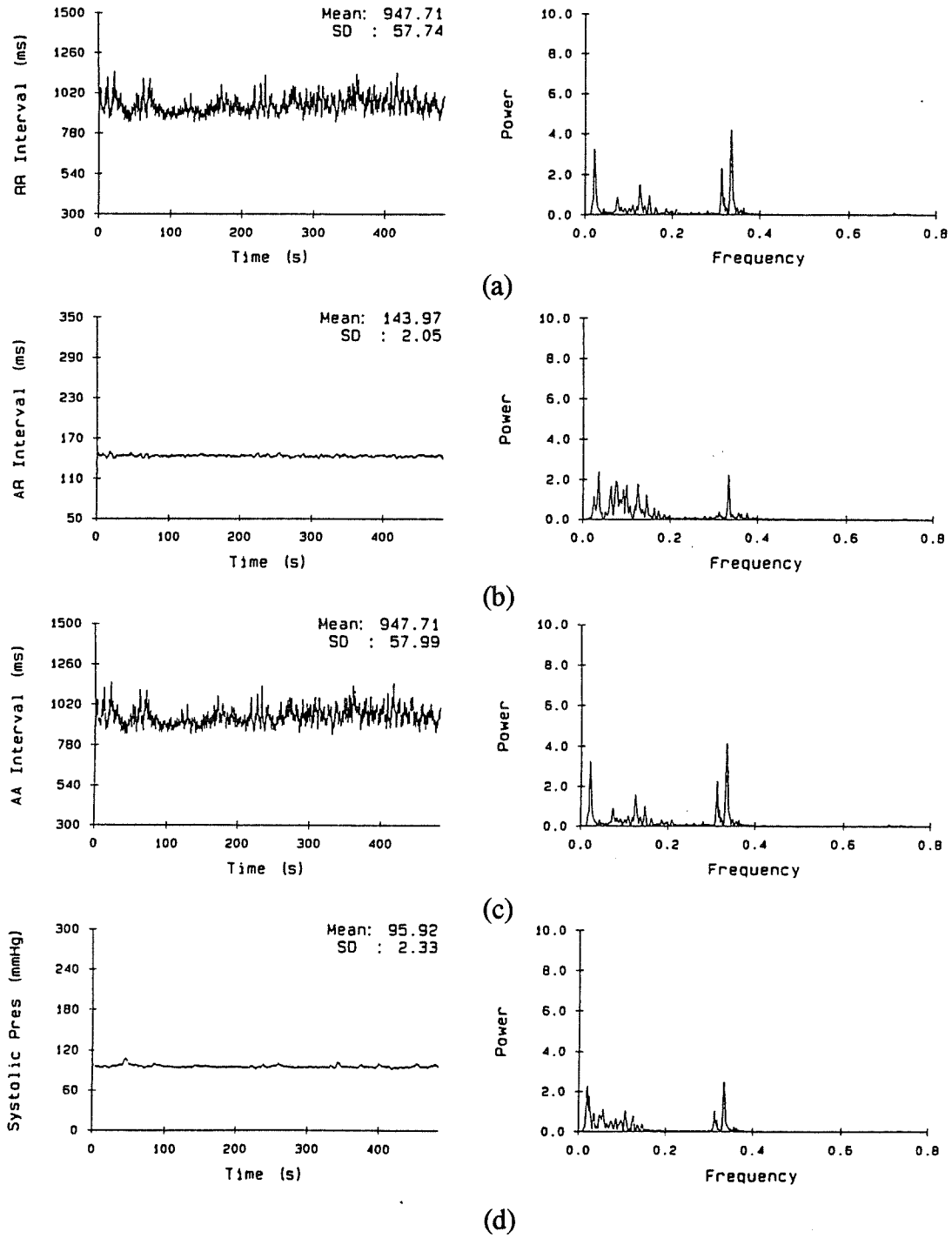

Figure 3.3 (ctd)

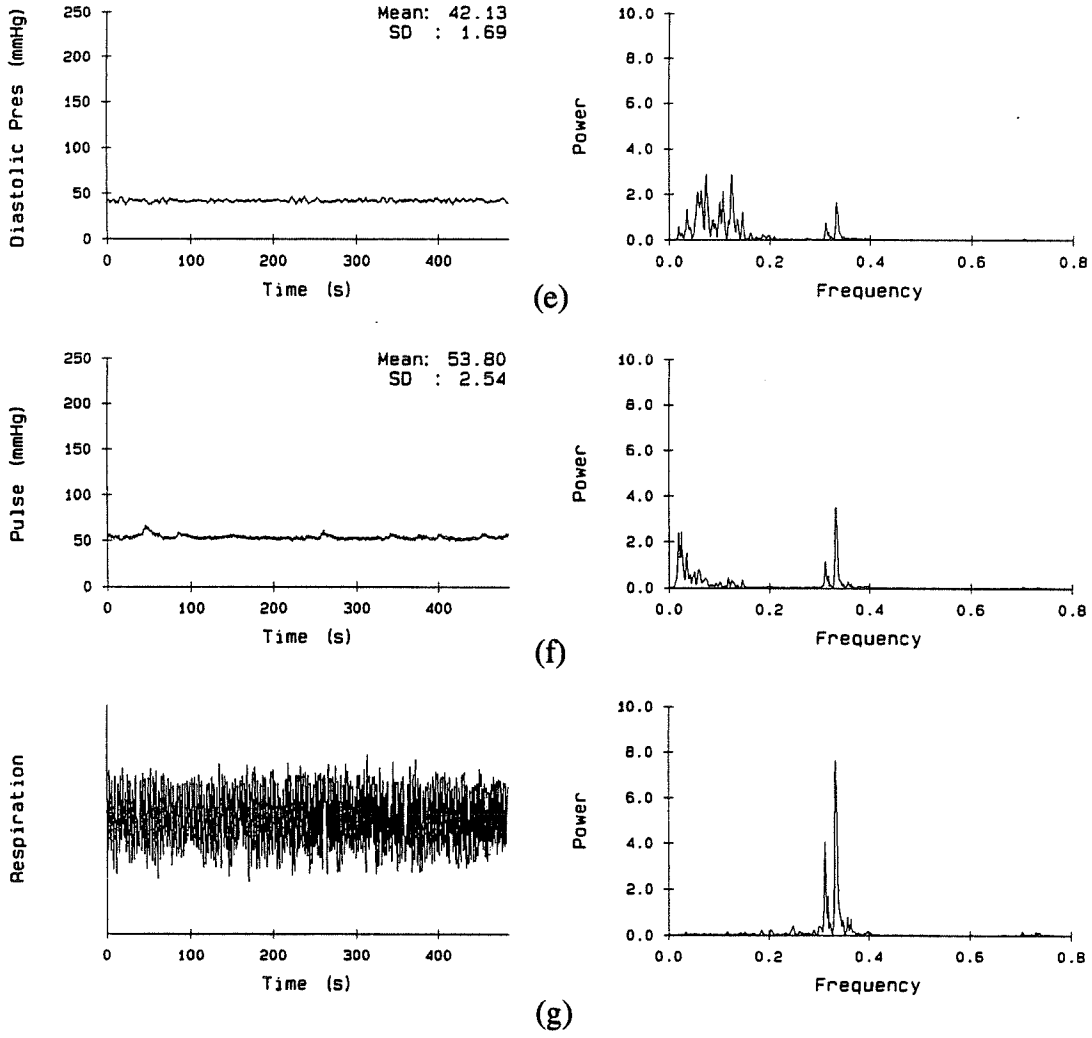

Figure 3.3: An example of tachograms (left column) and normalized spectra (right column) from a normal volunteer under spontaneous respiration.

a) RR interval, b) AA interval, c) AR interval,

d)systolic pressure, e) diastolic pressure,

f) pulse pressure, g) respiration.

the diastolic pressure spectrum (Fig 3.3e), the LF peak is more important than the other two peaks and the respiratory peak is much smaller. In the pulse pressure spectrum (Fig 3.3f), the VLF and HF peaks are greater than the 0.1 Hz peak.

By visual comparison of inter-subject spectra, it was observed that a lower respiration rate induced larger respiratory peaks in the spectra of RR and blood pressure variabilities. Evidence exists to show that a relationship between respiratory rate and spectral power of RR and SYS in the HF band is present. However, the nature of this relationship has only been shown in animals as a low-pass filter relationship. Here, this relationship has been examined by calculation of the correlation coefficient between relative power of a given variable in a given frequency band. Table 3.3 shows the correlation between spectral power of the three bands and the respiration frequency, for RR, SYS, DIAS and PULSE time series. Figures 3.4a-d give the plot of LF and HF power vs the respiration frequency for RR and SYS. Weak but significant trends were observed in the correlation between HF power in both RR and SYS with respiratory frequency. No correlation was found between respiratory rate and powers in DIAS, neither in PULSE. This correlation is carried out in inter-subjects not intra-subject. All the subjects breathed spontaneously and with an individual combination of depth and frequency of breathing.

To test the hypothesis that the spectral powers in the three bands are heart rate dependent, we calculated the correlation coefficient values between baseline mean RR interval and VLF, LF and HF powers in RR, SYS, DIAS and PULSE (Table 3.4). Results show that there are weak but significant correlations between the baseline mean RR interval and VLF power in SYS ($r=0.40$, $p=0.015$); the VLF and LF powers in DIAS ($r=0.43$, $p=0.006$; $r=-0.48$, $p=0.002$) and the LF power in RR

(r=-0.31, p=0.05). Figures 3.5 a) and b) plot the powers of RR (LF and HF respectively) vs baseline mean RR interval, c) and d) powers of DIAS (VLF and LF).

Table 3.3 Correlation of power spectra with respiration frequency (N=41)

	VLF	LF	HF
RR	0.34 p=0.032	0.112 p=0.48	-0.43 p=0.005
SYS	0.04 p=0.80	0.26 p=0.11	-0.36 p=0.02
DIAS	-0.04 p=0.80	0.17 p=0.3	-0.30 p=0.06
PULSE	0.25 p=0.11	-0.17 p=0.30	-0.21 p=0.19

Table 3.4 Correlation of power spectra with mean RR interval (N=41)

	VLF	LF	HF
RR	0.097 p=0.55	-0.31 p=0.05	0.16 p=0.33
SYS	0.40 p=0.015	-0.20 p=0.23	-0.234 p=0.14
DIAS	0.43 p=0.006	-0.48 p=0.002	0.08 0.63
PULSE	-0.06 p=0.71	-0.06 p=0.68	0.14 p=0.40

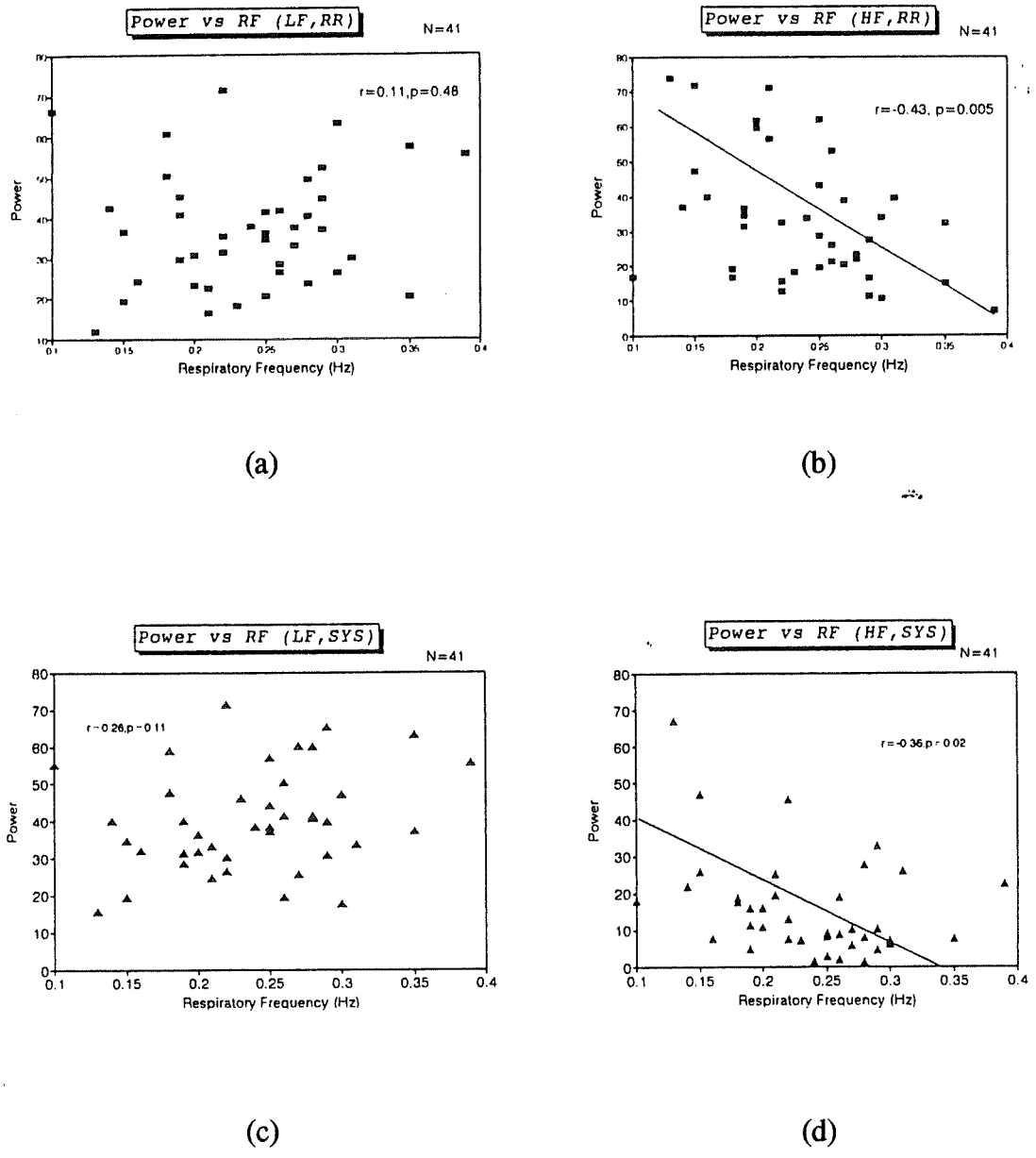

Figure 3.4: Correlation between either LF or HF power and respiration frequency (RF) in:
RR intervals: a) LF power, b) HF power,
and SYS pressures:c) LF power, d) HF power.

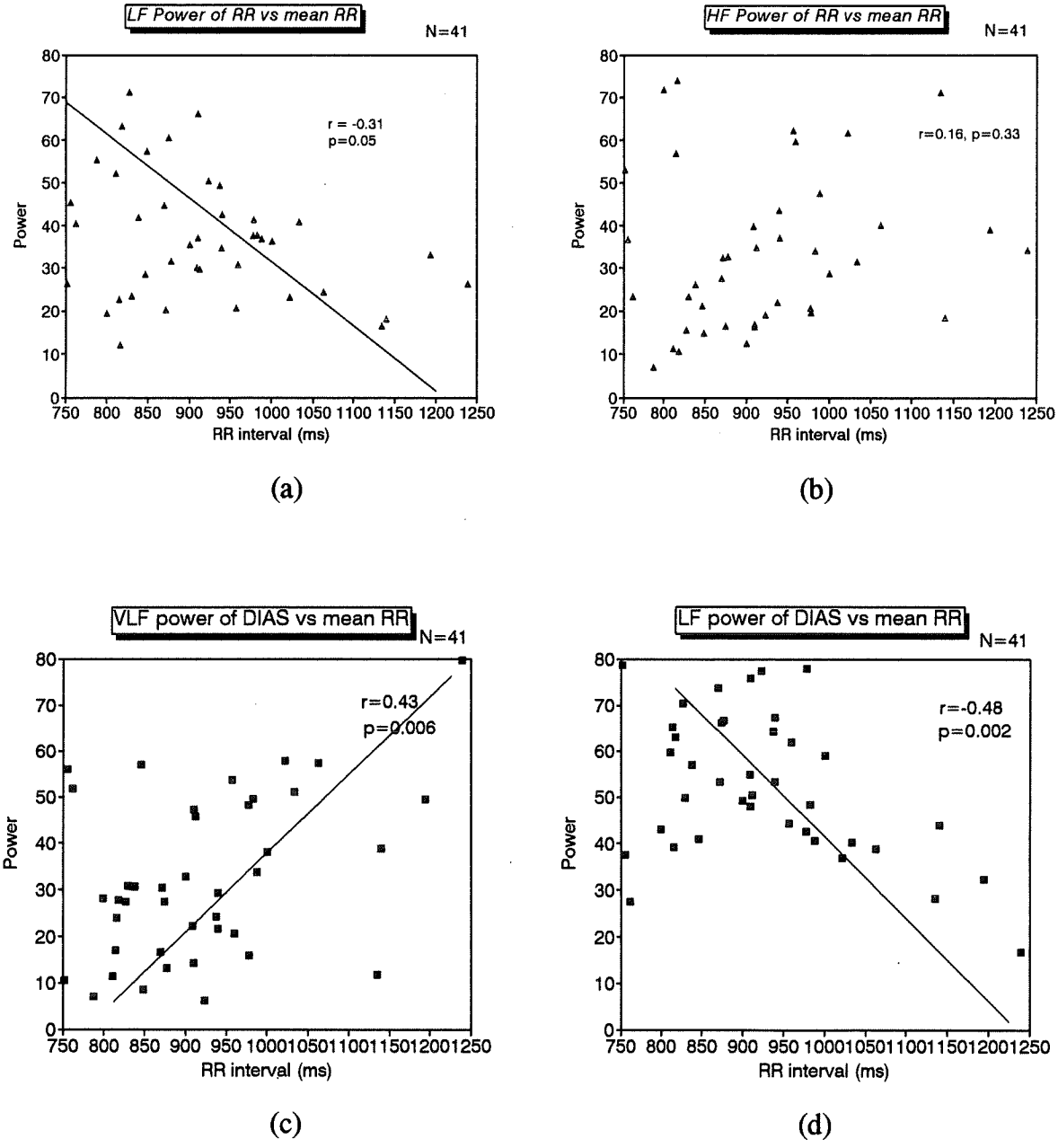

Figure 3.5 Correlation between powers in RR, DIAS and mean RR at rest.
a) LF power, b) HF power in RR.
c) VLF power, d) LF power in DIAS.

3.2.1.2 Response to passive head-up tilt:

Only heart rate and arterial blood pressure variables are presented in this section. AA and AR (AV conduction time) will be presented in section 3.2.4. Cardiovascular variables and their spectral components will be compared between both positions (supine and tilt). The power distribution in different frequency bands among cardiovascular variables (RR,SYS,DIAS,PULSE) will be discussed as well.

The initial reaction to tilt head up was characterized by a rapid shortening of RR intervals, then an overshoot followed by a gradual shortening of RR intervals (i.e., increase of heart rate) until a relatively stable value is obtained. This transient might last over 180 seconds (ref. Figure 3.6). After onset of the tilt, the systolic pressure dropped simultaneously with an increase in heart rate. This fall continues until it reaches a minimum value, then systolic pressure rise with an overshoot and fall again and finally stabilizes at a relative fixed level which is lower than the supine value. The diastolic pressure follows a time course similar to systolic pressure, except that the overshot is absent and the final stable value is higher than the rest value. The transient period is not analyzed because of its non stationarity.

Figure 3.7 gives an example of the characteristic appearance of the normalized power spectra and their corresponding tachograms for 512 consecutive a) RR interval, b) SYS, c) DIAS and d) PULSE at both rest and tilt positions in a normal subject. It shows an increase of LF power and a significant decrease of HF power in RR and SYS in response to tilt. This is interpreted as sympathetic stimulation and parasympathetic withdrawal.

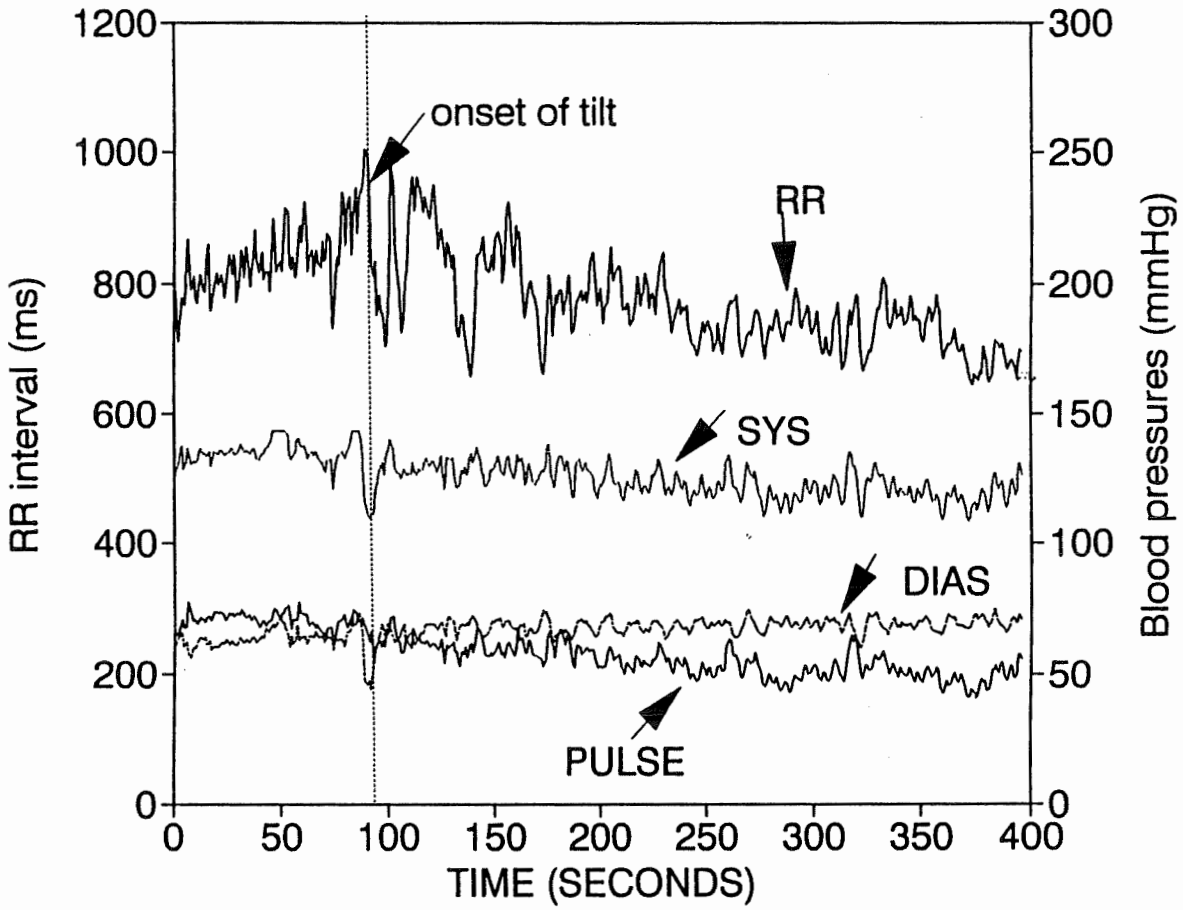

Figure 3.6 Response to passive head-up tilt in a normal subject.

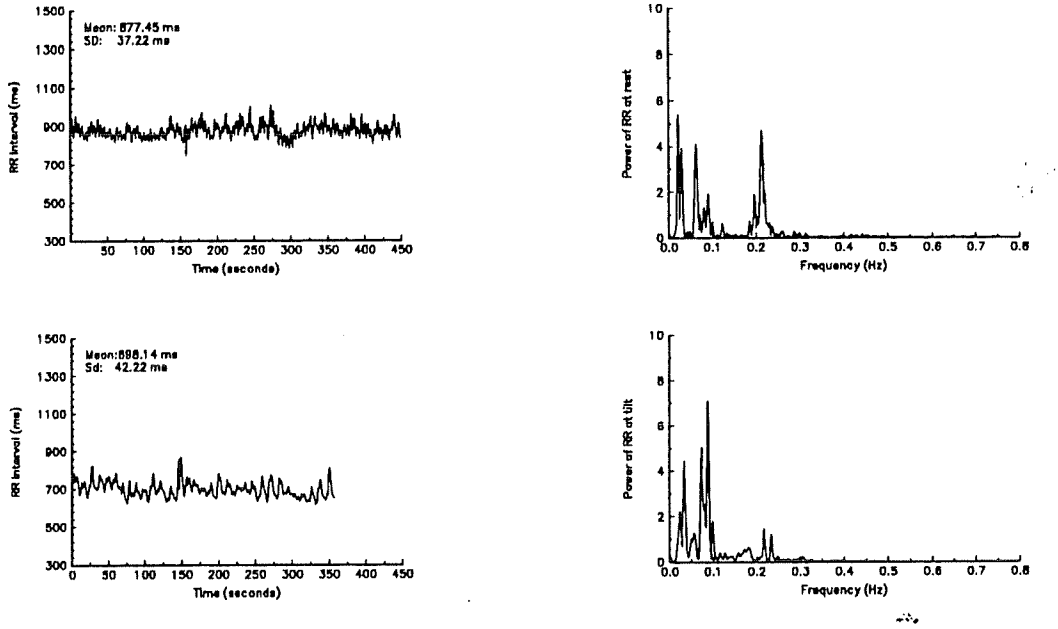

(a) signal of RR interval and its spectrum at rest (top)and tilt (bottom)

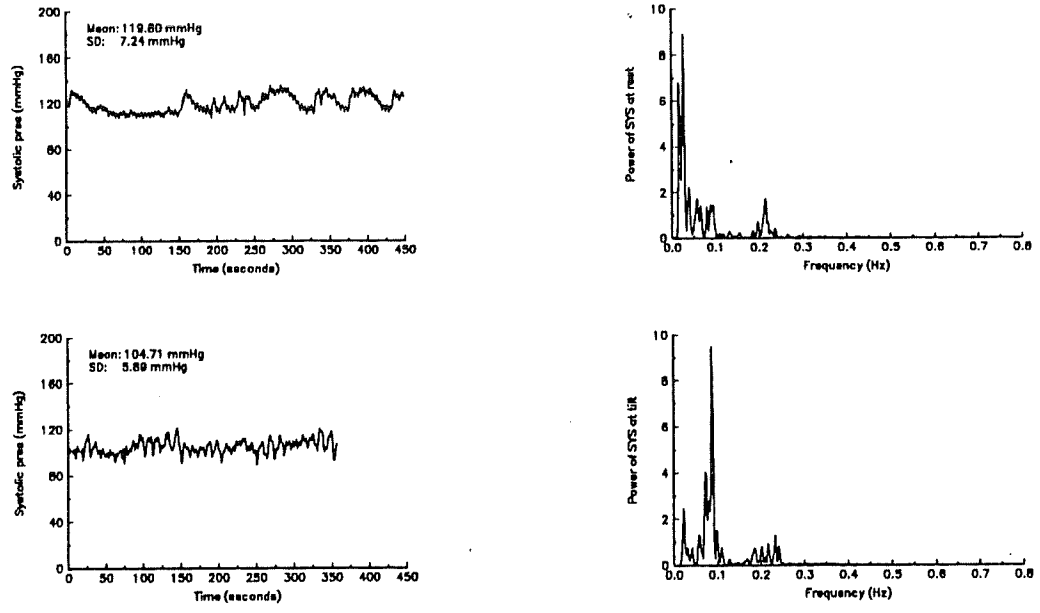

(b) signal of systolic pressure and its spectrum at rest (top) and tilt (bottom)

Figure 3.7 (ctd)

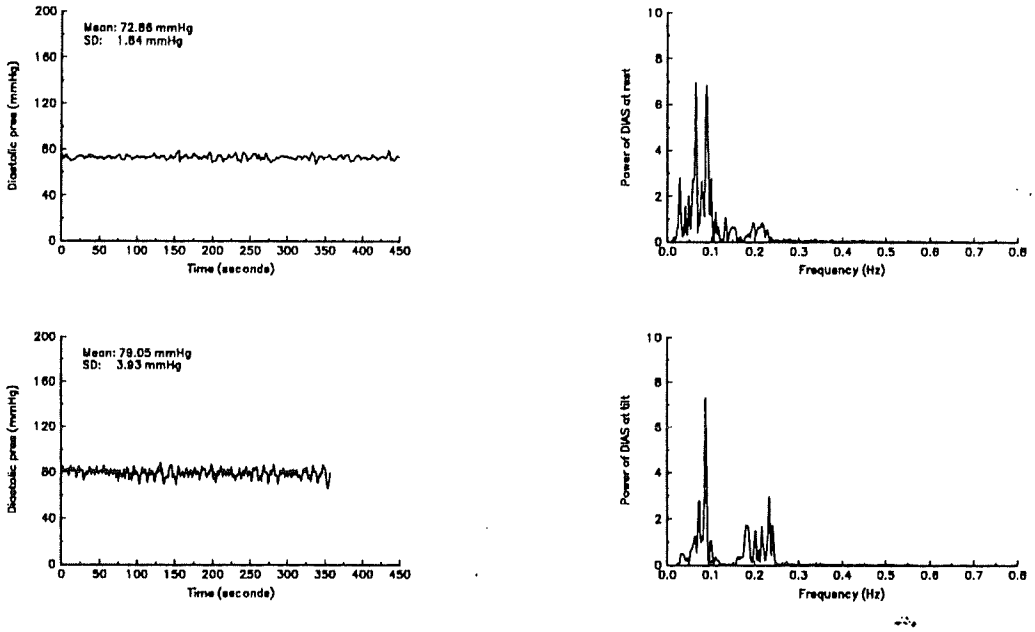

(c) signal of diastolic pressure and its spectrum at rest (top) and tilt (bottom).

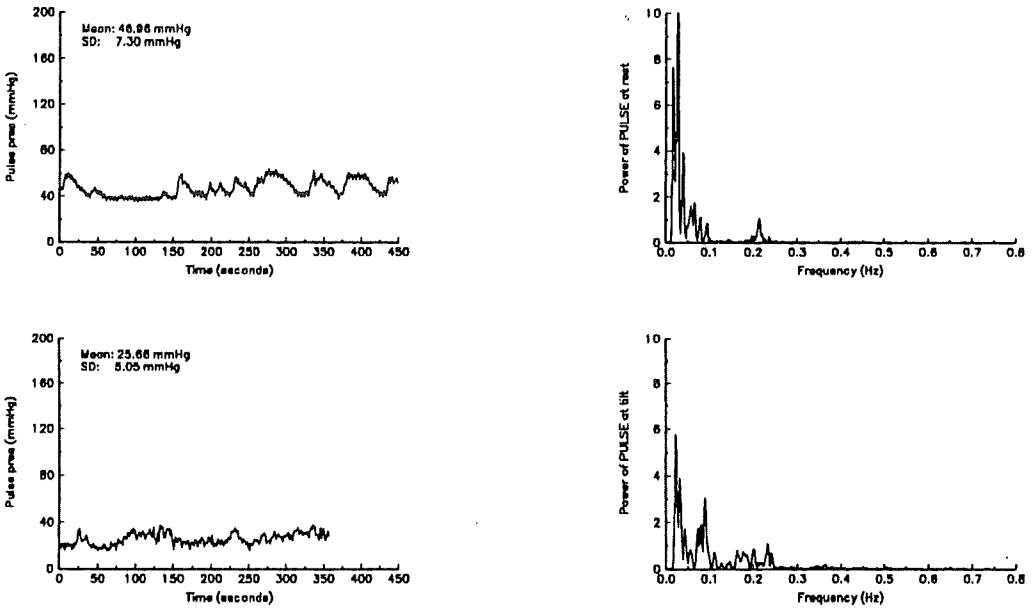

(d) signal of pulse pressure and its spectrum at rest (top) and tilt (bottom)

Figure 3.7 Examples of tachograms and their respective spectra both at rest and passive head-up tilt in a normal subject.

Responses of cardiovascular variables (heart rate and arterial blood pressures) to head up tilt in the normal group are summarized in Fig 3.8 A (RR interval) and B (blood pressures). Numerical data are presented in Table 3.5. The mean RR interval exhibited a statistically significant decrease after tilt from 921 ± 18 ms to 728 ± 14 ms ($p < 0.0001$). The mean standard deviation of RR intervals also decreased from 52 ms to 46 ms ($p = 0.05$). The mean systolic blood pressure decreased from 123 to 117 mmHg ($p < 0.007$), the diastolic pressure increased from 64 to 69 mmHg ($p = 0.003$) and the pulse pressure had a 10 mmHg decrease ($p < 0.0001$). The standard deviations of both systolic and diastolic pressures increased by 1 mmHg ($p = 0.002$ and $p < 0.001$), but the standard deviation of pulse pressure remained unchanged.

At both supine and tilt positions, correlations between mean RR interval and standard deviation were observed. But in tilt, this correlation was a little more important ($r = 0.43$, $p = 0.006$ vs $r = 0.40$, $p = 0.009$, ref. Fig 3.9). This means that subjects with a higher mean RR interval will have a more important beat-to-beat RR variation.

Changes of the cardiovascular variables in the frequency domain in response to head-up tilt are given in Fig. 3.10-12. Numerical data are also presented in Table 3.5. For the group, the HF power of the RR interval decreased significantly from 33.21 ± 2.84 to 18.57 ± 1.98 ($p < 0.0001$), while the LF power increased significantly from 36.91 ± 2.25 to 54.14 ± 2.74 ($p < 0.0001$). The VLF power did not change (ref. Figure 3.10). The LF over HF ratio also increased significantly from 1.8 to 7.8 ($p = 0.016$). To have an overall look at the individual response to tilt, we plot both LF and HF power subject by subject in rest and tilt in figures 3.11A and B.

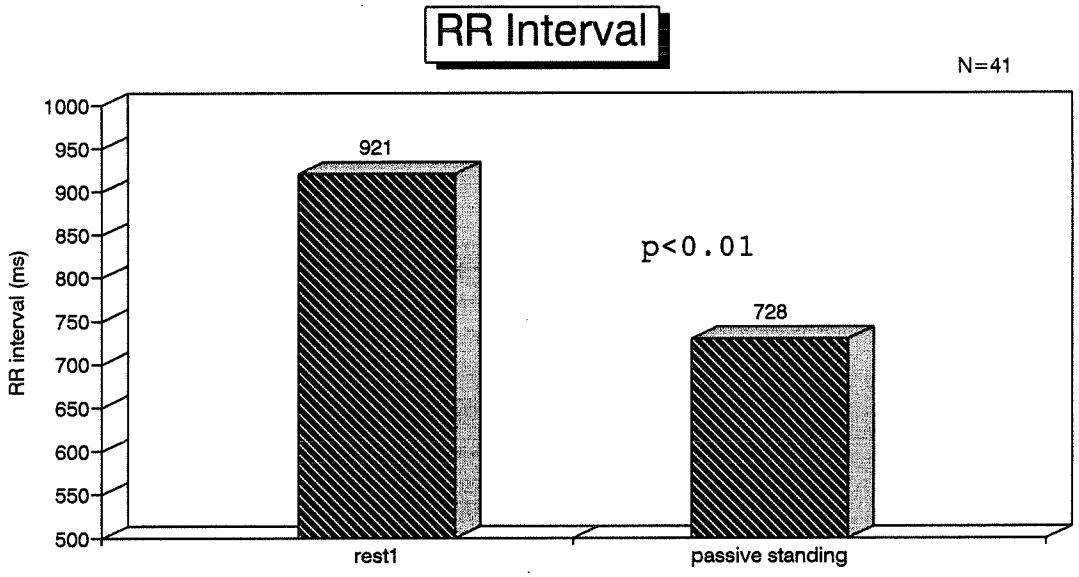

A

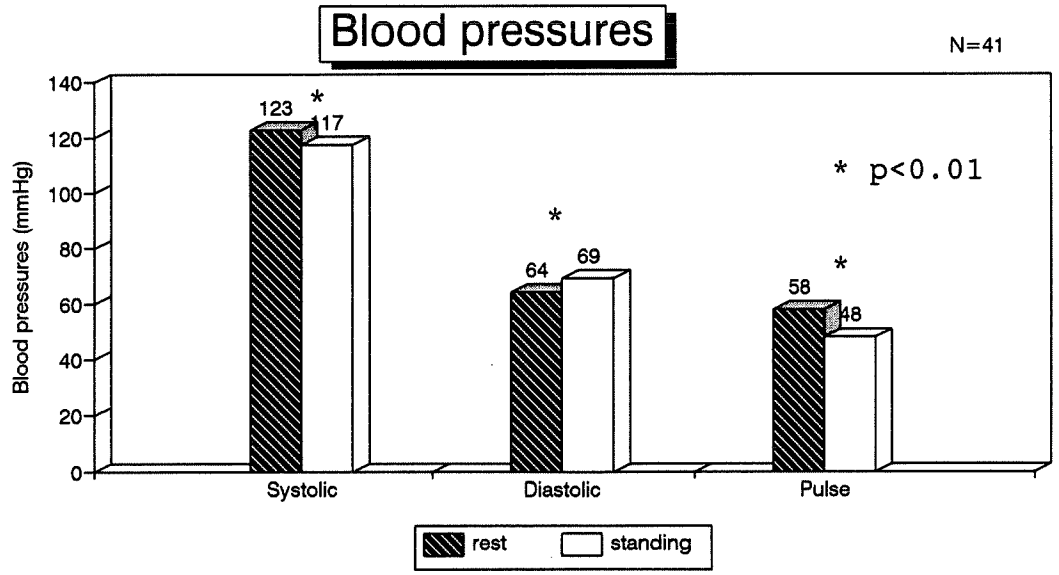

B

Figure 3.8 Average values of RR intervals and BP of the normal group at supine rest and passive tilt with spontaneous respiration. A) RR interval, B) Blood pressures.

Table 3.5 Effects of passive tilt in 41 volunteers

	Rest	Tilt	Mean difference	P values
RR (ms)	921±18	728±14	-192	<0.00001
SD (ms)	52±2	46±3	-7	0.05
VLF	23.8±2.1	23.3±2.3	-0.5	0.97
LF	36.9±2.3	54.1±2.7	+17.2	<0.00001
HF	33.2±2.8	18.6±2.0	-14.6	<0.00001
SYS (mmHg)	123±3	117±3	-6	0.007
SD (mmHg)	5±0.4	6±0.4	+1	0.002
VLF	41.8±2.6	18.9±1.7	-22.9	<0.00001
LF	40.1±2.1	48.9±2.6	+8.8	0.005
HF	15.6±2.1	28.7±2.6	+12.1	<0.00001
DIAS (mmHg)	64±2	69±1	+5	0.003
SD (mmHg)	2±0.12	3±0.2	+1	<0.00001
VLF	32.3±2.8	17.6±1.8	-14.6	<0.00001
LF	54.1±2.6	66.5±2.3	+12.4	0.0004
HF	10.3±1.6	13.3±1.8	+3.0	0.173
PULSE (mmHg)	58±2	48±2	-10	<0.00001
SD (mmHg)	5±0.3	5±0.3	0	0.053
VLF	48.0±3.0	26.7±2.2	-21.4	<0.00001
LF	28.8±2.2	38.0±2.4	+9.3	0.001
HF	19.8±2.6	30.3±2.8	+10.5	0.002

***Values are mean ± standard error.**

****differences are significant when p< =0.05.**

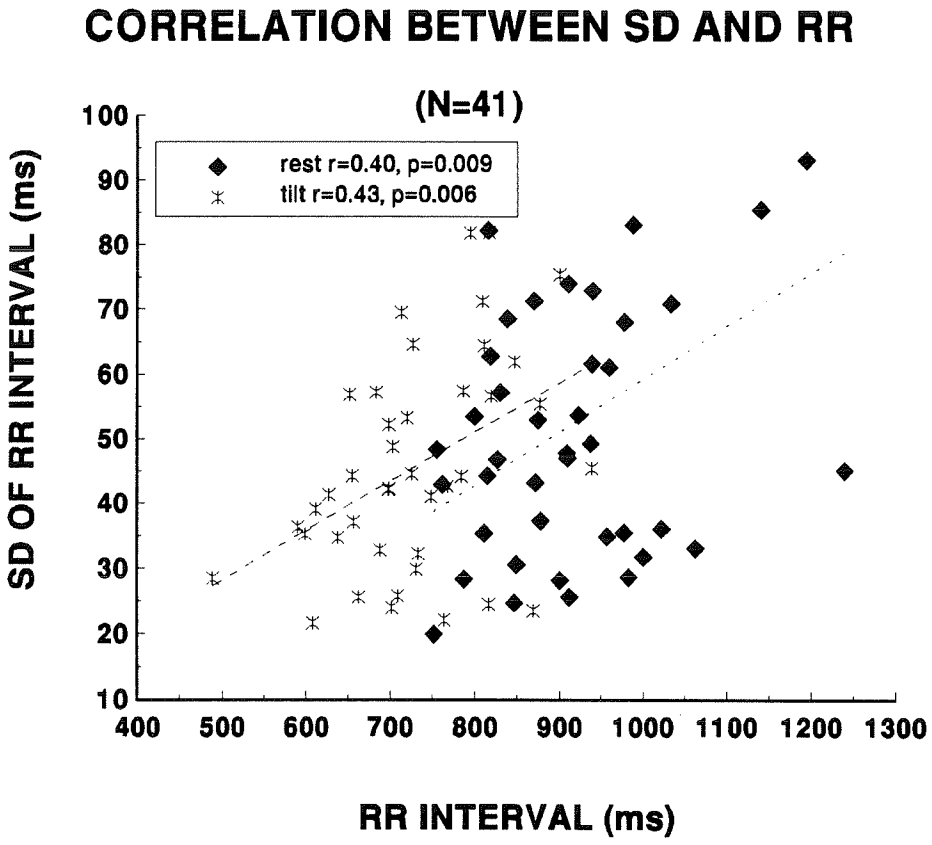

Figure 3.9 Correlation between mean RR interval and its standard deviation for all recordings in phases a) and b) of protocols I, II and III.

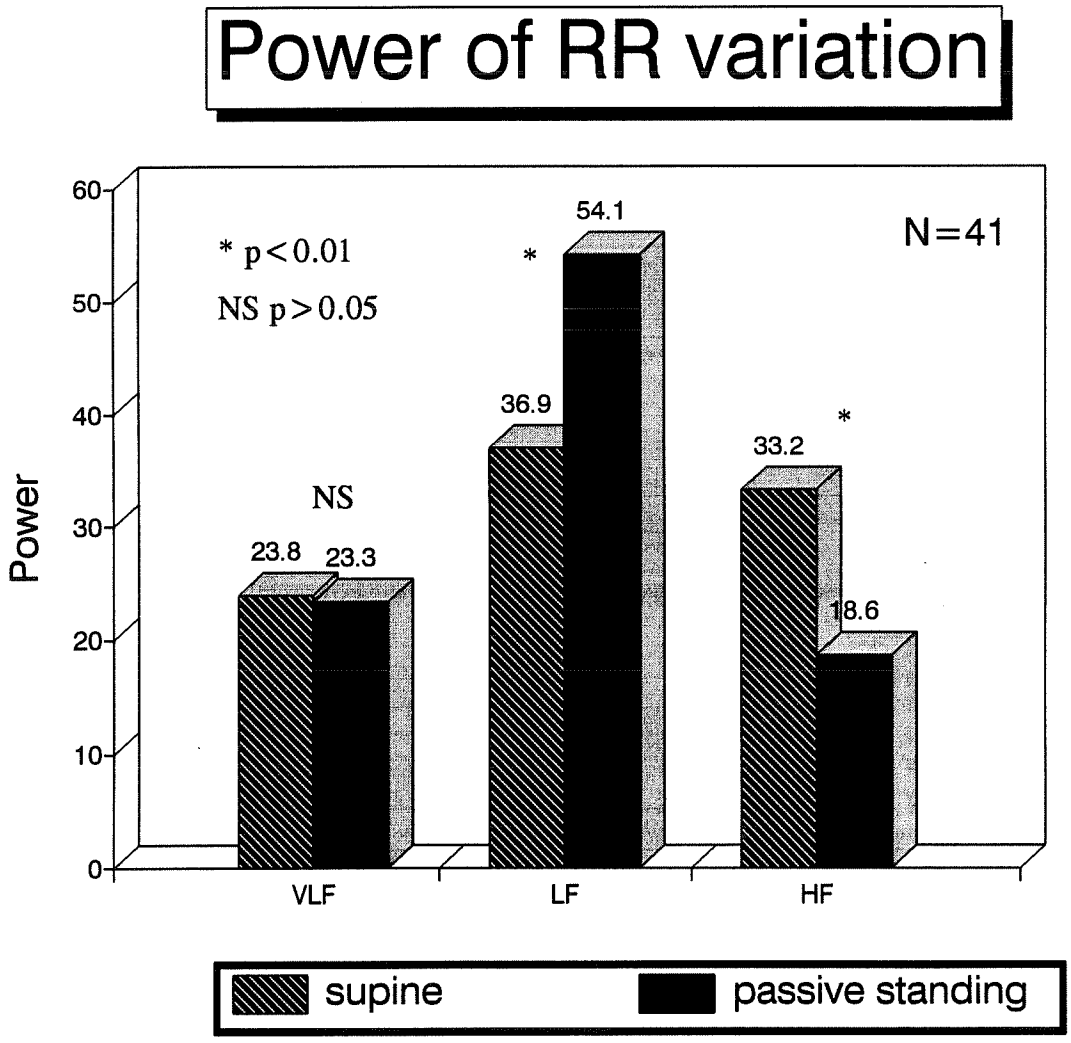

Figure 3.10 Comparison of RR power in VLF, LF and HF bands between supine phase a) and passive tilt phase b) in protocols I, II and III.

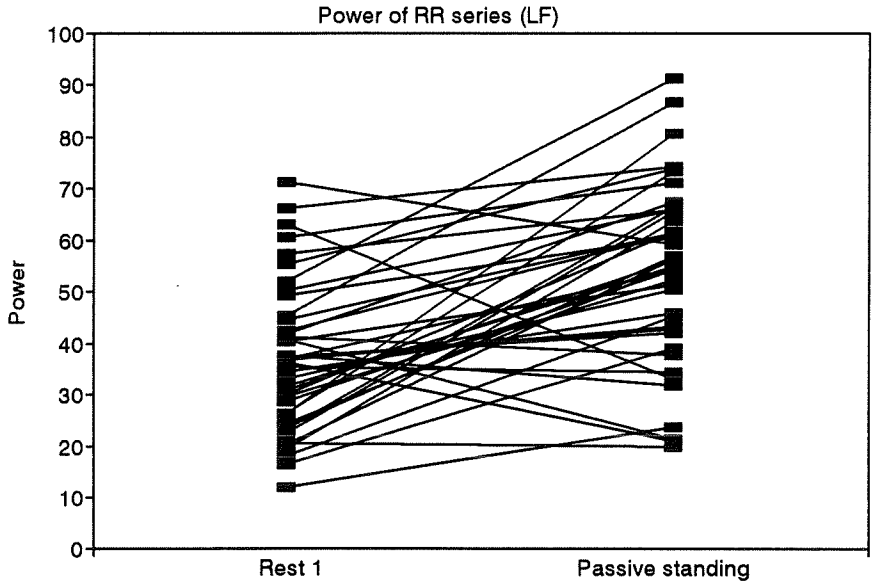

(a)

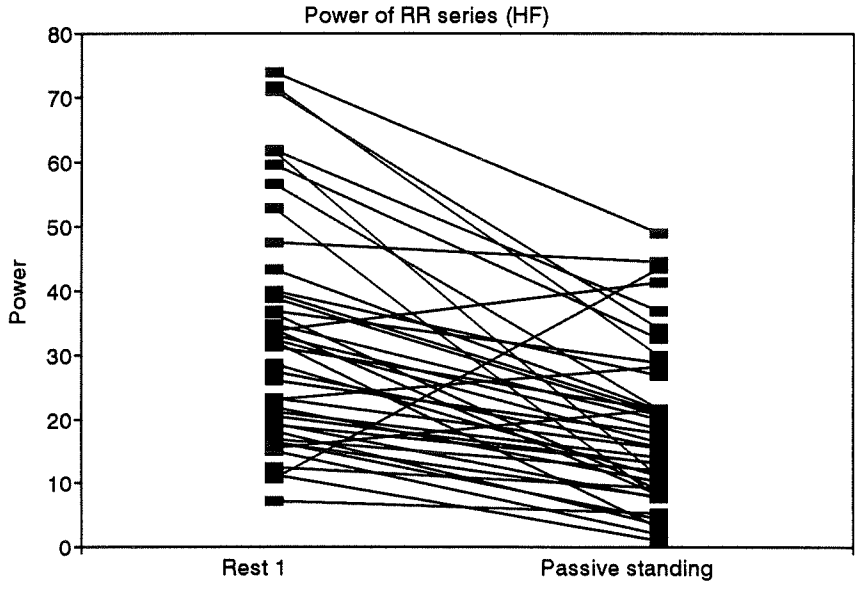

(b)

Figure 3.11 Changes of LF and HF power of RR in each normal subject in response to change in position from supine to tilt.

a) changes of LF power

b) changes of HF power

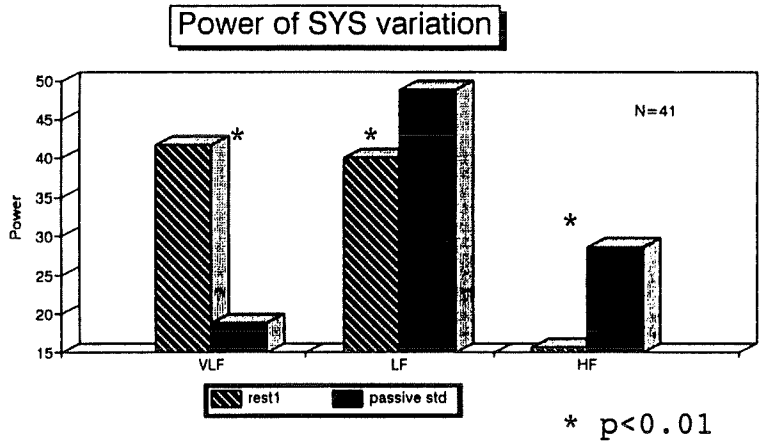

(a)

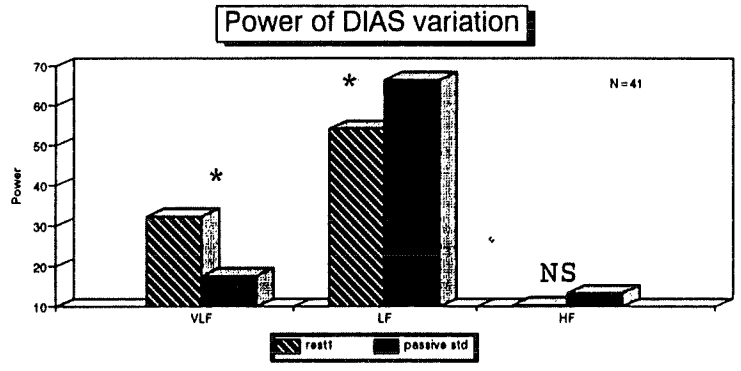

(b)

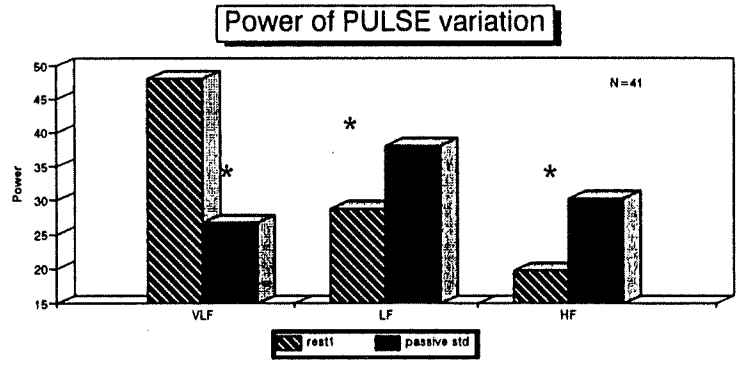

(c)

Figure 3.12 Spectral power of blood pressures at both rest phase a) and tilt phase b) in protocols I, II and III.
a) systolic pressure, b) diastolic pressure and c) pulse pressure

Although important inter-subject variation exists, we can see that most subjects had an increased LF power and a decreased HF power from supine rest to head-up tilt position. This is in accord with the common and global interpretation of power spectra: stimulation of the sympathetic system and withdrawal of parasympathetic system when changing from supine to upright position.

Figures 3.12a-c show the changes of mean power of blood pressures in three frequency bands from supine to passive head-up tilt. The LF powers of systolic (40.1 vs 48.9, $p=0.005$), diastolic (54.1 vs 66.5, $p=0.0004$) and pulse (28.8 vs 38.0, $p=0.001$) pressures increased. HF powers in both systolic (15.6 vs 28.7) and pulse pressures (19.8 vs 30.3) increased ($p<0.005$) while HF in diastolic (10.3 vs 13.3, $p=0.173$) did not change significantly. All VLF power in the blood pressures decreased significantly (SYS: 41.8 vs 18.9; DIAS: 32.3 vs 17.6; PULSE: 48.0 vs 26.1, $p<0.0001$). The LF/HF ratios for the pressures did not change significantly (SYS: 5.6 vs 3.4, $p=0.054$; DIAS: 12.2 vs 12.1, $p=0.9$; PULSE: 3.2 vs 2.4, $p=0.22$) due to the large inter-subject variability.

With the normalized power spectra, we can compare the distribution of energy in each of the three bands between different cardiovascular variables, RR and SYS for example. At rest, VLF relative energy is less important in RR than in SYS (23.8 ± 2.1 vs 41.8 ± 2.6, $p<0.0001$), while the relative energy in HF band is more important in RR than in SYS (33.2 ± 2.8 vs 15.6 ± 2.1, $p<0.0001$), the LF energy in both RR and SYS is not significantly different ($p=0.08$). In passive tilt VLF relative power was more important in RR than in SYS (23.3 ± 2.3 vs 18.9 ± 1.7, $p=0.045$), while the HF energy in SYS is 10.08 units more than that in RR ($p<0.0001$). Similar to rest, the proportion of LF energy in both signals is not statistically different

(p=0.051).

3.2.1.3 Passive standing vs Active standing:

Only twenty seven volunteers (21 males, 6 females) who participated in protocol II an III were recorded under the active standing condition, i.e. phase c and d. Compared to passive tilt (Table 3.6), the subjects breathed faster (Respiratory frequency RF of 0.28 Hz vs 0.23 Hz, p=0.04). The averages of cardiovascular variables were similar in both postures ($p > 0.2$), but the variation of RR interval were significantly larger in passive tilt (SD of 46 vs 39, $p < 0.05$). The variations of blood pressures in the HF respiration related frequency band were higher in the passive tilt (SYS: 28.7 vs 19.8, p=0.02; DIAS: 13.3 vs 8.4, p=0.038; PULSE: 30.3 vs 20.1, p=0.007). HF fluctuation in RR intervals was more important in passive tilt, but this difference did not reach statistical significance (p=0.06).

Table 3.6 Comparison of passive standing with active standing

	active std	passive std	difference	P values
no. of case	27	41		
RF	0.28 Hz	0.23 Hz	-0.05	0.04
RR (ms)	722±16	728±14	+7	0.7
SD (ms)	39±2	46±3	+07	0.05
VLF	26.2±2.9	23.3±2.3	-3	0.44
LF	55.7±3.0	54.1±2.7	-1	0.71
HF	13.5±1.8	18.6±2.0	+5	0.06
SYS (mmHg)	120±3	117±3	-3	0.46
SD (mmHg)	6±0.4	6±0.4	0	0.60
VLF	22.4±2.1	18.9±1.7	-4	0.2
LF	53.7±2.8	48.9±2.6	-4	0.211
HF	19.8±2.8	28.7±2.6	+9	0.02
DIAS (mmHg)	72±2	69±1	-3	0.27
SD (mmHg)	3±0.18	3±0.2	0	0.63
VLF	16.4±1.5	17.6±1.8	+1	0.61
LF	72.0±2.2	66.5±2.3	-5	0.08
HF	8.4±1.4	13.3±1.8	+5	0.038
PULSE (mmHg)	48±2	48±2	0	0.89
SD (mmHg)	5±0.3	5±0.3	0	0.96
VLF	30.8±2.8	26.7±2.2	-4	0.25
LF	43.5±2.6	38.0±2.4	-5	0.12
HF	20.1±2.3	30.3±2.8	+10	0.007

***Values are mean ± standard error.**

****differences are significant when p< =0.05.**

3.2.2 Hypertensive patients

Subjects and protocol

Fourteen patients (10 men and 4 women, age: 40-65 years old) with borderline arterial hypertension (diastolic arterial blood pressure between 90 and 115 mmHg at rest after at least 2 weeks of placebo) were studied. They had been recently diagnosed or had not been treated with an antihypertensive agent since at least two months. Patients all had a normal renal function (plasma creatinine $\leq$ 150 μmole/l, absent of proteinury). They had all signed a written consent.

The study included a) a 20 minutes rest on a tilt table, b) a 5 minutes isometric exercise (handgrip) with 30% of their maximal force, c) followed by another 20 minutes rest period and d) finally a 15 minutes orthostasis (active standing). Signals of 10 minutes duration were recorded and analyzed in both phases a) and d). Blood was sampled for measurement of catecholamine (NE and E) at the end of each phase. ECG lead II, arterial blood pressures with FINAPRES and respiration were recorded. The protocol was conducted in the ANSL.

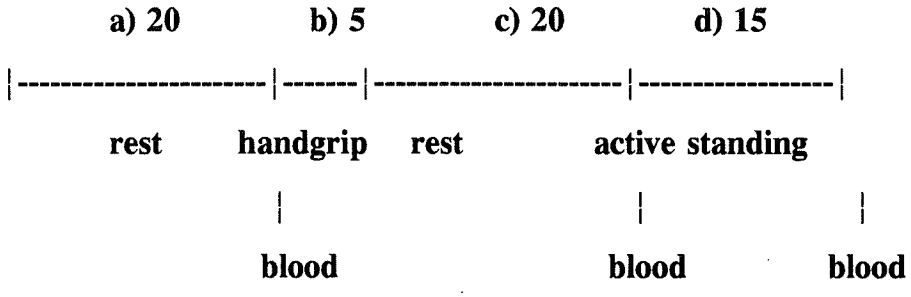

RESULTS

Rest:

Compared to the normal group at rest (Table 3.7), the hypertension group had an average lower breath rate than the normal group (13 breath/min vs 14 breaths/min, $p=0.057$ (not shown)) in supine position. This might be due to the higher mean age of the hypertension group. The hypertension group had a longer mean RR interval (962 ms vs 921 ms, $p<0.01$), but a smaller standard deviation of RR interval (46 ms vs 52 ms), i.e., the hypertension group had a smaller mean total energy in heart rate variation, even though those differences did not reach statistical significance ($p>0.4$). The spectral power of RR (ref Fig. 3.13a) variation in the LF band was not distinguishable between the two groups (34.9 vs 36.9, $p>0.6$). The VLF power was much higher (43.3 vs 23.8, $p<0.001$) while the HF power was smaller (19.6 vs 33.2, $p=0.002$) in the hypertension group.

In addition to a significantly higher systolic blood pressure in the hypertension group (166 mmHg vs 123 mmHg, $p<0.0001$), the variability of systolic pressure was also more important (SD=7 vs 5 mmHg, $p=0.017$). The comparison of spectral parameters in systolic pressure (ref. Fig. 3.14a) was in the same direction as RR. The VLF power was larger (55.2 vs 41.8, $p=0.021$) and the HF power was smaller (8.1 vs 15.6, $p=0.006$) in the hypertension group, but the LF power in both groups were not significantly different (35.6 vs 40.1).

The diastolic pressures was 25 mmHg higher (89 vs 64 mmHg,$p<0.01$) in the hypertension group. The diastolic pressure variation was also more than double

Table 3.7 Comparison between hypertension and normal groups

	Hypertension		Normal	
	Rest	**Active standing**	**Rest**	**Active standing**
	(N=14)	(N=14)	(N=41)	(N=27)
RR (ms)	*962±54	794±48	921±18	722±16
SD (ms)	46±6	47±10	52±2	39±2
VLF	*43.3±4.7	**34.5±4.8	23.8±2.1	26.2±2.9
LF	34.9±2.9	50.0±4.5	36.9±2.3	55.7±3.0
HF	*19.6±2.9	12.7±3.0	33.2±2.8	13.5±1.8
SYS (mmHg)	*166±5	**172±7	123±3	120±3
SD (mmHg)	*7±0.8	**10±1	5±0.4	6±0.4
VLF	*55.2±4.7	**25.0±4.2	41.8±2.6	22.4±2.1
LF	35.6±3.5	**60.4±4.6	40.1±2.1	53.7±2.8
HF	*8.1±1.5	**12.8±2.3	15.6±2.1	19.8±2.1
DIAS (mmHg)	*89±2	**98±4	64±2	72±2
SD (mmHg)	*5±0.6	**5±0.7	2±0.12	3±0.18
VLF	*51.3±5.1	**29.9±4.4	32.3±2.8	16.4±1.5
LF	*38.1±4.4	59.9±4.3	54.1±2.6	72.0±2.2
HF	8.7±2.7	8.3±1.4	10.3±1.6	8.4±1.4
PULSE (mmHg)	*77±4	**74±5	58±2	48±2
SD (mmHg)	5±0.4	**6±0.6	5±0.3	5±0.3
VLF	55.4±4.5	**21.2±3.5	48.0±3.0	30.8±2.8
LF	27.6±2.7	**53.0±4.7	28.8±2.2	43.5±2.6
HF	14.6±2.9	21.4±2.6	19.8±2.6	20.1±2.3

Values are mean ± standard error.

***Values are significantly different from normal at rest.**

****Values are significantly different from normal at active standing.**

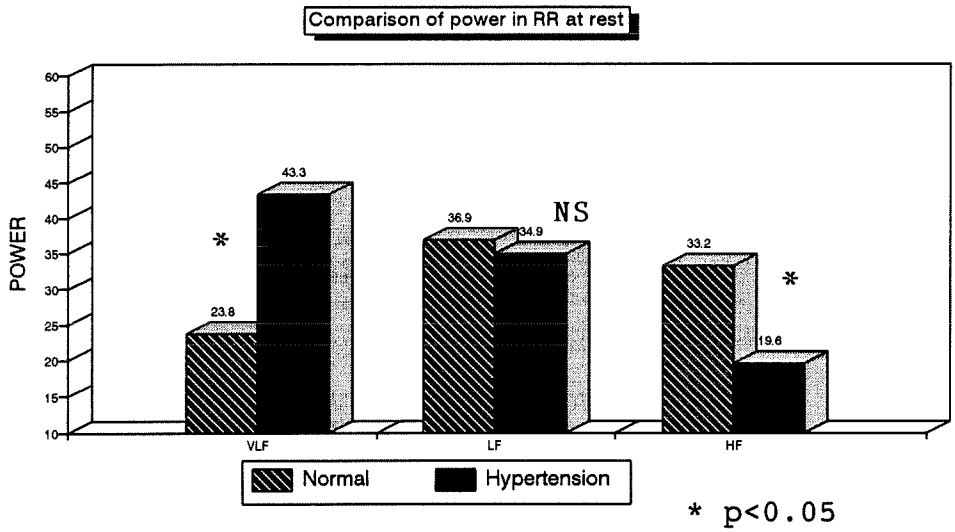

(a)

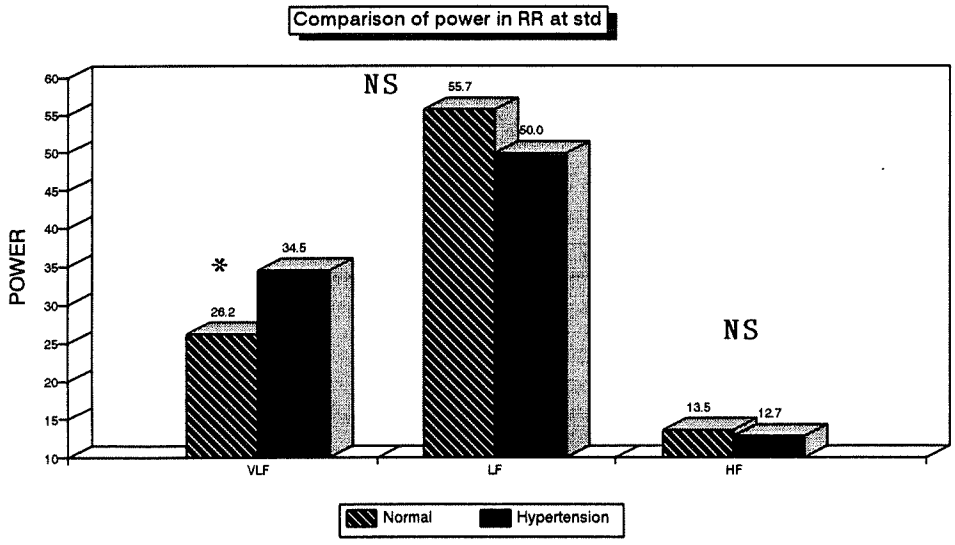

(b)

Figure 3.13 RR power comparison between normal and hypertensive groups.

(a) supine, (b) active standing

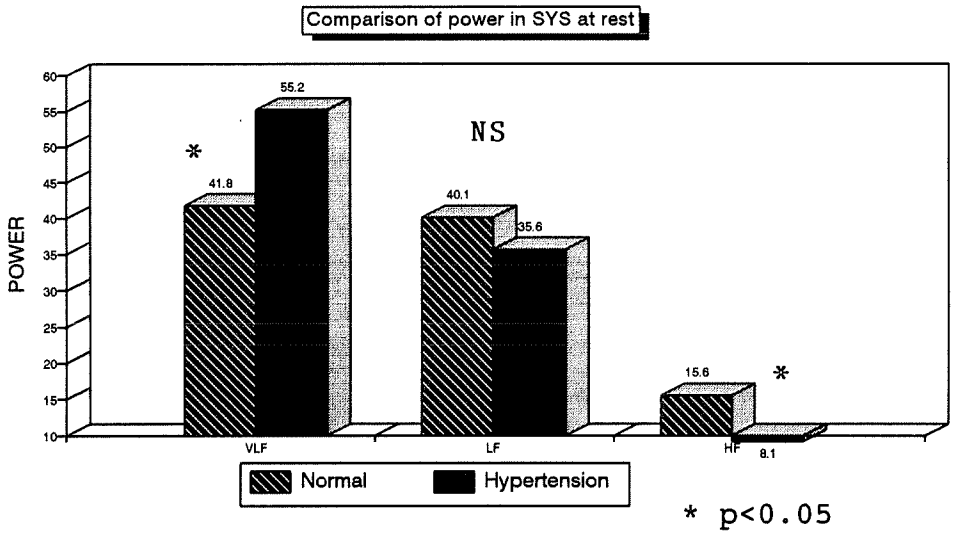

(a)

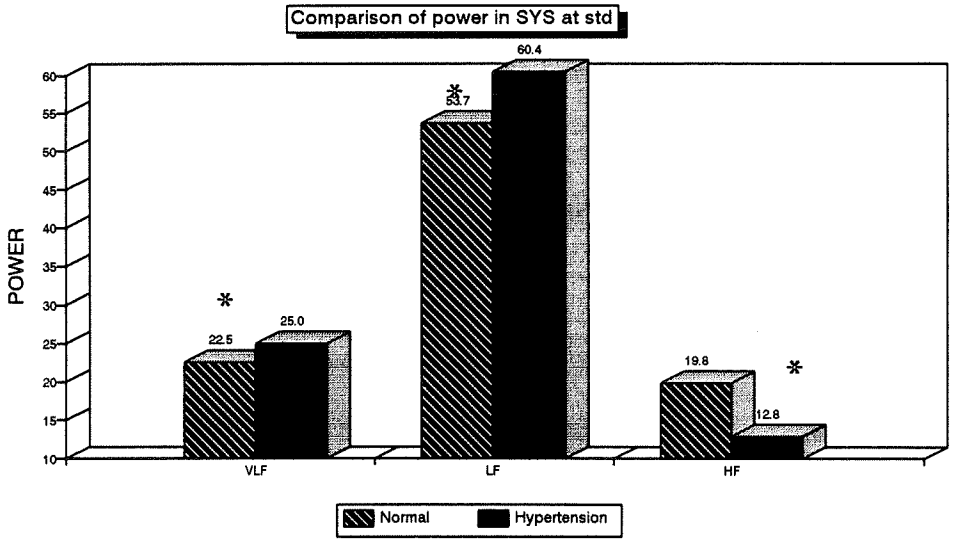

(b)

Figure 3.14 SYS power comparison between normal and hypertensive groups.
(a) supine, (b) active standing

(SD = 5 mmHg vs 2 mmHg, $p<0.01$) than in the normal group. There was no statistical difference in HF powers between two groups (8.7 vs 10.3), while the variation of the diastolic pressure in the VLF band was larger (55.3 vs 32.3, $p=0.004$) and the variation in the LF band was smaller (38.1 vs 54.1, $p=0.005$) in the hypertension group.

The mean pulse pressure was higher in the hypertension group (77 mmHg vs 58 mmHg, $p<0.0001$), but their standard deviations and spectral powers in each of the three bands were not statistically different.

Correlations of spectral powers with respiratory frequency and with mean RR interval at supine rest are given in Tables 3.8 and 3.9 (ref Tables 3.3, 3.4 in normal group). The correlation between HF power in RR with RF is stronger in hypertension group than in normal group (-0.557 vs -0.43). None of the spectral parameters is correlated with the rest mean RR interval in the hypertension group.

Standing:

Comparison of the response to active standing between the normal and the hypertensive is also presented in Table 3.7. Both groups (normal and hypertension) breathed at the same mean rate, 0.23 Hz, at standing (not shown in Table 3.7). The two groups had a similar heart rate at standing (RR = 794 ms vs 722 ms). Comparing powers of RR in different bands with normal group at tilt, only the VLF power was statistically different, which was higher in the hypertension group (34.5 ± 4.8 vs 26.3 ± 2.9, $p=0.04$) (ref Fig. 3.13b and 3.14b)

The blood pressures between the two groups were quite different at standing.

Of course, they were all higher in the hypertension group ($p<0.0001$) and their variations (SD) were also more important in the hypertension group ($p<0.05$). The HF power in systolic blood pressure variability was lower in the hypertension group (12.8 vs 19.8, $p<0.04$). The LF powers in SYS and PULSE were higher in the hypertension (SYS: 60.4 vs 53.7, PULSE: 53.0 vs 43.5, $p<0.05$) but the LF power in DIAS was not significantly different. The VLF power in both SYS and DIAS were higher in the hypertension group (25.0 vs 22.4; 29.9 vs 16.4, $p<0.05$). The VLF power in PULSE was higher in the normal group (30.8 vs 21.2, $p<0.05$).

Reaction to active standing:

Table 3.10 summarizes the tilt response of hypertensive patients. The mean of the RR decreased significantly compared to values at rest in both groups ($p<0.001$), but this decrease was more important in normal subjects (199 ms vs 168 ms ref. Table 3.7) even though this difference did not reach statistical significance ($p=0.2$). The SD of RR was relatively unchanged ($p>0.9$) in hypertension, but it decreased significantly (from 52 ms to 39 ms, $p<0.05$) in the normal group. The spectral power responses to posture change was in the same direction for both normal and hypertension groups. In response to active standing, the VLF power in RR did not change significantly, LF power increased from 34.9 to 50.0 ($p=0.006$) while the HF power decreased from 20.0 to 12.7 ($p=0.015$). The increase of LF power in RR was more important in the normal group than in the hypertension group (18.75 vs 15, $p<0.05$). The decrease of HF in RR was also more important in the normal group than in the hypertension group (19.7 vs 6.89, $p=0.02$).

The response of systolic pressure to tilt in the hypertension group was different

Table 3.8 Correlation of power spectra with respiration frequency in hypertension
(N=14)

	VLF	LF	HF
RR	0.391 p=0.167	-0.140 p=0.63	-0.557 p=0.04
SYS	-0.066 p=0.82	-0.066 p=0.823	0.246 p=0.41
DIAS	-0.011 p=0.87	-0.19 p=0.52	0.208 p=0.47
PULSE	-0.322 p=0.26	-0.175 p=0.55	0.557 p=0.039

Table 3.9 Correlation of power spectra with mean RR interval in hypertension
(N=14)

	VLF	LF	HF
RR	0.099 p=0.74	-0.433 p=0.12	0.30 p=0.29
SYS	0.29 p=0.320	-0.25 p=0.38	-0.302 p=0.294
DIAS	0.161 p=0.58	-0.076 p=0.80	-0.174 0.522
PULSE	0.405 p=0.15	-0.47 p=0.091	-0.17 p=0.05

from that in the normal group ($p=0.02$). The systolic pressure decreased 6 mmHg on tilt in the normal group, but it increased 3 mmHg in the hypertension group. The spectral power changes in response to active standing were in the same direction as in the normal group, but were quantitatively different. In response to active standing, VLF powers in all three pressure variables decreased ($p<0.002$) and LF power increased ($p<0.001$) significantly. There were no significant changes of the HF powers in blood pressure time series, while the HF powers of SYS and PULSE decreased significantly in the normal group in response to the head-up tilt. In SYS, the LF power increased more in hypertension (24.8 vs 13.6, $p=0.02$); in PULSE, VLF decreased more in hypertension (34.2 vs 17.2, $p<0.05$) and LF increased more in hypertension (25.4 vs 17.2, $p<0.05$). Other spectral parameter changes in response to standing were not significantly different between the two groups.

Relationship between RR variations and rest diastolic blood pressure:

To verify whether autonomic activity might be progressively altered with increasing severity of hypertension, we assessed the relationship between the resting diastolic blood pressure and the spectral powers of RR in the three bands. A significant positive correlation between VLF power in RR and resting diastolic blood pressure ($r=0.76$, $p<0.05$) and a negative correlation between the LF power and resting diastolic blood pressure ($r=-0.5$, $p<0.05$) were found in the hypertension group at the supine rest position (ref. Fig. 3.15), but no correlation was found between the HF power of RR and the resting diastolic blood pressure.

Table 3.10 Effects of standing in 14 hypertension patients

	Rest	Tilt	Mean difference	P values
RR (ms)	962±54	794±48	-168	<0.00001
SD (ms)	46±6	47±10	+1	0.919
VLF	43.3±4.7	34.5±4.8	-8.8	0.100
LF	34.9±2.9	50.0±4.5	+15.1	0.006
HF	19.6±2.9	12.7±3.0	-6.9	0.015
SYS (mmHg)	166±5	172±7	+6	0.315
SD (mmHg)	7±0.8	10±1	+3	0.097
VLF	55.2±4.7	25.0±4.2	-30.2	<0.00001
LF	35.6±3.5	60.4±4.6	+24.8	0.001
HF	8.1±1.5	12.8±2.3	+4.7	0.084
DIAS (mmHg)	89±2	98±4	+9	0.006
SD (mmHg)	5±0.6	5±0.7	-0.6	0.493
VLF	51.3±5.1	29.9±4.4	-21.4	0.002
LF	38.1±4.4	59.9±4.3	+21.8	0.003
HF	8.7±2.7	8.3±1.4	-0.4	0.903
PULSE (mmHg)	77±4	74±5	-3	0.362
SD (mmHg)	5±0.4	6±0.6	+1	0.034
VLF	55.4±4.5	21.2±3.5	-34.2	<0.00001
LF	27.6±2.7	53.0±4.7	+25.4	<0.00001
HF	14.6±2.9	21.4±2.6	+6.8	0.118

***Values are mean ± standard error.**

****differences are significant when p<=0.05.**

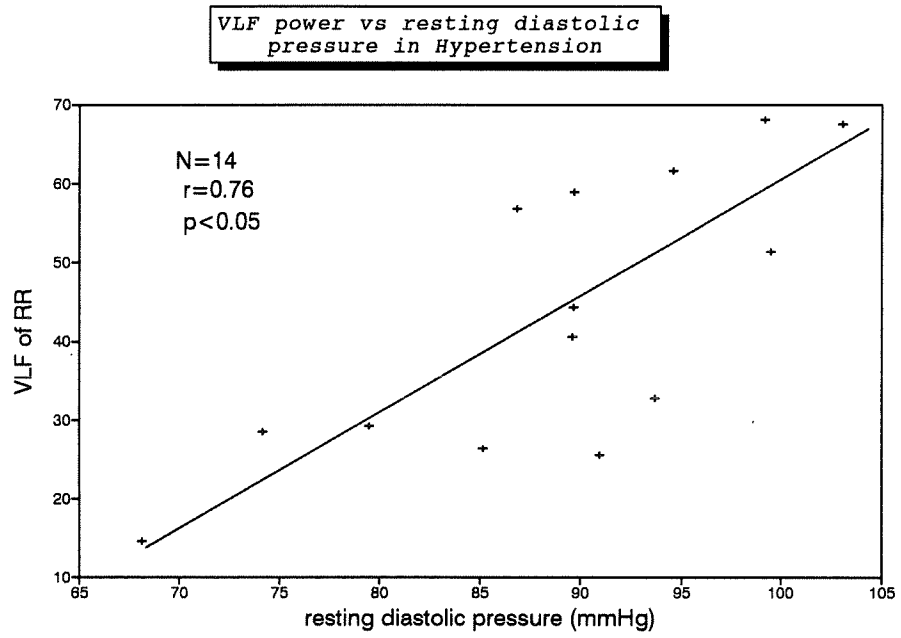

(a)

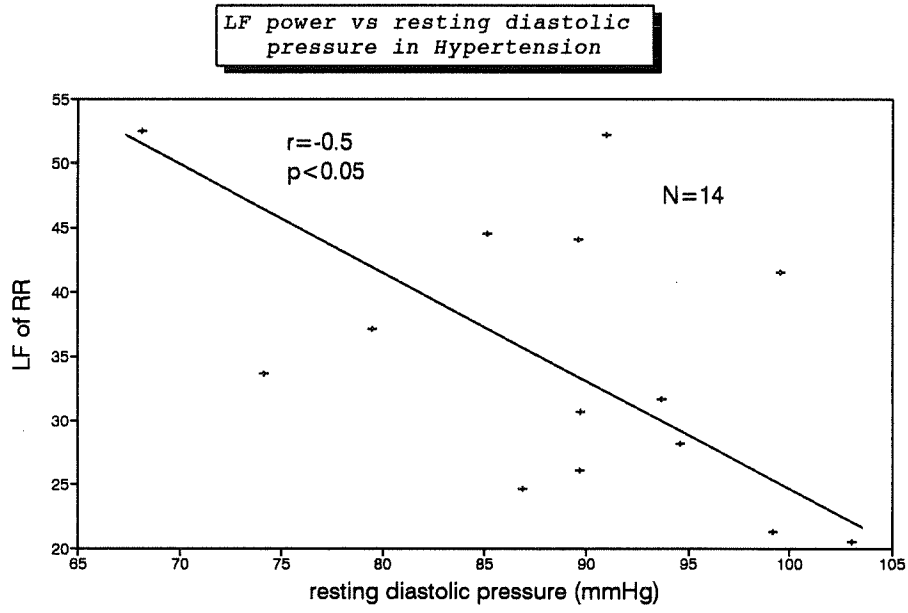

(b)

Figure 3.15 Correlation of spectral power in RR with resting diastolic pressure. a) VLF power and b) LF power.

3.2.3 Syncope patients

Syncope is defined as a transient loss of consciousness with spontaneous recovery. It may occur in as much as 30% of the general adult population [75]. Usually syncope occurs due to position change, exercise, emotional stress, after meals, or when one sees his or her own blood. Syncope results from a diversity of disorders from benign ones to those associated with mortality [76]. The cause of syncope remains unclear in many patients. In neurally mediated syncope, response to orthostasis is characterised by a rapid onset of bradycardia and hypotension. Reaction to orthostasis resembles the response to severe haemorrhage by a fast displacement of blood with consequent rapid decrease of venous return. Neurohumoral systems act to attempt to preserve cardiac output. Head-up tilt has been used to stimulate vasovagal reactions in adult subjects with unexplained syncope.

Subjects and protocol:

Twenty four patients (18 men and 6 women, age: 20-55) with recurrent unexplained reported syncope were included in this study. A series of clinical evaluations including physical and biochemical examinations, neurologic evaluation, electrophysiologic study and electrocardiography did not identify the origin of the syncope. The study included a 20 minutes rest on a tilt table followed by a tilt head-up from 15 minutes to 40 minutes. The analysis was limited to the recording of the last 10 minutes of the rest and 10 minutes during tilt without occurring of syncope. Patients were allowed to breath spontaneously. Again, ECG lead II, arterial blood pressures with FINAPRES and respiration were recorded. The protocol was conducted in the ANSL.

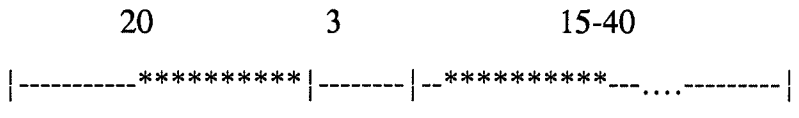

********** = 10 minutes and signals are recorded in these periods

Some patients developed syncope 6 to 20 minutes after tilt head-up, while others passed the whole tilt duration without fainting. The protocol was interrupted if patient developed syncope. For the analysis, we did not distinguish between patients who developed or did not develop syncope during the protocol. The first 3 minutes immediately after tilt were excluded from analysis because of the stationarity requirement.

Syncope occurred in some patients during tilt head up test between 6 to 20 minutes after the onset of the passive tilt. Fig. 3.16 shows a typical development of syncope in a patient. The syncope with bradycardia and hypotension occurred. We can see in this patient the syncope started by a simultaneous decline of both systolic and diastolic blood pressures followed by a marked drop in heart rate (from 540 ms to 1020 ms in this case) and a further fall in blood pressures. The RR interval reached its maximum almost at the same time as the blood pressures reached their minimum. The fall of arterial pressure is due to the drop of the peripheral resistance and cardiac output. Some investigators have observed also that the fall in stroke volume, cardiac output and arterial pressure usually precedes the bradycardia [56].

Because of stationarity requirement, analyses were not conducted in the period

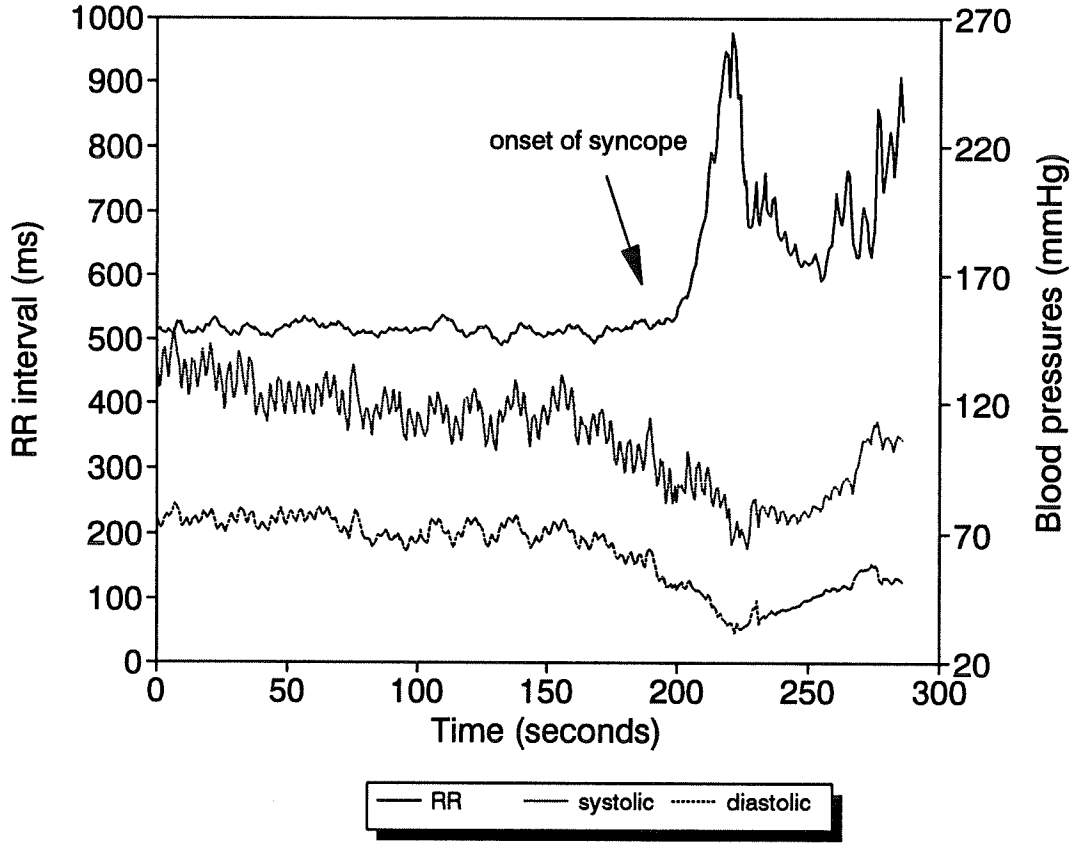

Figure 3.16 Signals of RR interval, systolic and diastolic pressures at head-up tilt in a syncope patient. Time 0 is not the onset of the test.

close to or during syncope, since the vasovagal response produces a highly non-stationary and complex process where many systems may be involved.

Results

The statistical parameters (mean and SD) of each variable and the spectral parameters will be compared with the normal group first at rest, secondly, during head-up tilt and thirdly the responses to tilt will be compared.

Rest:

Comparison of cardiovascular parameters between the normal and syncope groups during rest are given in Table 3.11. RR intervals of both groups are not different statistically, the systolic, diastolic and pulse blood pressures are higher in the syncope group ($p<0.05$). Three visible peaks were present in all the spectra of the analyzed variables (RR, SYS, DIAS and PULSE), and were similar to what was observed in the normal group. The spectral power in VLF fluctuation in RR interval was higher in the syncope group ($p=0.011$) while the respiration related HF variations in RR were more important in the normal group ($p=0.019$) (Fig. 3.17a and 3.18a). Other spectral parameters were not significantly different.

Correlations between spectral parameters with the respiratory frequency and the mean RR interval were also calculated in syncope (ref. Tables 3.12 and 3.13) in order to compare with the normal group. Similar to the normal group, the fluctuations of the RR interval and systolic pressure in respiration frequency (HF) are correlated negatively with the respiration frequency (RR: $r=-0.71$, $p<0.05$; SYS: $r=-0.46$, $p<0.05$) in syncope (ref. Figure 3.19), but these correlations are higher

Table 3.11 Comparison between syncope and normal groups

	Syncope(N=24)		Normal(N=41)	
	Rest	**Tilt**	**Rest**	**Tilt**
RR (ms)	927±37	745±24	921+18	728+14
SD (ms)	54±5	48±6	52+2	46+3
VLF	*34.8±4.2	29.0±3.5	23.8+2.1	23.3+2.3
LF	39.0±3.1	53.4±3.5	36.9+2.3	54.1+2.7
HF	*22.5±3.0	15.0±2.4	33.2+2.8	18.6+2.0
SYS (mmHg)	*132±5	**132±6	123+3	117+3
SD (mmHg)	6±0.5	**10±1.2	5+0.4	6+0.4
VLF	43.1±4.7	20.6±2.6	41.8+2.6	18.9+1.7
LF	42.1±4.5	**58.5±3.0	40.1+2.1	48.9+2.6
HF	12.7±2.2	**18.9±1.9	15.6+2.1	28.7+2.6
DIAS (mmHg)	*69±3	**77±4	64+2	69+1
SD (mmHg)	*4±0.34	**5±0.5	2+0.12	3+0.2
VLF	39.0±5.5	20.8±2.5	32.3+2.8	17.6+1.8
LF	49.5±4.6	65.7±2.8	54.1+2.6	66.5+2.3
HF	8.7±1.2	11.8±1.6	10.3+1.6	13.3+1.8
PULSE (mmHg)	*64±3	**55±4	58+2	48+2
SD (mmHg)	4±0.4	6±0.9	5+0.3	5+0.3
VLF	42.3±4.6	24.7±3.6	48.0+3.0	26.7+2.2
LF	34.3±3.9	44.2±3.7	28.8+2.2	38.0+2.4
HF	19.1±3.3	27.0±3.1	19.8+2.6	30.3+2.8

Values are mean ± standard error.

***Values are significantly different from normal at rest.**

****Values are significantly different from normal at tilt.**

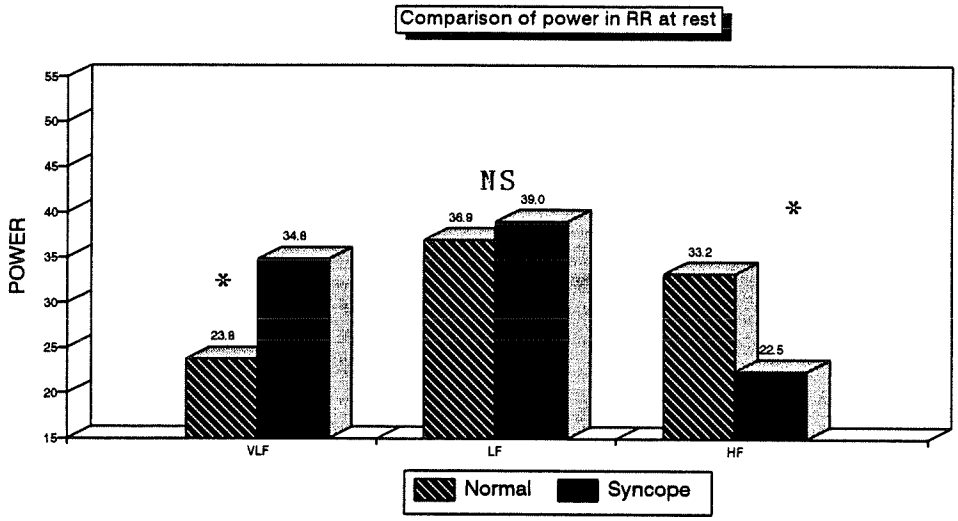

(a)

* p<0.05
NS P>0.05

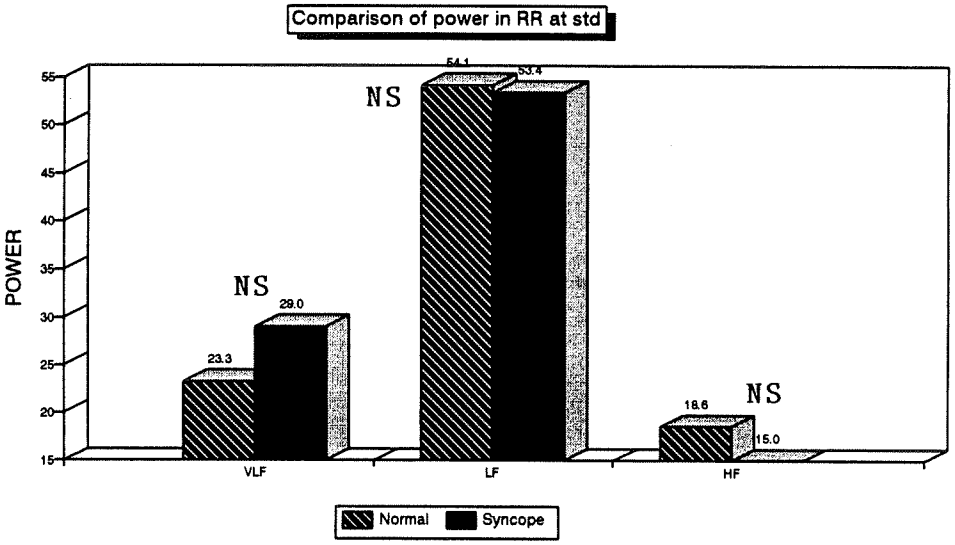

(b)

Figure 3.17 RR power comparison between normal and syncope groups.
(a) supine rest, (b) tilt

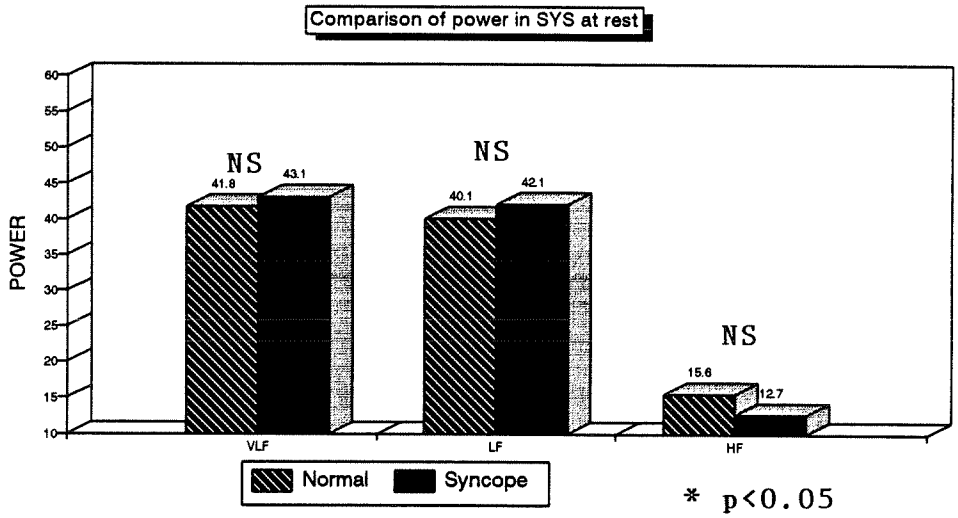

(a)

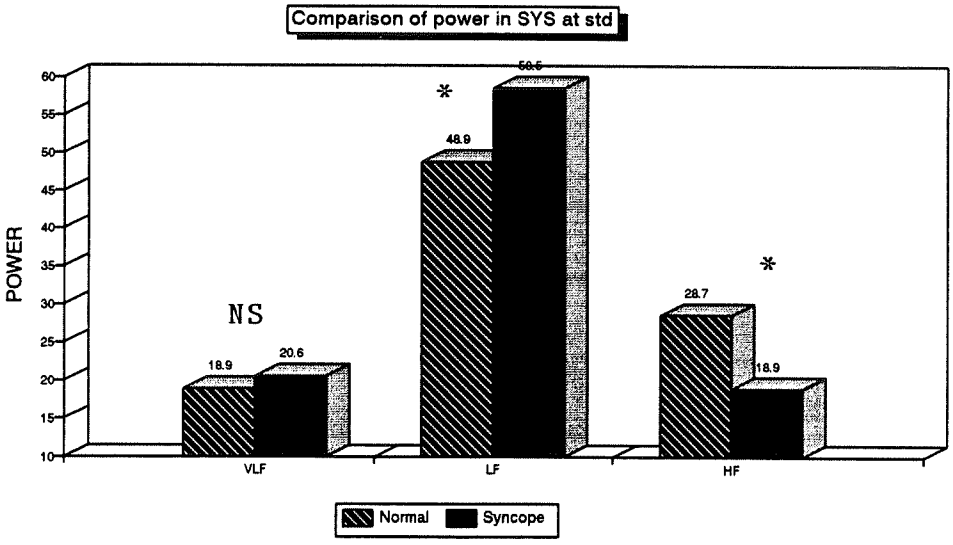

(b)

Figure 3.18 SYS power comparison between normal and syncope groups.
(a) supine rest, (b) tilt

Table 3.12 Correlation of power spectra with respiration frequency in syncope
(N=24)

	VLF	LF	HF
RR	0.38 p=0.065	0.156 p=0.466	-0.712 p=0.0001
SYS	-0.39 p=0.06	0.37 p=0.075	-0.46 p=0.024
DIAS	-0.462 p=0.023	0.508 p=0.011	-0.37 p=0.076
PULSE	-0.304 p=0.14	0.133 p=0.537	0.148 p=0.49

Table 3.13 Correlation of power spectra with mean RR interval in syncope
(N=24)

	VLF	LF	HF
RR	0.33 p=0.18	0.053 p=0.81	0.437 p=0.033
SYS	0.49 p=0.014	-0.363 p=0.08	-0.234 p=0.27
DIAS	0.46 p=0.023	-0.39 p=0.05	-0.134 0.53
PULSE	0.342 p=0.101	-0.125 p=0.56	-0.223 p=0.29

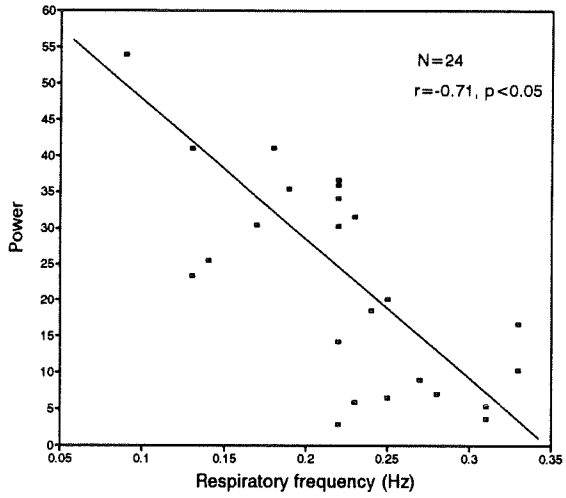

(a)

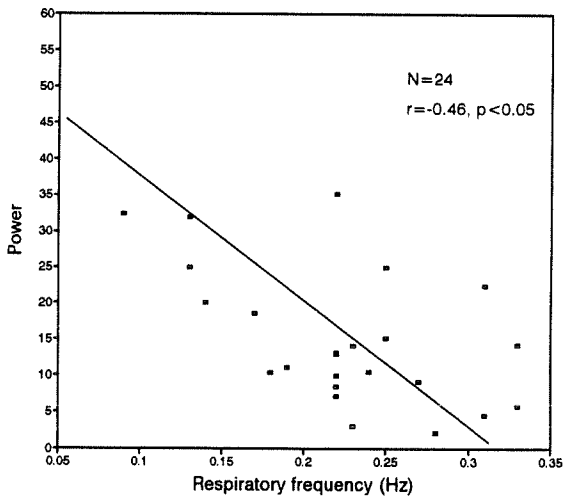

(b)

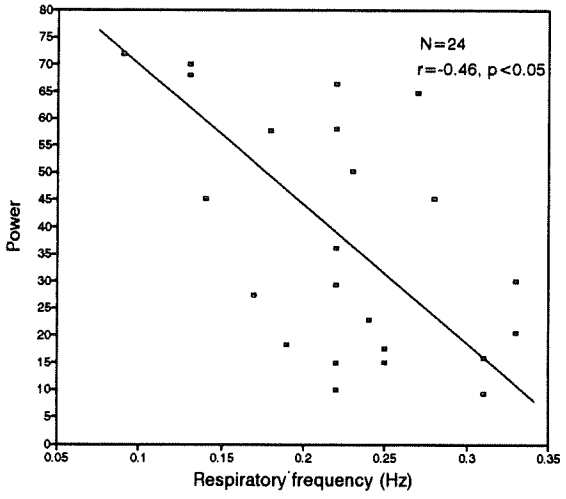

(c)

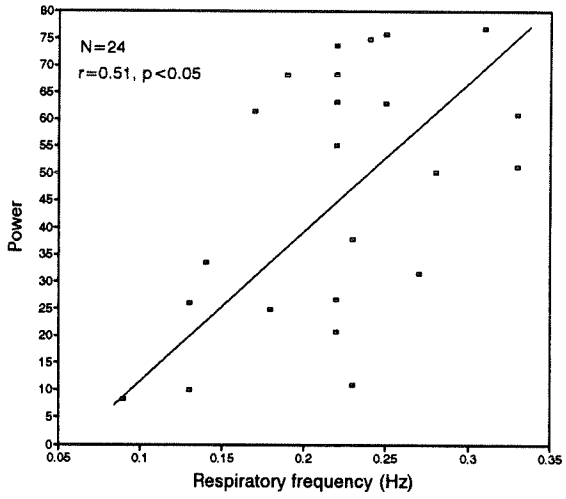

(d)

Figure 3.19 Correlations between spectral parameters and respiratory frequency in syncope group in supine position.
a) HF of RR, b) HF of SYS, c) VLF of DIAS, d) LF of DIAS

in the syncope group (RR: r=-0.71 vs r=-0.43; SYS: r=-0.46 vs r=-0.36, ref. Figures 3.19 and 3.4). The VLF power in DIAS is negatively correlated with RF (r=-0.46, p=0.020) while LF power in DIAS is positively correlated with RF (r=0.508, p=0.011). These correlations do not exist in the normal group. Similar to the normal group, the VLF and LF powers in DIAS are correlated with the mean RR interval (r=0.46, p=0.023; r=-0.39, p=0.05 respectively, ref. Table 3.13 and Fig. 3.20).

Tilt:

Mean RR intervals and RR spectral parameters were not significantly different between the group of syncope and the group of normal volunteers during tilt position. The blood pressures values were higher in the syncope group (SYS: 132 vs 117 mmHg, DIAS: 77 vs 69 mmHg, PULSE: 55 vs 48 mmHg, $p<0.05$). The spectral parameters of pressure variables were not statistically different between the normal and syncope groups during head-up tilt except the LF and HF powers in systolic pressure time series (LF: 48.851 vs 58.531, p=0.021; HF: 28.655 vs 18.871, p=0.011) (ref. Fig. 3.17b and 3.18b).

Reaction to tilt:

The responses to head-up tilt for the syncope group is summarized in Table 3.14. Similar to the normal group, RR intervals decreased significantly (745 ms vs 927 ms, $p<0.0001$) in response to tilt; the spectral power of RR in the VLF decreased but not significantly (from 34.8 to 29.0, p=0.25); the LF power of RR increased (from 39.0 to 53.4, p=0.007); the HF power dropped in response to tilt, but the drop did not reach statistical significance (from 22.7 to 15.0, p=0.063), while this drop was significant (33.2 to 18.6, $p<0.001$) in normal group (Table 3.5).

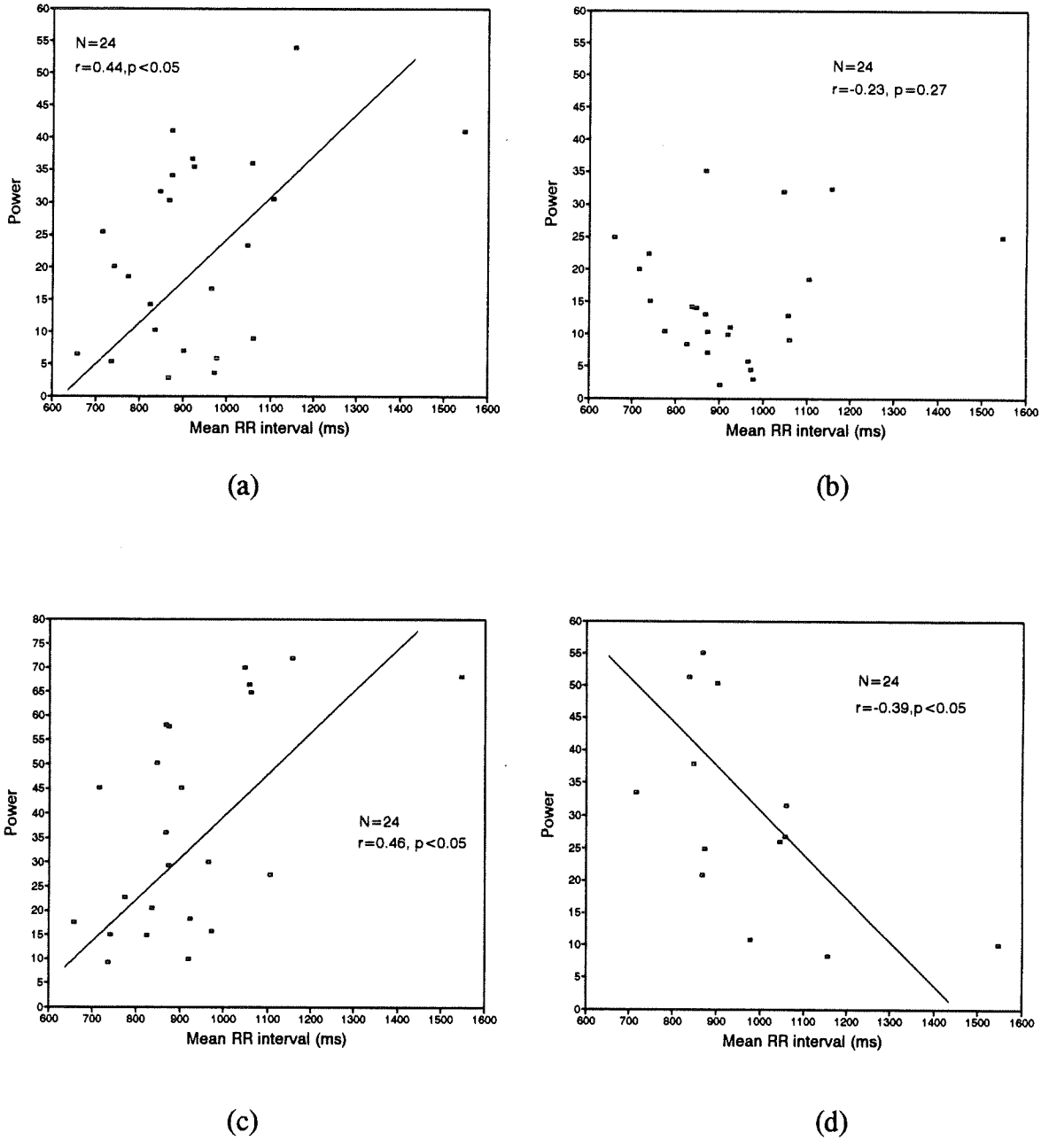

Figure 3.20 Correlation between spectral parameters and mean RR interval in syncope group in supine position.
a) HF of RR, b) HF of SYS, c) VLF and d) LF of DIAS.

Table 3.14 Effects of tilt in 24 syncope patients

	Rest	Tilt	Mean difference	P values
RR (ms)	927±37	745±24	-182	<0.00001
SD (ms)	54±5	48±6	-6	0.354
VLF	34.8±4.2	29.0±3.5	-5.8	0.254
LF	39.0±3.1	53.4±3.5	+14.2	0.007
HF	22.5±3.0	15.±2.4	-7.5	0.063
SYS (mmHg)	132±5	132±6	0	0.844
SD (mmHg)	6±0.5	10±1.2	-3.6	0.005
VLF	43.1±4.7	20.6±2.6	-22.5	<0.00001
LF	42.1±4.5	58.5±3.0	+16.5	0.007
HF	12.7±2.2	18.9±1.9	+6.2	0.002
DIAS (mmHg)	69±3	77±4	+8	0.019
SD (mmHg)	4±0.34	5±0.5	+1.5	0.013
VLF	39.0±5.5	20.8±2.5	-18.2	0.002
LF	49.5±4.6	65.7±2.8	+16.3	0.006
HF	8.725±1.223	11.769±1.555	+3.044	0.09
PULSE (mmHg)	64±3	55±4	-9	0.003
SD (mmHg)	4±0.4	6±0.9	+2	0.023
VLF	42.3±4.6	24.7±3.6	-17.6	0.001
LF	34.3±3.9	44.2±3.7	+10.0	0.046
HF	19.1±3.3	27.0±3.1	+7.9	0.011

***Values are mean ± standard error.**

****differences are significant when p< =0.05.**

The systolic pressure remained unchanged (132 mmHg vs 132 mmHg, $p=0.84$) in response to head-up tilt in syncope, but in the normal group (ref. Table 3.5) the systolic pressure dropped significantly (from 123 to 117 mmHg, $p=0.007$) by a mean of 6 mmHg. Diastolic pressure increased by 8 mmHg (from 69 to 77 mmHg, $p=0.019$) and the pulse decreased by 9 mmHg from rest values (from 64 to 55 mmHg, $p=0.003$). The changes of both diastolic and pulse pressures were not significantly different in response to tilt. Similar to the normal group, the VLF powers decreased (SYS: 43.1 to 20.6; DIAS: 39.0 to 20.8; PULSE: 42.3 to 24.7, $p<0.005$) and the LF powers increased (SYS: 58.5 vs 42.1; DIAS: 65.7 vs 49.5; PULSE: 44.2 vs 34.3, $p<0.005$) in all blood pressure variables. The increase of the HF power in diastolic pressure was not significant (11.8 vs 8.7, $p=0.09$). Increases of HF powers from rest to tilt in systolic and pulse blood pressure variables were less important than that in the normal group (ref. Table 3.5) (SYS: 6.2 vs 12.1, $p=0.03$; PULSE: 7.9 vs 10.5, $p=0.04$).

3.2.4 Atrioventricular conduction in normal volunteers and in patients in the electrophysiological laboratory

The atrioventricular (AV) junction plays an important role in regulating the sequence between atrial and ventricular systole. Its principal role is to transmit impulses from the atria to the ventricles with a delay of approximately 150 ms to allow the ventricles to be filled. Like the sinus node, the AV junctional region receives a rich supply of adrenergic and cholinergic nerve terminals as revealed by numerous histologic, histochemical and physiologic investigations [52,54,55,57,58]. Sympathetic and parasympathetic innervations of the heart are known to be bilaterally asymmetrical [55,58]. Furthermore, it has been established that there are several discrete excitatory and inhibitory autonomic nerves that project onto very specific cardiac regions such as the sinus node and the AV node.

Rate-dependent refractory properties at the AV node are well recognized; that is, when the heart rate is increased, the propagation of impulses through the AV node becomes slower. Sympathetic and parasympathetic neural inputs can modulate AV nodal conduction, both directly and indirectly [26,29,35,36,50,51,53]. The AV node is affected directly by parasympathetic activity, which impedes AV conduction and by sympathetic activity, which enhances impulse conduction. Indirectly, the ANS modifies AV conduction by changing the prevailing level of heart rate, which affects the AV nodal refractoriness. Thus AV conduction is influenced by complex relationships among the level of heart rate, sympathetic and parasympathetic activity.

O'Toole *et al.* [30] noted in anaesthetized dogs, the parallel efferent controls on the sinus nodal discharge and AV nodal conduction time in response to arterial

blood pressure changes. Warner, Loeb *et al.* [26,35,36] found that in dogs, the beat-to-beat AV conduction time varies in parallel with the respiration and the variation of the AV conduction time is independent of the simultaneous heart rate changes. They also reported that in the basal state, AV conduction time is mainly influenced by parasympathetic activity.

The aim of this study was to characterize non-invasively moment-to-moment variations of AV conduction time in human subjects. AV conduction time is represented by the AR interval, which was defined by the time difference between the A wave on OEG and the R wave on the ECG. Although AV interval includes both the atrial-His (A-H) and His-ventricular (H-V) intervals, it has been shown that the H-V interval remains constant during changes in either heart rate or autonomic neural activity, i.e, there is no beat-to-beat variation in the H-V intervals. Thus changes in the AR interval reflect predominately alterations in A-H conduction time.

Subjects and protocol:

Twenty-seven normal volunteers and 10 patients in the Electrophysiology Laboratory are included in this study. The protocol for the volunteer group was presented in section 3.2.1 and only subjects with recordings from an OEG electrode were included for the evaluation of the AR interval variation. In the electrophysiological laboratory, ECG lead II, pressure by FINAPRES, respiration by nasal thermistor and the electrogram of the high right atrium (HRA) were recorded. The patients were in the supine position. A 10 minute control recording was followed by one to five recordings with atrial stimulation at a fixed frequency. The duration of each stimulation session varied according to the pacing rate.

Results

Although the variation of AR is much less than that of RR, it is shown that AR duration can be determined by beat-by-beat measurements with a good precision using the method described in chapter 2. A small but visible variation is observed in the beat-to-beat AR interval time series and spectral estimation of the time series demonstrates also clearly three peaks (ref Fig. 3.3b). The preliminary results for the pacing group will be given in the discussion section.

Normal volunteers

AA vs RR:

Compared to RR intervals, at both rest and standing positions, the AA interval time series has almost identical statistical characteristics, such as mean and SD. For example, in the supine position, mean RR for the group was 899.15 $\pm$18.081 ms and mean AA was 899.049$\pm$18.059 ms; mean SD of RR 54.968 ms and mean SD of AA was 55.138. There were no significant differences for both mean values and their SD ($p > 0.9$). For the evaluation of the sinus rate, AA intervals should be used instead of RR interval time series, since the variation of RR intervals includes the variation of AV conduction time. But we can show that RR interval series is a good approximation of AA interval series. By definition,

$$AA_i = RR_{i+1} + AR_i - AR_{i+1} = RR_{i+1} + \delta AR_i \qquad (3.2)$$

Since mean AA is equal to mean RR, we can subtract mean RR from both sides of equation 3.2 and get

$$aa_i = rr_i + \delta AR_i \qquad (3.3)$$

where aa_i and rr_i are variations around their mean values, and δAR_i is the difference of two consecutive AR intervals. As shown in chapter 2, before doing FFT, the time series is divided by its standard deviation. The standard deviation for AA or RR is about 50 ms and 5 ms for AR interval, i.e., by dividing equation 3.3 by the SD of RR interval, the last term will have a less than 10% influence on the RR variation. Its contribution to AA interval spectrum will be less than 1% because of the square operation. Comparing the spectral parameters for both AA and RR time series, the mean power in each of the three bands was almost identical (VLF: 23.6/22.9, LF: 37.5/37.7; HF: 33.4/32.8). Figure 3.3a) and c) show tachograms and their spectra for both RR and AA in a normal subject supine at rest. We can see that both tachograms and spectra are very similar.

AV conduction time:

Our data show that there exist a positive correlation between AR interval and RR interval ($r=0.6$, $p<0.05$, Fig 3.21) at rest; namely, subjects with a short mean RR interval will have also a short AV conduction time. The discharge of the sinus node and the conductivity of the AV node are modulated in parallel by ANS. The beat-to-beat variations of heart rate and the AV conduction time will reflect the variation of the autonomic tone.

In the tilt position, both AA intervals and AV conduction times shortened significantly. Mean AA interval decreased from 899 ± 18 ms to 711 ± 13 ms ($p<0.0001$), while the mean AR interval decreased by 11 ms for the normal group ($p<0.0001$). Contrary to the refractory theory, the AR interval decreased when the

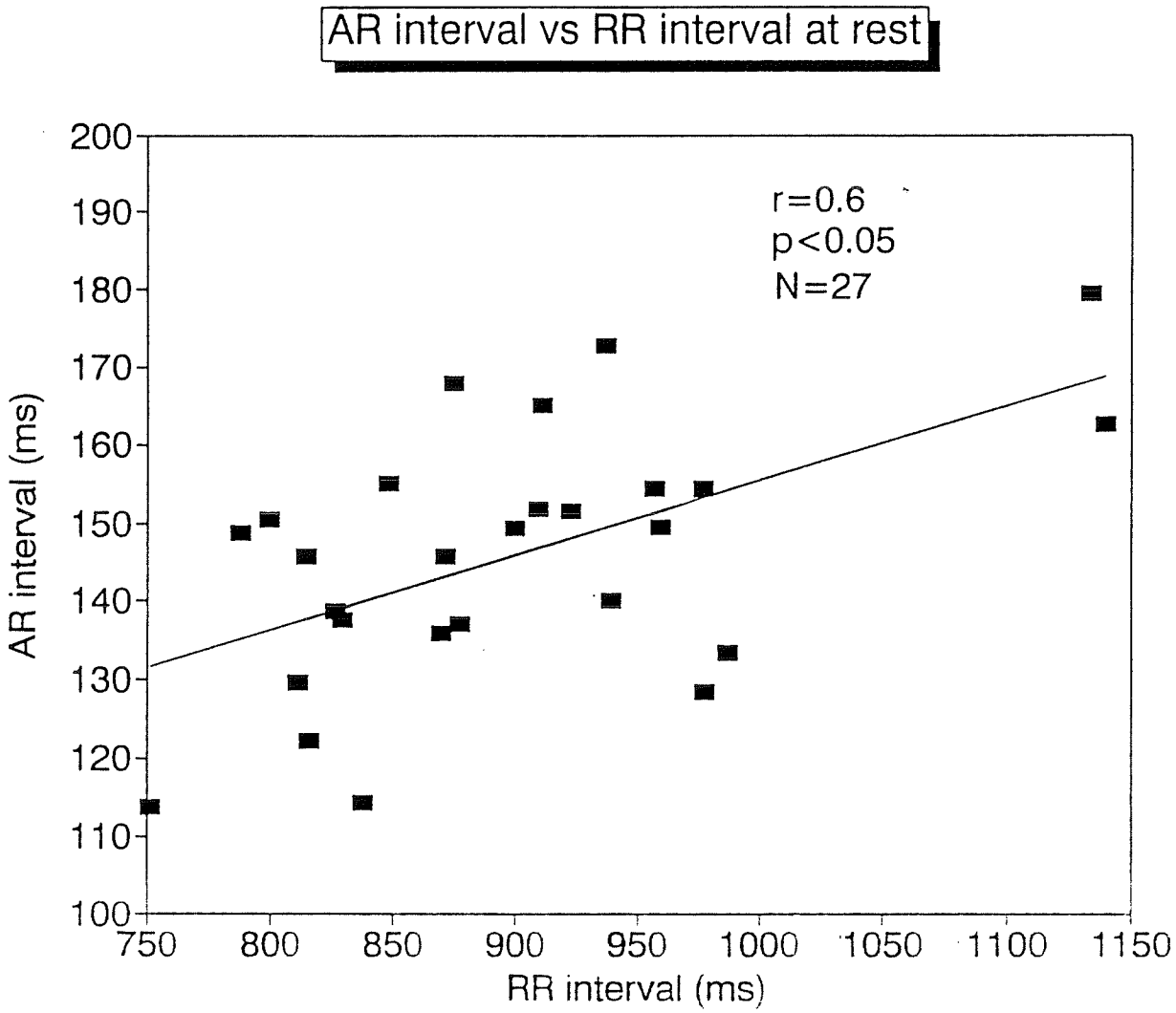

Figure 3.21 Correlation between mean AV conduction time and the mean RR interval.

heart rate increased in response to tilt. This means that under normal physiological conditions, the refractory effect on AV conduction can be ignored. The AV node conductivity is in harmony with the sinus discharge rate under normal physiological conditions to insure that every sinus discharge will be conducted. Consequently, AV conduction is influenced directly by the ANS under normal physiologic conditions while the indirect effect of the sinus rate on AV conduction time through the mechanism of refractoriness is less important. Thus the decrease of AV conduction time in tilt is mainly due to the enhancement of sympathetic activity and the reduction of parasympathetic activity.

Spectral analysis shows that not only is AA (or RR) affected by the autonomic tone but also that the AV conduction is modulated in a similar fashion (ref. Fig. 3.3a-c). In response to tilt, both VLF and LF power decreased non significantly ($p=0.067$ and 0.225 respectively), but HF power increased from 23.580 to 33.879 ($p=0.015$) (Fig. 3.22). Contrast to RR, the LF/HF ratio of AR power decreased significantly from 2.71 to 1.33 ($p=0.029$). But the AR spectra show a more important parasympathetic influence than the AA spectra. Our data show that both at rest and during tilt, the spectra of AR has a lower LF/HF ratio than that of RR. The LF/HF ratio increased significantly ($p<0.005$) during tilt in the spectra of RR which is due to the increase of the sympathetic tone, but decreased in the AR spectra.

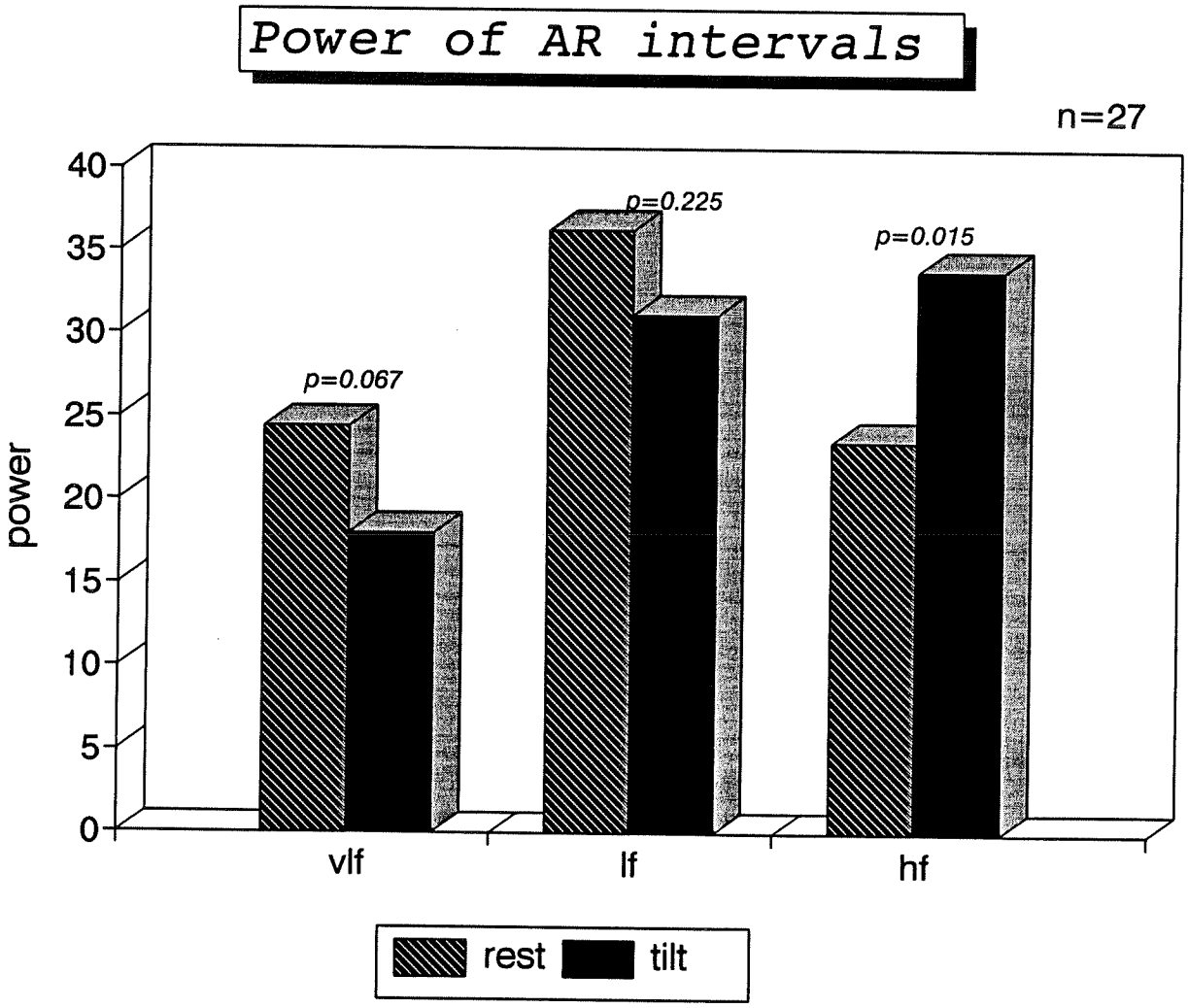

Figure 3.22 Spectral power in AR interval at rest and tilt positions.

3.3 Spectral analysis in anaesthetized dogs

The objective of analyzing the data from an animal experimental protocol was to demonstrate the effects different manipulations on ANS, such as stimulation, deactivation or activation of presynaptic receptors and parasympathetic blockade; also to show that the method developed may be applied in anaesthetized dogs.

The ANS regulates the heart rate, contractility, the peripheral resistance in order to respond to demands of the peripheral tissue under different physiological conditions, such as exercise, emotion, stress, through the peripheral circulation. It controls the cardiovascular system through the two branches (sympathetic and parasympathetic) by the release of neurotransmitters at the terminal neural fibres and the interactions between neurotransmitters and effector cells. Usually, we consider sympathetic and parasympathetic tones as the discharge rate of nerve fibres, but recent studies suggest that local mechanisms are also responsible for regulating the release of neurotransmitters and neurohormones by the demonstration of multiple auto- or heteroreceptors found presynaptically on sympathetic and parasympathetic fibres [45]. Figure 3.23 gives a schematic representation of presynaptic modulatory influences by autoreceptors for adrenergic peripheral neurons.

The release of the neurotransmitters and neurohormones are dependent on the number of nerve impulses, and are modulated by the presynaptic autoreceptors. The expression of autonomic tone may thus also depend on the number of functional adrenergic, cholinergic and neurohormone receptors. The number of functional receptors are highly variable [45], due to desensitization mechanisms which respond to the degree of activation of agonist neurotransmitters.

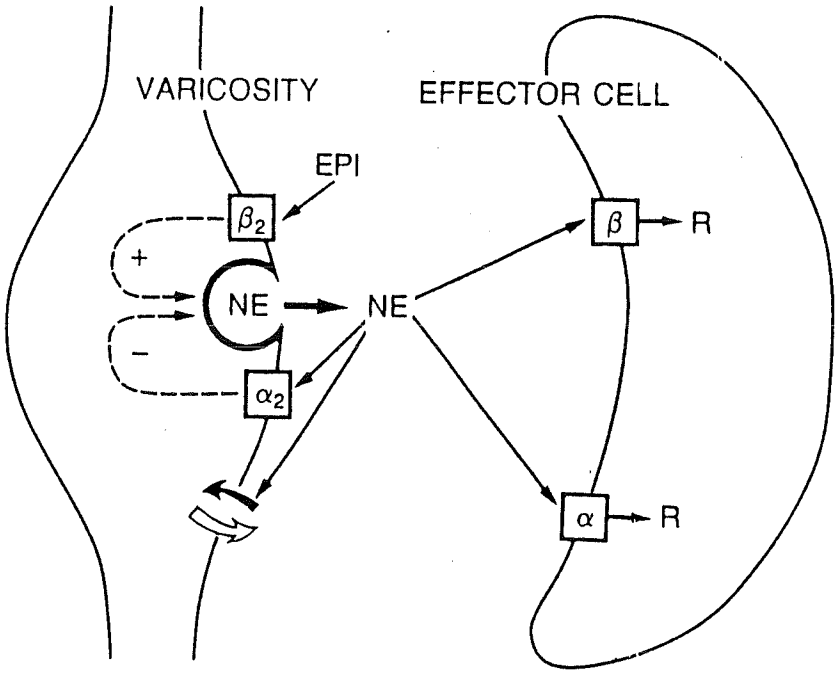

Role of the presynaptic α- and β-adrenoceptors in the regulation of norepinephrine release during nerve stimulation. During norepinephrine (NE) release at low frequencies of nerve stimulation (when the concentration of the released transmitter in the synaptic cleft is rather low), circulating or locally released epinephrine (EPI) can activate presynaptic β-adrenoceptors, of the β_2 subtype, leading to an increase in transmitter release. As the concentration of released NE increases, a threshold is reached at which the negative feedback mechanism mediated by presynaptic α-adrenoceptors of the α_2 subtype is triggered, leading to inhibition of transmitter release. Both presynaptic receptor mechanisms are present in nerves, irrespective of the α or β nature of the postsynaptic receptors that mediate the response (R) of the effector organ. As shown in the figure, NE is a substrate for the presynaptic transporter which represents the main inactivating mechanism for the transmitter.

Figure 3.23 Presynaptic autoreceptor modulation of NE release in sympathetic nerves ending (adapted from ref. 115).

Subjects and protocol

Eight mongrel dogs (18-30 kg) were utilized in these experiments. Anaesthesia was induced by intravenous administration of Penthotal (15 mg/kg, i.v.) and α-chloralose (80 mg/kg + 10 mg/kg/h). The animals were artificially ventilated by a respirator (Harvard pump, model 607) and the rate of ventilation was regulated to produce an inspiration pressure of 20 cm of H_2O (15 cycles/min). The temperature of the animals was maintained at 37°C. The detailed surgical procedure was described by Boudreau [114]. ECG of standard lead II was recorded on a polygraph Nihon-Kohden, model RM-6000.

The experimental protocol is summarized as follow (for detailed protocol, see ref. [114] and Fig. 3.24): After 10 minutes baseline recording (recording A), the dog received one hour intravenous injection of epinephrine. Two ECG of 5 minute duration each were recorded; the first at 5 minutes after the beginning (recording B) and the second 5 minutes before the end (recording C) of the injection. 5 minutes of baseline anaesthesia signal (recording D) was recorded after surgery. The left stellate ganglion (LSG) was stimulated at 4 Hz for one minute followed by 15 minutes of rest. Recording E was collected during the last 5 minutes of rest. The one minute of stimulation at 4 Hz was followed by a period of 10 minutes rest and one minute of stimulation at 10 Hz. Then a specific α_2 receptor blocker (yohimbine or YHMB, 0.3 mg/kg, i.v.) was injected i.v. 5 minutes of signal was recorded 5 minutes after the start of YHMB (recording F). After this, the LSG was stimulated again at 4 Hz for one minute then $ß_2$-adrenergic agonist (fenoterol, 0.5 μg/kg, i.v.) was administrated and the ECG was recorded 5 minutes later for 5 minutes (recording G).

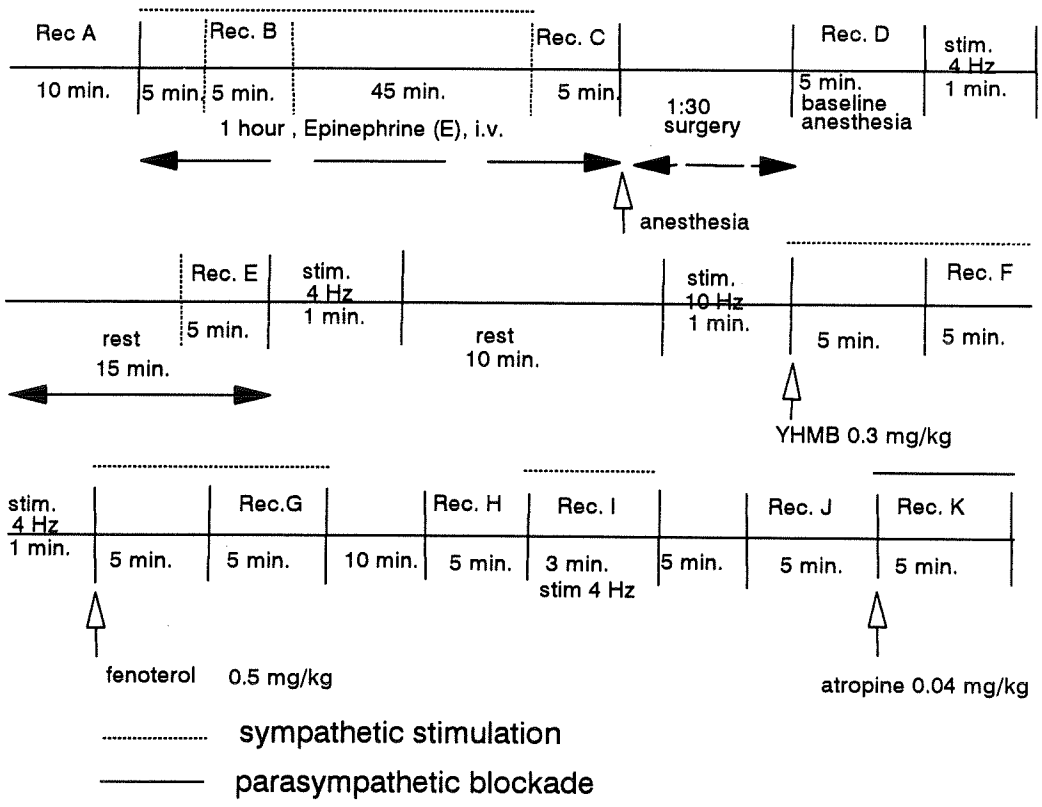

Figure 3.24 Schematic representation of the experimental protocol

The ECG before LSG stimulation (recording H) and during a 3 minute stimulation at 4 Hz (recording I), before atropine (recording J) and after atropine (recording K) were recorded.

Results and discussion

The recording of dog 3 was of very bad quality and was excluded from the group analysis. Moreover, only dog 1 had recording A. Consequently, there are no statistical data for baseline recording (recording A). The original protocol (recording A to G) was designed by Boudreau [114] and we added a segment (recording H to K) at the end of his protocol in order to study the effects of LSG stimulation and atropine. We did not analyze the effect of stimulation in his protocol because the stimulation segments were too short to be analyzed.

Table 3.15 gives the statistics for the group in different phases of the protocol. The same data are also presented in graphics (Fig. 3.25).

Five minutes after the start of perfusion of epinephrine, the mean of 512 consecutive RR intervals shortened in dog 1 from 928 ms to 743. After one hour of perfusion, the mean RR did not show further decline. The spectra of RR interval of this dog (dog 1) at each recording was plotted in Fig. 3.26. Compared to the baseline, the spectrum at recording C (Fig. 3.26a, dotted line) shows a significant increase in 0.1 Hz peak, while the respiratory band is similar to that in baseline (at this stage, the dog breathed spontaneously). The comparison between recording A and C is not available. Increases of the heart rate and the LF power are due to the accumulation of the epinephrine (EPI) in terminals of sympathetic nerves, which

Table 3.15 Comparison among recordings:
statistical value and spectral components for RR intervals

Recording	mean RR	SD (RR)	VLF	LF	HF
B 5' EPI	625.2±136.3	81.5±50.5	11.6± 5.6	26.1±13.1	43.9±19.3
C 55' EPI	592.9±214.6	91.9±86.2	17.2± 9.4	23.3±10.8	28.9±7.1
D BLN	399.9± 68.4	8.5±13.3	27.5±18.1	69.3± 9.3	21.0±4.9
E BLN	369.5± 35.1	8.8±10.3	11.0± 9.7	23.6± 6.4	38.5±6.6
F YHMB	337.0±122.8	10.7±12.5	9.3± 5.6	38.0±11.5	36.6±8.1
G FENO	316.8± 37.8	9.3± 9.9	8.7±11.4	36.4±12.2	53.1±12.3
H BLN	510.2±184.0	9.0±11.8	13.0±16.4	25.6±12.6	44.9±28.1
I STIM	424.6± 93.0	23.0±33.1	23.4±27.7	36.9±15.1	38.0±19.7
J BLN	415.4± 97.4	9.0± 5.0	12.3±13.3	33.3±10.9	34.2±12.8
K ATR	317.0± 51.5	4.4± 2.0	14.4±18.4	18.1± 6.0	21.2± 6.9

* data presented in this table are means±SD

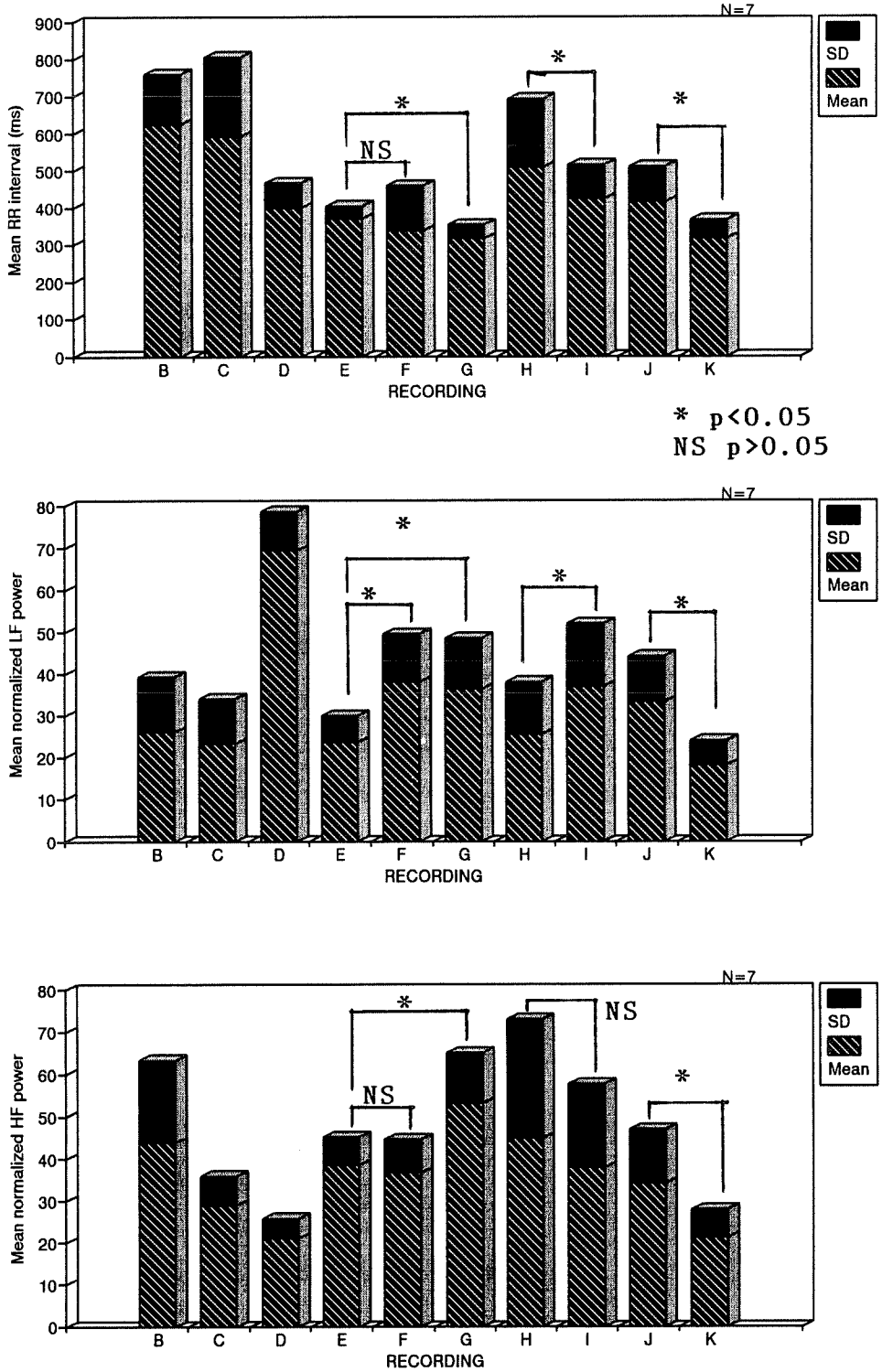

Figure 3.25 Effects of different manipulations of the sympathetic system on mean RR interval (top), normalized LF power (middle) and normalized HF power (bottom). Definitions of recordings B to K were given in figure 3.24

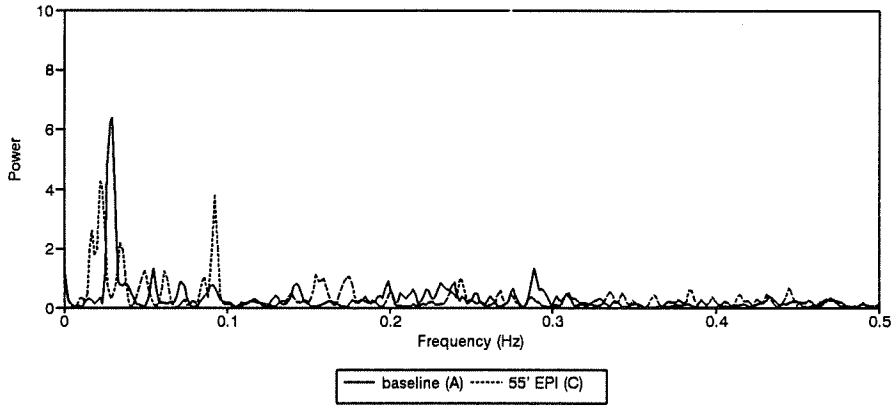

(a)

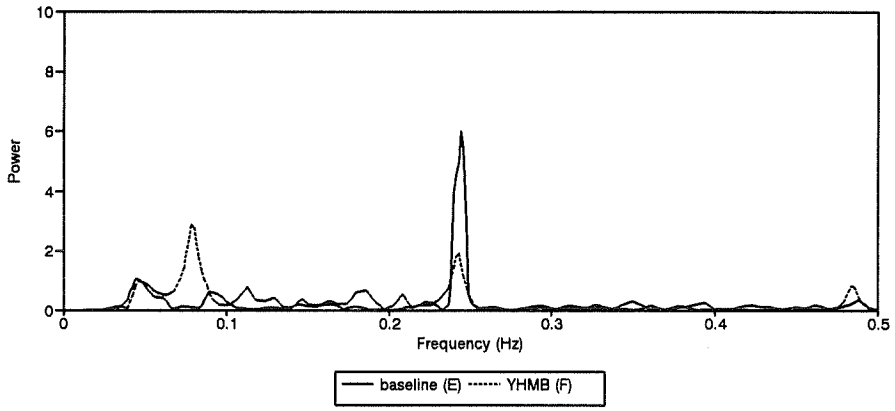

(b)

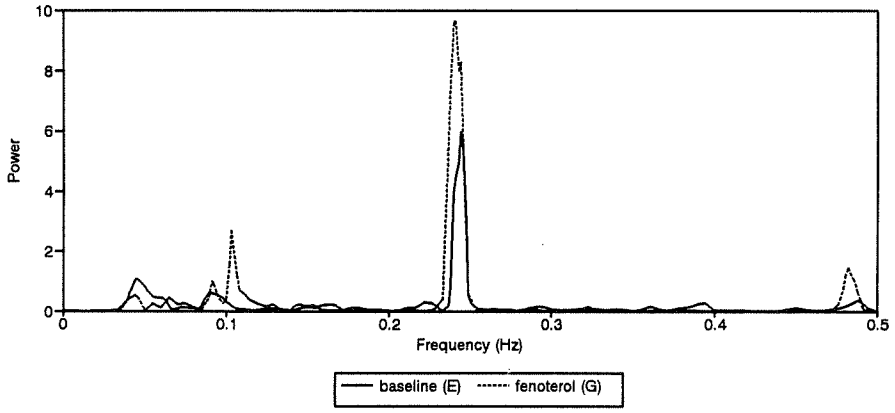

(c)

Figure 3.26 (ctd)

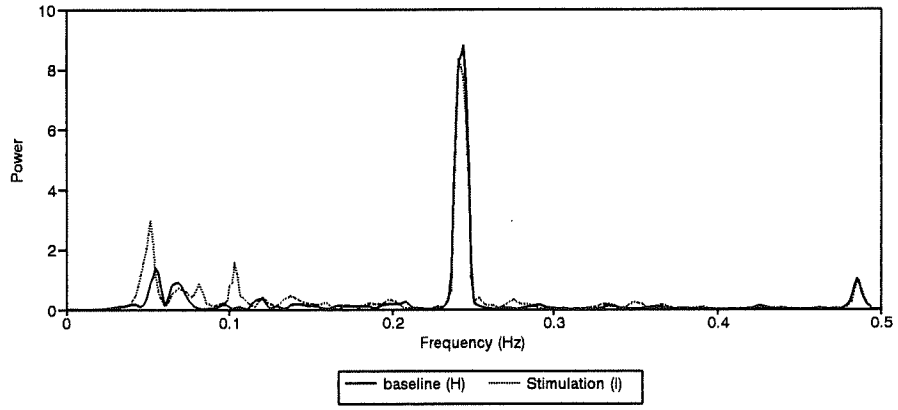

(d)

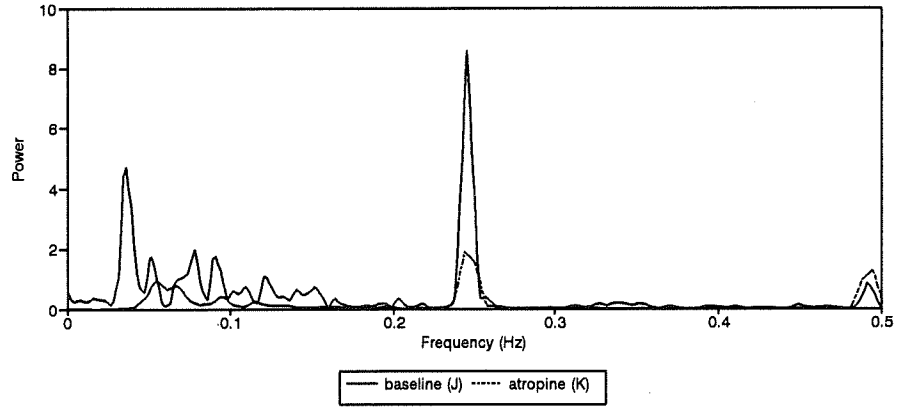

(e)

Figure 3.26 An example of spectral analysis for dog #1.
Examples of comparison of spectra between a) baseline (A) and 55' after EPI perfusion (C); b) baseline (E) and YHMB (F); c) baseline (E) and fenoterol (G); d) before (H) and after (I) 3' stellate stimulation; e) baseline (J) and atropine (K)

suggest that the circulating and locally released EPI can activate presynaptic ß-adrenoceptors, of the $ß_2$ subtype, leading to an increase in neurotransmitter release [114,115].

Our data show that there are no significant differences in mean heart rate and LF power between recording B and C (Table 3.15) even though the durations of perfusion of EPI were 50 minutes apart. Boudreau [114] showed that a longer duration of perfusion of EPI will give a higher norepinephrine (NE) concentration under left stellate stimulation. This difference may be explained by the fact that the response of the heart rate variability may be not linearly related to the NE concentration or the NE concentration may be different under these two conditions only with stimulation.

In the recording of baseline anaesthesia (recording D), a significant decrease of RR interval ($p<0.05$), an increase of LF power ($p<0.01$) and a decrease of HF power ($p<0.05$) are shown. This is due to the open chest operation.

Comparing results before (recording E) and after (recording F) the administration of yohimbine (YHMB) (ref. Fig. 3.26b), RR interval did not decrease significantly (Table 3.15), HF power remained unchanged while the LF power in the RR variability increased from 23.6 ± 6.4 to 38.0 ± 11.5 ($p<0.05$). This specific α_2 adrenergic blocker deactivates the feedback mechanism of NE concentration control at the sympathetic terminals, which is mediated by presynaptic α adrenoceptor of the α_2 subtype, leading to a decrease of the inhibition of transmitter release and a facilitation of NE release. Boudreau [114] demonstrated that in the dog treated by YHMB, NE concentration was two times higher than that in the control group when

the left stellate ganglion was stimulated. The blockade of the postsynaptic α receptor in the vessels reduces peripheral resistance, which then reflexively increases overall sympathetic activity. Thus the higher LF peak after injection of YHMB reflects the increased sympathetic tone caused directly by the increase of NE concentration with masking the presynaptic α_2 autoreceptor and indirectly by the reduced peripheral resistance with the blockade of the α receptor in the vessel.

After the administration of the $ß_2$ agonist fenoterol (recording G), the heart rate increased significantly ($p < 0.05$) compared with both baseline (recording E) and after the injection of α_2 blocker (recording F) (Fig. 3.25). The LF power was significantly higher than that at baseline (recording E) but was not different from that in recording F. The HF power was higher than that in both of preceding recordings ($p < 0.05$). The $ß_2$ agonist leads to an increase of the transmitter release, again this increase can not activate the presynaptic α_2 adrenoceptor to inhibit the NE release because the α_2 receptor was blocked in the preceding step. Boudreau showed a higher NE concentration in both plasma and the peripheral tissue after administration of fenoterol.

At this stage, two mechanisms function together to facilitate the release of NE. The first is the blockade of α receptor and the second is the $ß_2$ agonist. The blockade of α receptor leads to a reduction of peripheral resistance, and the $ß_2$ agonist leads to vasodilation, which again reduces the peripheral resistance. The vasodilation of the vessel will reflexively increase the sympathetic tone, then increase the LF fluctuation in the RR variability.

But the increase of the HF power in the RR variability in this recording seems

questionable. Because the increased sympathetic tone will inhibit the release of parasympathetic tone by the prejunctional adrenergic-cholinergic interaction from intramural vagal nerve endings [116]. This inhibition of Ach release appears to be mediated by α_1-adrenergic receptors on the vagal terminals. Another mechanism which may also inhibit the release of Ach is the release of neuropeptide Y. This peptide, which is released along with NE from sympathetic nerve terminals, is thought to attenuate cardiac vagal actions by inhibiting the release of Ach from vagal nerve endings. This may suggest that the increased HF power may not be due necessarily to increased parasympathetic tone, but may be the result of an increased vagal response. This is confirmed by a mechanism termed accentuated antagonism [116], which describes an exaggerated inhibitory response to vagal stimulation is elicited by an augmented level of tonic sympathetic activity. The vagal tone in this stage may be unchanged or even attenuated, the exaggerated vagal response may cause this increased fluctuation of RR interval when the vagal discharge has a small variation around the average vagal tone. Thus the power of RR interval fluctuation at a given frequency band not only represents the corresponding autonomic nervous tone, but also shows the response of heart rate to the variability of that autonomic tone.

With stimulation of the left stellate ganglion (recording I), RR interval shortened significantly ($p<0.05$) compared with the baseline before stimulation (recording H). LF power increased from 25.6 to 36.9 ($p<0.05$) while the HF power decreased non significantly. The increase of sympathetic tone caused the increase of LF fluctuation in the RR interval time series. This confirms the hypothesis that the LF power reflexes the sympathetic tone.

The last phase of the protocol is to test the effect of parasympathetic blockade. The plot of mean RR and the mean LF and HF normalized power before (recording J) and after (recording K) administration of atropine was given in Figure 3.25. Vagal blockade decreased the RR interval from 415.5 ± 97.4 ms to 317.0 ± 51.5 ms ($p < 0.02$) and at the same time the RR variability (SD) decreased ($p < 0.05$) from 9.0 ± 5.0 ms to 4.4 ± 2.0 ms. Both LF and HF power decreased significantly after atropine. Figure 3.26 e) illustrates the effect of parasympathetic blockade in dog No.1. It shows clearly that the spectrum amplitude is abolished in the whole frequency band. Our results confirm the results of Akselrod *et al.* [1,2]. Their experiments showed that the low and high frequency peaks were abolished after parasympathetic blockade with glycopyrrolate, while the amplitude of the very low frequency peak was reduced. Our data of VLF power did not show a significant difference after vagal blockade. This may be due to the fact that the VLF band we chose was different from that used by Akselrod. In our case, the VLF band was from 0.01 to 0.05 Hz, while their VLF band was defined as 0.02 to 0.09 Hz. The abolishment of the LF and HF power in RR variability after atropine provides evidence that the parasympathetic system is responsible for both LF and HF fluctuations in RR variability.

Chapter 4 Discussion

4.1 Methodology: Assessment of ANS function by spectral analysis of the hemodynamic variable time series

Spectral analysis was widely applied on heart rate, blood pressure, respiration or other cardiovascular variables to assess parasympathetic (high frequency component) and sympathetic system (low frequency component) function [1-6,16,19,32], to evaluate alterations in neural control mechanisms in different conditions such as head up tilt, mental tasks, exercises, myocardial infarction and hypertension. Some features of our methodology of spectral estimation need to be underlined here for their relevance to the observed results.

1) We used a systematic and standardized approach to perform the analyses, which includes signal recording, event detection, time series construction, detrending, filtering, windowing, spectra estimation (FFT) and parameter extraction. This standardized process improved the reproducibility of observations. A PC-based bedside system has been developed for this project. The software needed for each step was developed for this project and the quality of performance was under our control.

2) We expressed the spectra in normalized rather than absolute units to facilitate intersubject and with group spectral comparisons. In absolute units, even in normal

subjects, spectra may easily vary from one to another by a factor of 10, which makes a specific spectral parameter for a group disperse in a very wide range and a comparison between different maneuvers in a group not possible. The normalized inter-subject spectra can be easily plotted in the same range.

3) Our normalization was different from others [1,105]. Akselrod *et al.* normalized heart rate power spectrum so that the integral of s(v) is the variance of the heart rate fluctuations divided by the square of the mean heart rate, while Pagani *et al.* normalized the power spectrum by dividing the power of a given component by the total variance (from which the very low frequency component was subtracted) and multiplying by 100. Our normalized power spectra was based on the normalized time series, which was normalized to a process of unit variance and zero mean. This normalization process assured that our spectral estimation was performed on time series with the same statistical properties. As in Pagani's method, the very low frequency was not clear or arbitrarily chosen, moreover, the relative ratio between the very low frequency component, assumed noise in their method, and the remainder of the signal may vary considerably. By this way, the normalization varied from one spectrum to another and was not uniform.

4) With our normalization process, the absolute power spectrum, if needed, can be easily produced by multiplying the normalized power by the total variance of the time series under study. But with the method of Akselrod *et al.* [1-2], to obtain the absolute spectrum, the FFT needs to be applied again.

5) VLF is located below 0.05 Hz. This band was not addressed by some authors [27,31,43,62,65,104,105], because it cannot be properly assessed with some

methods, such as with autoregressive algorithms. This band may contain significant physiological information. Usually it shows important inter-subject variation because the very low frequency (almost DC) component has a large amplitude and it varies importantly from subject to subject. With our trend removal of a moving 4th order polynomial, the periods of fluctuations greater than minutes were eliminated from the analysis. Thus, it makes the study of fluctuations between 0.01-0.05 Hz possible.

6) High frequency band limits were determined according to the spectrum of respiration signal instead of being imposed arbitrarily. Parasympathetic activity is reflected in the HF of cardiovascular variable fluctuations. The proper selection of band limits is important to assess vagal activity. The HF band limits varied from one investigator to the other, for example, 0.15-0.8 Hz [3], 0.224-0.28 Hz [32], 0.15-0.4 Hz [49]. This makes the results difficult to compare. Furthermore, the respiration rate varies among subjects, large band limits may not give a precise measurement of HF power for an individual. As the HF power is related to respiration, it is natural to select the HF band limits from the respiration signal. We choose HF band limits according to the individual's spectrum of respiration signal. So, this band reflects the subjects' breathing pattern and can also be uniformly applied to all subjects.

Spectral analysis assumes a stationary time series. However, in practice this is not a problem because the objective of most studies is to determine autonomic functioning or balance of both systems in a particular situation (i.e., a stationary condition, for example, during sleep, supine rest, orthostasis, exercise, or mental activity). Such a condition should be stable for about 8 to 10 minutes for spectral analysis to be applicable (5 minutes is acceptable). The cardiovascular system must accommodate itself to each new situation, and time series plots of the signals show

that an adaptation period of about 2 minutes is usually enough to obtain a stationary situation. This adaptation period should not be included in the analysis. Thus, as our experiences confirm, there will be no problems with the assumption of stationary time series.

Spectral analysis of cardiovascular variables, such as heart rate and arterial blood pressure, has been proved to be a valuable non-invasive tool to assess short term autonomic nervous control of the cardiovascular system. Compared to time domain cardiovascular variability measurements, the main advantage of spectral analysis is its accuracy. It can be used to evaluate physiological variations of sympathovagal tone in individuals. Variations in CV variables in specific frequencies are related to the sympathetic and parasympathetic systems. Quantitative measurements of spectral power in each frequency band may be useful to understand the physiological origins and their functioning. In patients with impaired autonomic functioning, spectral analysis of variability of heart rate and ABP will be useful to evaluate effectiveness of treatments or for prognosis.

4.2 Studies of normal subjects

We assessed autonomic nervous control of the heart rate (RR interval), arterial blood pressure by measuring the power spectra of spontaneous RR intervals, AV conduction time and blood pressure (systolic, diastolic and pulse) fluctuations in normal human subjects in supine rest, passive head-up tilt and active standing positions.

4.2.1 Fluctuations of cardiovascular variables in specific frequencies

Cardiovascular variables, such as heart rate and blood pressure, fluctuate at specific rhythms. Each of the rhythms may reflect the output of individual systems superimposed on the overall system output. Sayers [42] described three frequency peaks in human heart rate variability, Akselrod *et al* [1,2] presented similar peaks in animals. Our data show that in spectra of both RR intervals and systolic pressure, three peaks were evident in most subjects. However, in some subjects, one of the peaks may disappear in a given spectrum because of low amplitude or overlap. In the spectra of diastolic pressure, HF peak were absent or had a very low amplitude in most of the subjects. While in the spectra of pulse pressure, the LF fluctuation were less important than the other two peaks. Our results were in agreement with previous observations of an oscillating cardiovascular control system [1,2,13,40-42,112,113]. The LF (10 s) fluctuations in cardiovascular variables were generally accepted as being sympathetic in nature and with some parasympathetic contribution, while the respiration-related rhythms were solely mediated by the vagal system [1,2,31,32,112].

The origins of periodic fluctuations in blood pressure and heart rate in the frequency lower than 0.05 Hz (VLF), ie. periods of more than 20 s, are controversial in the literature. These VLF fluctuations have been described as 1) being possibly caused by properties of the thermoregulatory systems [25,40-42], 2) being modulated by the renin-angiotensin system [1,2,112], or 3) being jointly mediated by the sympathetic and parasympathetic nervous systems[1,2,32,70]. Our spectra show VLF variabilities in both RR and blood pressure time series in every stage of our protocols. All three systems mentioned earlier may contribute to the regulation of cardiovascular

variables in the VLF fluctuations, but only the possible contributions of the sympathetic and parasympathetic systems will be discussed since our study was not designed to address the control of VLF fluctuations by neither thermoregulatory nor renin-angiotensin systems. The origins of the VLF fluctuations in heart rate and arterial blood pressure may differ. de Boer [13] showed that for frequencies under 0.05 Hz the coherence between RR and blood pressures was low. This indicates that the blood pressure is not linearly related to the heart rate. Akselrod *et al* [2] showed that during pacing the VLF fluctuations in ABP did not decrease significantly and they suggested that this fluctuation was not caused by the variability in heart rate but by variability in peripheral vasomotor activity. They suggested also that the local vascular beds regulate local resistance to match flow to demand and the renin-angiotensin system plays a role in controlling the resultant variability in peripheral resistance, whereas residual variability is compensated for by the heart rate variation through the baroreceptor reflex. Saul *et al.* [11] demonstrated also a low transfer function magnitude and a low coherence for frequencies less than 0.05 Hz between respiration and heart rate variability with a broad-band respiration method. This implies that the variation of heart rate in that frequency range is not linearly related to the blood pressure variations induced by respiration movements.

Of the spectra of diastolic pressure, the lack of HF power was explained by de Boer [13] as an effect of counteracting between the influence of systolic pressure on diastolic pressure and the baroreflex [92]. The diastolic pressure is a function of the total peripheral resistance. The low HF fluctuations in the diastolic pressure may also be due to less influence of parasympathetic activity on peripheral resistance which is mainly mediated by the sympathetic system through the slow temporal response of the α-adrenergic effector mechanisms [28]. This is also supported by the experiment of

Sanders *et al* [34]. They found a strong correlation between diastolic pressure and efferent muscle sympathetic nerve activity (MSNA).

The respiration-related modulation of heart rate may be explained by mechanisms generally referred to in the literature: 1) a direct influence of medullary respiratory neurons on cardiomotor neurons (central irradiation) [84]; 2) an indirect influence on heart rate of blood pressure changes secondary to respiration activity, respiration movements affects mechanically the blood pressure through two possible ways (venous return and direct deformation of great arteries) and further change in blood pressure is mediated via arterial baroreceptors or atrial stretch receptors [85] and 3) a reflex response to lung inflation mediated by thoracic stretch receptors, most likely from the lungs and chest wall [86]. The blood pressure may be influenced by respiration through 1) RR interval variation that is modulated by medullary respiratory neurons in cardiomotor center and 2) direct and indirect mechanical effects as mentioned previously.

4.2.2. LF and HF powers of RR correlated with mean RR interval

The intersubject plot of LF power versus its corresponding mean RR interval shows a significant negative correlation between the two parameters. This may be related to the baseline sympathetic activity. In normal subjects, higher sympathetic activity results in higher mean heart rate. As mentioned earlier, LF fluctuation in heart rate variability is related mainly to the sympathetic activity. Although the correlation between mean RR and the HF power of RR in our normal group was not significant, but we can see clearly (ref. Fig. 3.5b) that there are three clusters: cluster

A in the upper left part (6 subjects), cluster B on the diagonal (32 subjects) and cluster C in the lower right (3 subjects). The low correlation was caused by the dispersion of clusters A and C. In cluster B, there is a visible positive correlation between HF power and the mean RR. This may reflet parasympathetic activity; a higher vagal activity, may result in a longer RR interval and at the same time cause a more important respiration related fluctuation in the RR time series.

4.2.3 HF power correlated with respiratory frequency

Our data shows that the HF power in both RR and SYS variations were respiratory frequency-dependent. The negative correlations of HF power in RR and SYS with respiration frequency can be explained as the effect of roll-off of the parasympathetic system and this observation confirms the results of previous studies [10,11,19]. Thus the HF power in both RR and SYS is weakly frequency-dependent. Hirsch *et al* [19] demonstrated that RSA amplitudes are stable at low frequency of breathing below the corner frequency and decreased significantly at higher frequencies greater than the corner frequency of 8.9 cycles/min. The slope of the roll-off was estimated at 19.4 db/decade. In our case, spontaneous breathing had higher frequencies than the corner frequency defined by Hirsch *et al.* With a broad band respiration method, Berger, Saul *et al.* [10,11] demonstrated also that respiratory sinus arrhythmia was a frequency-dependent phenomenon with the magnitude and phase characteristics of a low-pass filter and the average transfer function magnitude fell with frequency above 0.1 Hz. Another possible explanation of the negative correlation between the respiratory rate and the HF power is that with longer respiratory cycle length, the longer expiratory period allows the RR interval to

continuously increase and possibly to reach a plateau, since it is in this period that the parasympathetic impulse rate is higher and the heart rate decreases. Thus, the longer respiratory cycle length causes the larger variability of RR interval and so the larger variations in ABP. In the frequency domain, this appears as a larger power in the respiration related frequency band.

4.2.4 Response to posture change

The typical normal response to passive head-up tilt is an activation of sympathetic and suppression of parasympathetic mechanisms [27,87]. The posture change results in increases in heart rate and diastolic blood pressures [ref. Table 3.5 and Fig. 3.7]. For spectral parameters, many studies [27,65,87,89,105,111] demonstrated that LF power increase and HF power decrease in normal subjects in response to posture change from supine rest to tilt. With reference to RR interval fluctuations, our results are in good agreement with the findings of previous studies [31,32,37,72] for the response of LF and HF power spectral parameters for posture change. The increased sympathetic activity may be due to an increase of discharge rate of sympathetic nerves, or a facilitation of norepinephrine release at sympathetic endings through some presynaptic autoreceptor modulation, or an increase of sensitivity of α and ß receptors in the effector cells. The suppression of vagal activity may be the result of withdrawal of parasympathetic discharge or/and inhibition by the increased sympathetic tone which inhibits the release of parasympathetic neurotransmitters at the presynaptic level. Spectral analysis can show the global change of the ANS, but we can not specify which part plays a major role. Another possible interpretation of the decrease of the HF power of RR in response to tilt is that the effective characteristics of filter for the response of the cardiac pacemaker to

modulation of vagal tone depend on the mean level of parasympathetic tone. Berger *et al.* [10] showed with broad band vagal stimulation that the filter becomes progressively more selective for lower frequency fluctuations in vagal activity (i.e., rolls off faster) as the mean vagal level falls. Thus the RR response to the vagal modulation (HF) decreases at tilt because the filter becomes more low frequency selective.

Concerning LF fluctuations, some authors [31,43,62,65,104,105, 110] suggested that the LF variations in cardiovascular variables were mediated by the sympathetic system, but others [1,2,32,98] have suggested that the parasympathetic system may also modulate fluctuations in this band. In human subjects, Pomeranz [32] and Weise [98] demonstrated that under parasympathetic blockade (atropine), both HF and LF power decreased significantly. During tilt, the vagal influence on LF fluctuations is reduced because of the overall decreased vagal tone. This means that during standing, the LF power is mainly mediated by sympathetic activity. During supine rest, the parasympathetic system modulates the fluctuations of all the frequency range, however the HF power is solely modulated by the parasympathetic system [1,32,98]. Our data show that during supine rest HF peaks are very visible and during tilt the LF peaks are important [ref. Fig. 3.9 and Table 3.5]. Thus it is reasonable to use the LF power in tilt position and the HF power in supine position to assess the sympathetic and parasympathetic activities, respectively.

Blood pressure variability during orthostatic stress was examined by Pagani *et al* [31] using direct arterial pressure measurement. These experiments showed a predominant LF component in systolic and diastolic pressure after upright tilting compared with recumbency. Rossberg and Penaz studied the systolic, diastolic, mean

and pulse pressure variabilities using the non-invasive Penaz method in squatting, standing and sitting positions [59]. They showed similar responses. Our studies also used the Penaz method for measurement of the blood pressure [59] and our results confirm these findings. On the HF power in pulse pressure time series, Rossberg and Penaz [59] found that this parameter was more important in the sitting position than during standing. Our data indicate that the HF fluctuations in systolic and pulse pressure were more important during tilt than during supine rest. These increased HF fluctuations in systolic and pulse pressure may be due to the mechanical influence of respiration. Since respiration during tilt is deeper, the respiratory movements influence more strongly the venous return and squeeze the great arteries more strongly. This suggests that the HF component of blood pressure variabilities are likely to depend on the mechanical effect of the respiration movements. This is different from what was observed in dogs by Akselrod *et al* [1,2]. They speculated that the HF fluctuation of ABP resulted from heart rate variation at this frequency, and not vice versa. This may be due to the difference of mechanisms of HF fluctuations in ABP in dogs and human subjects. Our data of patients with atrial pacing also showed that the fluctuations of ABP in HF frequency were still important, instead of decreasing by two folds in the HF power. The HF fluctuation in RR interval was decreased in response to tilt because of the baroreceptor damping mechanism and the withdrawal of vagal activity.

Pulse pressure is proportional to the stroke volume. In tilt, stroke volume decreases because of shortened filling period and augmentation of afterload. We noted a decrease in mean pulse pressure [ref. Table 3.5].

The VLF power of RR remains unchanged in response to tilt while the VLF

powers in all blood pressure variables decreased significantly. This may be explained again by the hypothesis that the origins of VLF fluctuations in RR and ABP variables are different. Assuming that the posture change does not alter the properties of the thermoregulatory and renin-angiotensin systems, the increased sympathetic activity, decreased parasympathetic activity and reduced baroreflex (because of the reduced VLF fluctuations in ABP) might be responsible for keeping the VLF variation in RR from changing. The increased sympathetic activity (increased peripheral resistance) and the decreased parasympathetic activity as well as the increased vasomotor and venomotor tone might be responsible for the decrease of the VLF fluctuations in ABP.

4.2.5 Active standing versus passive head up tilt

Wieling *et al* [63,103] showed that there is a significant difference in the initial response to active standing and to passive head up tilt, whereas steady state differences in the circulation between active standing and passive standing have received little attention. The aim of this study is to compare the autonomic response to active and passive standing in steady state conditions. Our results showed that in all blood pressure variables the HF fluctuations were less important during active standing than during head up tilt. The HF fluctuations in RR were in the same direction although the difference was not significant. This means that during active standing, the withdrawal of parasympathetic activity is more important than that during head-up tilt.

4.2.6 Autonomic control of AV conduction time

The influence of ANS on the heart rate in humans was investigated extensively, whereas the influence of the autonomic system on the variability of the atria-ventricular conduction time in frequency domain has received little attention. Our study shows that the AV node is also influenced by the ANS, and that the spectral analysis of AV conduction time variability appears to be useful for the assessment of the influence of the ANS. Also our results show also that the patterns of fluctuations in AV conduction time and in RR intervals are different and that the AV node is more influenced by the parasympathetic system than the sinus node.

To avoid the indirect influences of the variation of sinus rate on the AV conduction time, a protocol was conducted in the electrophysiology laboratory with atrial pacing. Because of poor recording in some patients, valid results can not be given for the group. But through case by case analysis, preliminary observations can be given:

1) increase of mean AR interval compared to the control due to refractory effect;
2) visible peaks in the spectra of AR;
3) AR interval variations increased (both its standard deviation and its spectrum);
4) even though the AA intervals are fixed, the systolic and diastolic blood pressures vary on a beat-to-beat basis and their spectra clearly show peaks.

The observations from the pacing patients imply that 1) the variations of the AV conduction time is not caused by changes in the refractory properties of the AV node through variations of the sinus rate and 2) the conductivity of AV node is modulated by the ANS.

4.2.7 A conceptual model to explain interaction among blood pressures, AA,AR,RR and Respiration

A conceptual model (Fig. 4.1) is proposed to explain the interaction among cardiovascular variables. The objective of the cardiovascular control system is to maintain an adequate blood pressure in order to satisfy metabolism needs. As illustrated in Fig. 4.1, the mean blood pressure BP_m is the sum of the BP (product of the cardiac output (CO) and the total peripheral resistance (R)) and the dp caused by the respiratory movements on the great arteries. CO is the product of heart rate (HR) and the stroke volume (SV), while the SV is influenced by HR (AA interval, related to the duration of atrial filling period), ventricle contractility (E), change of venous return (dv) by respiration movement and AV conduction time (AR, related to the ventricular filling duration). The HR and AV are mediated by both sympathetic (S) and parasympathetic (P-S) nervous systems in responses to the blood pressure and central respiratory drive. Functions H_x in the diagram are transfer functions of the corresponding input to output. We can see that the interactions between cardiovascular variables are complex. For example, HR can affect the blood pressure, but the blood pressure in turn can modulate the HR though the baroreceptors and the ANS. The respiration influences CV variables by the direct coupling between respiratory center and the vasomotor center and by the mechanical effect of the respiration movement on the blood pressure (venous return and the squeezing of the great arteries). Study of this model in time and frequency domains with a systems identification approach may give insight of the interaction among CV variables and may reveal the autonomic control mechanism of the overall system. We have established this conceptual model from the literature and the observations in our studies.

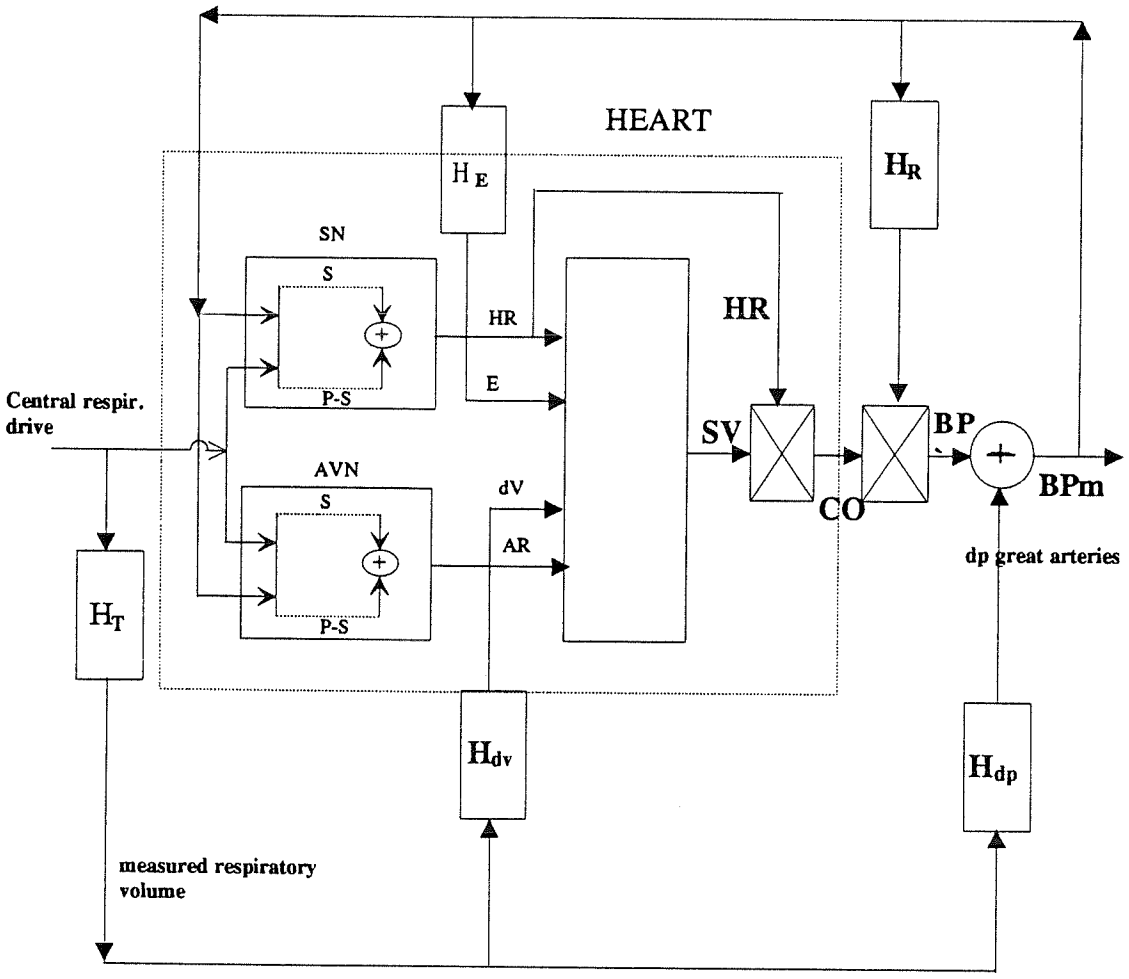

Figure 4.1 Block diagram of short term cardiovascular control mechanisms
The mean blood pressure (BPm) is the product (BP) of the total resistance (R) and the cardiac output (CO) plus the mechanical influence of respiration on the great arteries (dp). Stroke volume (SV) is influenced by HR, ventricle contractility (E), change venous return (dv) by respiration movement and AV conduction time (AR). The HR and AR are regulated by both sympathetic (S) and parasympathetic (P-S) systems. Hx are transfer functions of the corresponding input to output. Respiration influences the BPm by 1) direct coupling to cardiovascular center, 2) venous return (dv) and 3) squeezing the great arteries (dp).

4.3 Studies in hypertensive patients and patients prone to syncope

Hypertension

Comparing the hypertensive with normotensive controls in supine rest, it was found that the SD of RR was less and the SD of pressures variables were higher in hypertensive patients, suggesting that the neural buffering mechanisms appear attenuated in essential hypertension. For spectral parameters in RR and SYS, HF power was less important in hypertension. This confirms the result of Guzzetti *et al* [105]. But for the LF power our data are different from theirs. This difference is due to the LF band definition. Their LF band is our VLF and LF together. Our data showed that for the VLF power, all hemodynamic variables are significantly higher in hypertensive than in normotensive. If we combine VLF and LF powers, the results will be consistent with theirs. In supine rest the hypertensive can be characterized by loss of RR variability, increase of BP variabilities, larger VLF power and lower HF power in all variables.

With sympathetic stimulation (standing up), we found a depressed response of the parasympathetic system in hypertensive patients. This was marked by a smaller decrease of the HF power in RR and no change of the HF power in all BP variables due to a lower parasympathetic activity at baseline. This suggests a lower vagal activity in the hypertensive patients. Changes of systolic pressure in hypertensives was opposite to changes in normotensives. This may be due to different contributions to pulse pressure, which in normal subjects, is caused by a reduced stroke volume while in hypertension, it is caused by an exaggerated increase of peripheral resistance. This is confirmed by the larger increases of LF power in SYS and PULSE. The increase of LF power in RR was not different between the two groups, suggesting

again an attenuated baroreceptor sensitivity. This indicates that study of RR variability alone in the frequency domain may not be adequate to characterize the alterations in autonomic control in hypertension.

Syncope

Our results showed a higher VLF variability in RR in both supine rest and head up tilt in syncope prone subjects, while VLF fluctuations in blood pressure variables were similar to those in the control group. This instability of heart rate control in the VLF band may contribute to fainting in syncope prone subjects. Our data suggest another possible reason to explain the vasovagal syncope during tilt: insufficient withdrawal of parasympathetic activity with posture change from supine to tilt, not the absolute tone. HF power in RR, SYS and PULSE changed less than that in normal group when posture change from supine rest to head up tilt [ref. Tables 3.5 and 3.8].

4.4 Suggestions for further studies

1) A great portion of the power was found in the VLF band in each of the cardiovascular variables and power in this band changed also with stimuli, such as head up tilt. Study of the variation of CV variables in this band may give important physiological information. Very little studies have been done concerning the information content of VLF power. Thus, studies may be conducted to investigate which systems play roles in the VLF fluctuations.

2) It is assumed that fluctuations of cardiovascular variables reflect the functioning of the ANS. But the quantitative relationship between autonomic tone and variability is not clear. Further investigations could be conducted to distinguish

contributions of the variability (or stability) of autonomic tone or autonomic tone itself on the fluctuations of cardiovascular variables, such as heart rate, blood pressures, etc.

3) Since most components of the cardiovascular regulation system are involved in establishing a new equilibrium during the transition period from one physiological condition to another (supine to tilt, for example), study of changes of CV variables in this period will give more information about the cardiovascular control system. Thus, new methods (such as time domain and/or frequency domain, modelling) has to be used or developed to study these transients and non stationary processes [90].

4) Since the irregularity of the respiration can contribute to the LF power in the spectra of RR and BP variables, it will be useful to use controlled instead of spontaneous breathing. As a standardized approach, the subject can be asked to breath regularly at a rate close to his mean spontaneous rate.

Chapter 5 Conclusion

Our contributions to this domain are summarized as:

* Our data confirm the previous studies on the ANS control of the heart rate and blood pressures. The new results of our study are the detection of the spontaneous fluctuations of systolic, diastolic and pulse pressures together with the RR, AA and AV conduction time variability in supine, passive standing and active standing positions using a non-invasive method. These results represent the fluctuations of the cardiovascular variables in healthy subjects and could be used as a reasonable base for the study of impaired cardiovascular responsiveness.

* The reproducibility of VLF power in the seven studied variables was acceptable with our standardized and systematic approach. This parameter in BP variabilities shows significant decreases with a change in posture from supine rest to head up tilt in the normal group. Some of VLF power parameters differ between the normal group and the patient groups (hypertension and neurally mediated syncope). This suggests that VLF power can also be used to evaluate the functioning of the cardiovascular regulation system.

* Our data confirmed that the AV node is also modulated by the ANS and demonstrated that the pattern of ANS influence on the AV node is different from the one on the sinus node. The spectra of the beat-to-beat variations of the AV conduction time show three peaks. The spectra of the AV conduction

time variability showed a parasympathetic dominance on the regulation of the AV conduction velocity. Our data also showed that the contribution of the sinus rate on AV conduction time was of little importance in normal subjects under normal physiological conditions. This was also confirmed by using atrial pacing. Thus, spectral analysis may give new insight into the autonomic control of the AV node conduction.

* In essential hypertension, our results showed a reduction of parasympathetic activity and enhanced VLF fluctuations in the cardiovascular variables.

* In syncope prone subjects, our results showed exaggerated VLF fluctuations in cardiovascular variables and the insufficient withdrawal of parasympathetic activity response to head up tilt.

* Time and frequency domain analyses of the RR variability in anaesthetized dogs with autonomic manipulations confirm mechanisms involved in responses to drugs used by pharmacological studies in the literature.

* A standardized bedside system has been developed to evaluate non-invasively the functioning of the ANS in different physiological conditions. The complete system allowed analysis of a patient to be performed, starting from bedside signal recording to extraction of time domain and frequency domain parameters without help of other software. Normalized spectra were used.

References

1) AKSELROD, S., GORDON, D., UBEL, F.A., SHANNON, D.C., BARGER, A.C. and COHEN, R.J., Power Spectrum Analysis of Heart Rate Fluctuation: A Quantitative Probe of Beat-to-beat Cardiovascular Control. Science 213:220-223, 1981.

2) AKSELROD, S., GORDON, D., MADWED, J.B., SNIDMAN, N.C., SHANNON, D.C. and COHEN, R.J., Hemodynamic regulation: Investigation by Spectral Analysis. Am. J. Physiol. 249 (Heart Circ. Physiol. 18): H867-H875,1985.

3) ARAI, Y., SAUL, J.P., ALBRECHT, P., HARTLEY, L.H., LILLY, L.S., COHEN, R.J. and COLUCCI, W.S., Modulation of Cardiac Autonomic Activity During and Immediately After Exercise. Am. J. Physiol. 256 (Heart Circ.Physiol. 25):H132-H141, 1989.

4) BASELLI, G., CERUTTI, S., CIVARDI, S. and PAGANI M., A Model for the Evaluation of the Interactions Between Heart Rate and Arterial Blood Pressure Variability Signals. Comp. Cardiol., IEEE pub. #87CH2544-5:405-408, 1987.

5) BASELLI, G., CERUTTI, S., CIVARDI, S and RIZZO G, Toward a Modelling Heart Rate and Blood Pressure Interaction Through Parametric Bivariate Analysis. Comp. Cardiol. IEEE pub. #87CH2476-0:431-434, 1987.

6) BASELLI, G., CERUTTI, S., SILVIA, C. and GIOVANNA, R., Spectral Analysis of Heart Rate and Arterial Blood Pressure Variability Signals for Physiological and Clinical Purposes. Comp. Cardiol. IEEE 0276-6574/87/0000/0435, 1987.

7) BASELLI, G., CERUTTI, S., CIVARDI, S, LIBERADI D, LOMBARDI, F, MALLIANI, A and PAGANI, M, Spectral and Cross-spectral Analysis of Heart Rate and Arterial Blood Pressure Variability Signals. Computer and

Biomedical Research 19, 520-534, 1986.

8) BASELLI, G, CERRUTI, S, CIVARDI, S, MALLIANI, A and PAGANI, M, Cardiovascular Variability Signals: Towards the Identification of a Closed-loop Model of the Neural Control Mechanisms, IEEE Trans. Biomed. Eng., vol. 35, No. 12, Dec. 1988.

9) BERGER, RD, AKSELROD, S, CIRDON, D and COHEN, RJ, An Efficient Algorithm for Spectral Analysis of Heart Rate Bariability, IEEE Trans. Biomed. Eng., vol. 33, No. 9:900, Sept. 1986.

10) BERGER, R.D., SAUL, J.P and COHEN, R.J, Transfer Function Analysis of Autonomic Regulation I. Canine Atrial Rate Response, Am. J. Physiol. 256 (Heart Circ. Physiol. 25): H142-H52, 1989.

11) SAUL, J.P, BERGER, R,D., CHEN, M.H. and COHEN, R.J, Transfer Function Analysis of Autonomic Regulation II. Respiratory Sinus Arrhythmia, Am. J. Physiol. 256 (Heart Circ. Physiol. 25):H153-H161, 1989.

12) BILLMAN, G.E. and HOSKINS, R.S., Time-series Analysis of Heart Rate Variability During Submaximal Exercise, Evidence for Reduced Cardiac Vagal Tone in Animals Susceptible to Ventricular Fibrillation, Circulation 80:146-157,1989.

13) DE BOER, R.W. KAREMAKER, J.M. and STRACKEE, J., Relationship Between Short-term Blood Pressure Fluctuations and Heart Rate Variability in Resting Subjects I: A Spectral Analysis Approach, Med. & Biol. Eng. & Comput. 23, 352-358,1985.

14) BORST, C. and KAREMAKER, J.M, Time Delays in the Human Baroreceptor Reflex, J. of Autonomic Nervous System, 9, 399-409, 1983.

15) CHEN, M.H., BERGER, R.D., SAUL, J.P., STEVENSON, K. and COHEN, R.J, Transfer Function Analysis of the Autonomic Response to Respiratory Activity during Random Interval Breathing, IEEE Comp. Cardiol.,

0276-6574/87/0000/0149, 149-152, 1987.

16) CRAELIUS, W, CHEN, VKH, RESTIVO, M. and EL-SHERIF, N., Rhythm Analysis of Arterial Blood Pressure, IEEE Trans. Biomed. Eng., vol. 33, No. 12, Dec. 1986.

17) DEBOER, RW, KAREMAKER, JM and STRACKEE, J, Comparing Spectra of a Series of Point Events Particularly for Heart Rate Variability Data, IEEE Trans. Biomed. Eng.,vol. 31, No. 4, 384-387, April 1984.

18) FALLEN, E, KAMATH, MV and GHISTA, DN, Power Spectral of Heart Rate Variability: a Non-invasive Test of Integrated Neural Cardiac Function, Clinical and Investigative Medicine, vol. 11, No. 5, 331-340, 1988.

19) HIRSCH, J.A. and BISHOP, B., Respiratory Sinus Arrhythmia in Humans: How Breathing Pattern Modulates Heart Rate, Am. J. Physiol. 241 (Heart Circ.Physiol. 10):H620-H629, 1981.

20) BERGER, R.D., SAUL, J.P., COHEN, R.J, Assessment of Autonomic Response by Broad-band Respiration, IEEE Trans. Biomed. Eng., vol. 36, No. 11, 1061-1065, Nov. 1989.

21) KALLI, S, GRONLUND, J, IHALAINEN, H, SIIMES, A, VALIMAKI, I and ANTILA, K, Analysis of Blood Pressure and Heart Rate Variability Using Multivariate Autoregressive Modelling, IEEE Comp.Cardiol., 0276-6574/87/0000/0427, 1987.

22) KALLI, S, GRONLUND, J, IHALAINEN, H, SIIMES, A, VALIMAKI, I and ANTILA, K, Multi Autoregressive Modelling of Autonomic Cardiovascular Control in Neonatal Lamb, Computer and Biomed. Res. 21, 512-530, 1988.

23) KITNEY, RI, FULTON, T and MCDONALD, A, Transient Interaction Between Blood Pressure, Respiration and Heart Rate in Man, J. Biomed. Eng. vol. 7, 217-224, July 1985.

24) KOLLAI, M., Cardiovascular Reflexes and Interrelationships between Sympathetic and Parasympathetic Activity. J. of the Autonomic Nervous System, 4, 135-148, 1981.

25) LINDQVIST, A., PARVIAINEN, P., KOLARI, P., TUOMINEN, J., VALIMAKI, I., ANTILA, K. and LAITINEN, L.A, A Non-invasive Method for Testing Neural Circulatory Control in Man, Cardiovascular Research, 23, 262-272, 1989.

26) LOEB, JM and DETARNOWSKY, JM, Integration of Heart Rate and Sympathetic Neural Effects on AV Conduction, Am. J. Physiol. 254 (Heart Circ. Physiol. 23):H651-H657,1988.

27) LOMBARDI, F, SANDRONE, G, PERNPRUNER, S, SALA, R, GARIMOLDI, M, CERRUTI, S, BASELLI, G, PAGANI, M and MALLIANI, A, Heart Rate Variability as an Index of Sympathovagal Interaction After Acute Myocardial Infarction, Am. J.Cardiol. 60:1239-1249, 1987.

28) MADWED, J.B., ALBRECHT, P., MARK, R.G. and COHEN, R.J, Low-frequency Oscillation in Arterial Pressure and Heart Rate: A Simple Computer Model, Am. J. Physiol. 256 (Heart Circ. Physiol. 25):H1573-H1579, 1989.

29) MANCIA, G, BONAZZI, I, POZZONI, A, FERRARI, M, GARDUMI, L, GREGORINI, L, and PERONDI, R, Baroreceptor Control of Atrioventricular Conduction in Man, Circ. Res. 44:752-758, 1979.

30) O'TOOLE, M., Parallel Baroreceptor Control of Sinoatrial Rate and Atrioventricular Conduction, Am. J. Physiol. 246 (Heart Circ.Physiol. 15):H149-H153, 1984.

31) PAGANI, M,LOMBARDI, F, GUZZETTI, S, RIMOLDI, O, FURLAN, R, PIZZINELLI, P, SANDRONE, G, MALFATTO, G, DELL'ORTO, S, PICCALUGA, E, TURIEL, M, BASELLI, G, CERRUTI, S and MALLIANI,

A, Power Spectral Analysis of Heart Rate and Arterial Pressure Variability as a Marker of Sympatho-vagal Interaction in Man and Conscious Dog, Circ. Res. 178-193, 1986.

32) POMERANZ, B., MACAULAY, RJB., CAUDILL, MA., KUTZ, I., ADAM, D., GORDON, D., KILBORN, KM., BARGER, AC., SHANNON, DC., COHEN, RJ., and BINSON, H., Assessment of Autonomic Function in Humans by Heart Rate Spectral Analysis, Am. J. Physiol. 248 (Heart Circ. Physiol.17):H151-H153, 1985.

33) RIENZO, M.D., CASTIGLIONI, P., MANCIA, G., PARATI, G. and PEDOTTI, A., 24 h Sequential Spectral Analysis of Arterial Blood Pressure and Pulse Interval in Free-moving Subjects, IEEE Trans.Biomed. Eng. vol. 36, No. 11, 1066-1075, Nov. 1989.

34) SANDERS, J.S. and FERGUSON, D.W., Diastolic Pressure Determines Autonomic Responses to Pressure Perturbation in Humans, J. Appl. Physiol.66(2):800-807, 1989.

35) WARNER, MR and LOEB, JM, Beat-by-beat modulation of AV conduction I. Heart Rate and Respiratory Influences, Am. J. Physiol. 251 (Heart Circ.Physiol. 20):H1126-H1133, 1986.

36) WARNER, MR, DETARNOWSKY, JM, WHITSON, CC and LOEB, JM, Beat-by-beat Modulation of AV Conduction II. Autonomic Neural Mechanisms, Am. J. Physiol. 251(Heart Circ. Physiol.20):H1134-H1142, 1986.

37) ZWIENER, U., Physiological Interpretation of Autospectra, Coherence and Phase Spectra of Blood Pressure, Heart Rate, and Respiration Waves in Man, Automedica, vol. 2, 161-169, 1978.

38) APPEL, ML, SAUL, JP, BERGER, RD and COHEN RJ, Assessment of the HR Baroreflex in Human Subjects Using Parametric System Identification, Computer in Cardiology, IEEE PUB. 89CH2770-6, 4-5, 1989.

39) LUDWIG, L., Beitrage Zur Kenntnis des Einflusses der Respirations-bewegungen auf den Blutulauf im Aortensystem, Arch. Anat. Physiolo., 242-257, 1847.

40) HYNDMAN, BW, KITNEY, RI and SAYERS, BMcA, Spontaneous Rhythms in Physiologic Control Systems, Nature Lond. 233:399-341, 1971.

41) KITNEY, RI and ROMPOLMAN, O., The Study of Heart Rate Variability, Oxford: Clarendon, 59-107, 1980.

42) SAYERS, B.McA, Analysis of Heart Rate Variability, Ergonomics 16:17-32, 1973.

43) CERUTTI, S, BIANCHI, A, BONTEMPI, B, COMI, G, GIANOGLIO, P and SORA, MG, Power Spectrum Analysis of Heart Rate Variability Signal in the Diagnosis of Diabetic Neuropathy, Comp. Cardiol., IEEE PUB. 89CH2770-6, 12-13, 1989.

44) TREMBLAY, G. and LEBLANC, A-R., Near-optimal Signal Processor for Positive Cardiac Arrhythmia Identification, IEEE Trans. Biomed. Eng., vol. BME-32, No. 2, Feb, 1985.

45) DE CHAMPLAIN, J., Pre- and Postsynaptic Adrenergic Dysfunction in Hypertension, Journal of Hypertension, 8 (suppl 7): S77-S85, 1990.

46) KAPLAN, DT., FURMAN, MI., PINCUS, SM., RYAN, SM. and LIPSITZ, LA., Aging and the Complexity of Cardiovascular Dynamics, Biophys. J., volume 59, 945-949, April 1991.

47) GRIESEN, GM, JANNETT,TC., JADALLAH, MA., YATES, SL., QUINT, SR. and NAGLE, HT., A Comparison of the Noise Sensitivity of Nine QRS Detection Algorithms. IEEE Transactions on Biomedical Engineering, VOL. 37. NO. 1. January 1990.

48) PAHLM O. AND SORNMO L., Software QRS Detection in Ambulatory

Monitoring a Review, Med. & Biol. Eng. & Comput., 22, 289-297, 1984.

49) RYAN, SM., GOLDBERGER, AL., RUTHAZER, R., MIETUS, J. and LIPSITZ, L., Spectral Analysis of Heart Rate Dynamics in Elderly Persons with Postprandial Hypotension, Am J. Cardiol. 69, 201-205, 1992.

50) LOEB, JM. and DETRARNOWSKY, M., Modulation of the Atrioventricular Conduction in Vivo: Integration of the Heart Rate and Autonomic Neural Input, a chapter in "Electrophysiology of the Sino-Atrial and Atrioventricular Nodes: Integrative Physiologic, Morphologic, Autonomic, and Pharmacologic Aspects, Edited by Leonard Dreifus, Yoshio Watanabe, and Todor Mazgalev, Alan R. Liss, Inc., New York, 1988.

51) PAGE, RL., TANG, ASL. and PRYSTOWSKY, EN., Effect of Continuous Enhanced Vagal Tone on Atrioventricular Nodal and Sinoatrial Nodal Function in Humans, Circulation Research, 68, 1614-1620, 1991.

52) WALLICK, DW., and MARTIN, PJ., Separate ParaSympathetic Control of Heart Rate and Atrioventricular conduction of dogs, Am. J. Physiol. 259, H536-H542, 1990

53) NAYEBPOUR, M., TALAJIC, M., VILLEMAIRE, C. and NATTEL, S., Vagal Modulation of the Rate-Dependent Properties of the Atrioventricular Node, Circulation Research, 67, 1152-1166, 1990.

54) WALLICK, DW., XU, RG. and MARTIN, PJ., Dynamic Interaction of Vagal Activity and Heart Rate on Atrioventricular Conduction, Am. J. Physiol, 262 (Heart Circ. Physiol. 31): H792-H798, 1992.

55) NEELY, BH. and URTHALER, F., Quantitative Effects of Sympathetic and Vagal Nerve Stimulations on Sinus and AV Junctional Rhythms, Journal of the Autonomic Nervous System, 37, 109-120, 1992.

56) VAN LIESHOUT, JJ., WIELING, W., KARENAKER, JM. and ECKBERG, DL., The Vasovagal Response, Clinical Science, 81, 575-586, 1991.

57) CANALE, E.D., CAMPBELL, G.R., SMOLICH, J.J. and CAMPBELL, J.H., Innervation of the heart. In: A. Oksche and L. Vollrath (eds), Handbook of Microscopic Anatomy, Vol. II/7, Springer-Verlag New York, pp. 104-142, 1986.

58) LEVY, M.N., and MARTIN, P.J., Neural Control of the Heart. In R. Berne and N. Sperelakis (Eds.), Handbook of Physiology -The Cardiovascular System, The American Physiological Society, Bethesda, MD, pp. 581-620, 1980.

59) ROSSBERG, F. and PENAZ, J., Heart Rate and Arterial Pressure Variability in Humans During Different Orthostatic Load, Physiol. Res. 41: 19-23, 1992.

60) SCHWEITZER A., Rhythmical fluctuations of the Arterial Blood Pressure. J. Physiol (lond), 104:25P, 1945.

61) MAYER S., Uber Spontane Blutdruckschwankungen, Sber. Akad. Wiss. Wien, 74, 281, 1876.

62) MALLIANI A., PAGANI M., LOMBARDI F. and CERUTTI S., Cardiovascular Neural Regulation Explored in the Frequency Domain, Circulation, vol. 84, No. 2, 482-492, August 1991.

63) WIELING W., BORST C., KAREMAKER J.M. and DUNNING A.J., Testing for Autonomic Neuropathy: Initial Heart Rate Response to Active and Passive Changes of Posture,

64) EWING D.J., NEILSON J.M.M, SHAPIRO C.M., STEWART J.A. and REID W., Twenty Four Hour Heart Rate Variability: Effects of Posture, Sleep, and Time of Day in Healthy Controls and Comparison with Bedside Tests of Autonomic Function in Diabetic Patients, Br. Heart J., 65:239-44, 1991.

65) BIANCHI A., BONTEMPI B, CERUTTI S., GIANOGLIO P., COMI G. and NATALI SORA M.G., Spectral Analysis of Heart Rate Variability Signal and

Respiration in Diabetic Subjects, Med. & Biol Eng. & Comput. 28, 205-211, 1990.

66) HAYANO J, SAKAKIBARA, Y, YAMADA, M, OHTEM, N, FUJINAMI, T, YOKOYAMA, K, WATANABE, Y and TAKATA, K, Decreased Magnitude of Heart Rate Spectral Components in Coronary Artery Disease, Its Relation to Angiographic Severity, Circulation, vol 81, No. 4, April 1990.

67) KARAGUEUZIAN HS, KHAN, SS, PETERS, W, MandEL, WJ and DIAMOND, GA, Nonhomogeneous Local Arterial Activity During Acute Fibrillation: Spectral and Dynamic Analysis, Pace, vol 13, 1937-42, Dec. 1990.

68) BIGGER JT, KLEIGER, RE, FLEISS, JL, ROLNITZKY, LM, STEINMAN, RC, MILLER, JP, and the Multicenter Post-Infaction Research Group, Components of Heart Rate Variability Measured During Healing of Acute Myocardial Infarction, Am. J. Cardiol., 61:208-215, 1988.

69) KLEIGER RE, MILLER, JP, BIGGER, JR and MOSS, AJ, Decreased Heart Rate Variability and Its Association with Increased Mortality After Acute Myocardial Infarction, Am. J. Cardiol., 59:256-262, 1987.

70) SAUL JP, ARAI, Y, BERGER, RD, LILLY, LS, COLUCCI, WS and COHEN JR, Assessment of Autonomic Regulation in Chronic Congestive Heart Failure By Heart Rate Spectral Analysis, Am. J. Cardiol., 61:1292-1299, 1988.

71) BIGGER JT, FLEISS, JL, STEINMAN, RC, ROLNITXKY, LM, KLEIGER, RE and ROTTMAN JN, Correlation Among Time and Frequency Domain Measures of the Heart Rate Variability Two Weeks After Acute Myocardial Infarction, Am. J. Cardiol., 69:891-898, 1992.

72) LIPSITZ LA, MIETUS, J, MOODY, GB and GOLDBERGER, AL, Spectral Characteristics of Heart Rate Variability During Postural Tilt, Relations to Aging and Risking of Syncope, Circulation, 81:1903-1810, 1990.

73) LERMAN-SAGLE T, RECHAVIA, E, STRASBERG, B, SAGIE, A, BILEDEN, L and MOMOUNI, M, Head-up Tilt for the Evaluation of Syncope of Unknown Origin in children, J. Pediatr., 118:676-9, 1991.

74) PERRY JC and GARSON, A, The Child with Recurrent Syncope: Autonomic Function Testing and Beta-Adrenergic Hypersensitivity, J. Am. College of Cardiol., vol 17, No. 5, 1168-71, April 1991.

75) SRA JS, andERSON, AJ, SHEIKH, SH, AVITALL, B, TCHOU, PJ, TROUP, PL, GILBERT, CJ and AKHTAR, M, Unexplained Syncope Evaluated by Electrophysiologic Studies and Head-up Tilt Testing, Annals of Internal Medicine, 114:1013-19, 1991.

76) SCHAAL SF, NELSON, SD, BOUDOULAS, H and LEWIS, RP, Syncope, Current Problems in Cardiology, vol. 17, No. 4, April 1992.

77) WADDELL S., Vasovagal Syncope, Critical Care Nurse, vol 9, No. 6, 35-43, 1985.

78) TUCK M.L., Obesity, the Sympathetic Nervous System and Essential Hypertension, Hypertension, 19[suppl I]:I-67--I-77, 1992.

79) SAFAR M., Clinical Research in Essential Hypertension, Schattauer, 76-132, 1989.

80) ZATSIORSKY V.M. and SAESANIYA S.K., Avtokor Relatsionnyi Analiz Dlitelnostey Serdechnykh Ciklov Cheloveka, Ciofizika, 11, 928-931, 1966.

81) TAYLOR M.G., Use of Random Excitation and Spectral Analysis in the Study of Frequency-Dependent Parameters of the Cardiovascular System, Circ. Res., 18, 585-595, 1966.

82) PENAZ J. and FISHER B., Amplitudove Spektrum Spontanich Vln Pletysmogramu a Tepove Frekvence u Cloveka (Amplitude Spectrum and Heart Rate in Man), Cs. Fysiol., 15, 517, 1966.

83) PENAZ J., ROUKENS J. and WAAL H.J.V.D., Spectral Analysis of Some Spontaneous Rhythms in the Circulation, in Biokybernetik (Ed. H. Drischel and N. Tiedt), K. Marx Universitat, Leipzig, 233-236, 1968.

84) JORDAN D., The inhibitory Control of Vagal Cardiomotor Neurons, J. Physiol., London, 301:54p-55p, 1980.

85) MELCHER C., Respiratory Sinus Arrythmia in Man, A Study in Heart Rate Regulating Mechanisms. Acta Physiol. Scand Suppl. 435:1-31, 1976.

86) CLYNES M., Respiratory Sinus Arrhythmia: Laws Derived from Computer Simulation, J. Appl. Physol. 15:863-874, 1960.

87) VYBIRAL, T., BRYG, R.J., MADDENS, M.E. and BODEN W.E., Effect of Passive Tilt on Sympathetic and Parasympathetic Components of Heart Rate Variability in Normal Subjects, AM J Cardiol, 63:1117-1120, 1989.

88) ROBBE, H.W.J., MULDER, L.J.M., RUDDEL, H., LANGEWITZ, W.A., VELDMAN, J.B.P. and MULDER, G., Assessment of Baroreceptor Reflex Sensitivity by Means of Spectral Analysis, Hypertension, 10:538-543, 1987.

89) KAMATH, M.V., FALLEN, E.L. and GHISTA, D., Microcomputerized On-line Evaluation of Heart Rate Variability Power Spectra in Humans, Comput. Biol. Med. Vol. 18, No. 3, 165-171, 1988.

90) NOVAK, P. and NOVAK, V., Time Frequency Mapping of the Heart Rate, Blood Pressure and respiratory Signals, Medical & Biological Engineering & Computing, volume 31, pp.103-110, 1993.

91) BILLMAN, G.E. and DUJARDIM J.P., Dynamic Changes in Cardiac Vagal Tone as Measured by Time-Series Analysis, Am. J. Physiol. 258 (Heart Circ. Physiol. 27):H896-H902, 1990.

92) DE BOER R.W., KAREMAKER, J.M. and STRACKEE, J., Relationships Between Short-Term Blood Pressure Fluctuations and Heart Rate Variability

in Resting Subjects II: a Simple Model, Med. & Biol. & Comput., 23, 359-364, 1985.

93) DE BOER R.W., KAREMAKER, J.M. and STRACKEE, J., Hemodynamic Fluctuations and Baroreflex Sensitivity in Humans: a Beat-to-Beat Model, Am. J. Physiol. 253 (Heart Circ. Physiol. 22):680-689, 1987.

94) SAUL, J.P., BERGER, R.D., LABRECHT, P., DTEIN S.P., CHEN. M.H. and COHEN R.J., Transfer Function analysis of the Circulation: Unique Insights into Cardiovascular Regulation, Am. J. Physiol. 258 (Heart Circ. Physiol. 30):H1231-1245, 1991.

95) SAUL, J.P., REA, R.F., ECKBERG, D.L., BERGER, R.D. and COHEN, R.J., Heart Rate and Muscle Sympathetic Nerve Variability During Reflex Changes of Autonomic Activity, Am. J. Physiol. 258 (Heart Circ. Physiol. 27):H713-H721, 1990,

96) DIXON E., KAMATH, M.V., MCCARTNEY N. and FALLEN E.L., Neural Regulation of Heart Rate Variability in Endurance Athletes and Sedentary Controls, Cardiovascular Research, 26:713-719, 1992.

97) WOMACK, B.F., The Analysis of Respiratory Sinus Arrhythmia Using Spectral Analysis ans Digital Filtering, IEEE Trans. on Bio-medical Eng., Vol. BME-18, No. 6, 399-409, November 1971.

98) WEISE F., BALTRUSCH, K. and HEYDENREICH, F., Effect of Low-dose Atropine on Heart Rate Fluctuations During Orthostatic Load: a Spectral Analysis, J. of the Antonomic Nervous System, 26:223-230, 1989.

99) KUNITAKE, T. and ISHIKO N., Power Spectrum Analysis of Heart Rate Fluctuations and Respiratory Movements Associated with Cooling the Human Skin, J. of the Autonomic Nervous System, 38:45-56, 1992.

100) DE BOER, R.W., KAREMAKER J.M. and STRACKEE J., Comparing Spectra of a Series of Point Events Particularly for Heart Rate Variability

Data, IEEE Trans. on Biomedical Engineering, Vol. BME-31, No. 4, 384-387, April 1984.

101) FALLEN, E.L., KAMATH, M.V., GHISTA, D.N. and FITCHETT, D., Heart Rate Variability Power Spectra in Normal Subjects and in Patients with Cardiac Dysfunction, IEEE/Ninth Annual Conference of the Engineering in Medicine and Biologi Society, CH2513-0/87/0000-0523-0524, 0523-0524 1987.

102) AKSELROD, S., ARBEL, J., OZ, O., BENARY, V. and DAVID, D., Spectral Analysis of the HR Fluctuations in the Evaluation of Autonomic Control During Acute Myocardial Infarction, IEEE Comput. Cardiol., 0276-6574/85/0000/0315-0318, 315-316, 1985.

103) BORST, C., Initial Heart Rate Response to Standing, IEEE/Ninth Annual Conference of the Engineering in Medicine and Biology Society, ch2513-0/87/0000-0893, 0893-0894, 1987.

104) PAGANI, M., FURLAN, R., DELL'ORTO, S., PIZZINELLI, P., BASELLI, G., CERUTTI, S., LOMBARDI, F. and MALLIANI, A., Simultaneous Analysis of Beat by Beat Systemic Arterial Pressure and Heart Rate Variability in Ambulatory Patients, Journal of Hypertension 3(suppl 3):S83-S85, 1985.

105) GUZZETTI, S., PICCALUGA, E., CASATI, R., CERUTTI, S., LOMBARDI, F., PAGANI, M. and MALLIANI, A., Sympathetic Predominance in Essential Hypertension: a Study Employing Spectral Analysis of Heart Rate Variability, Journal of Hypertension, 6:711-717, 1988.

106) SANDS, K.E.F., APPEL, M.L., LILLY, L.S., SCHOEN, F.J., MUDGE, G.H. and COHEN, R.J., Power Spectral Analysis of Heart Rate Variability in Human Cardiac Transplant Recipient, Circulation, 79:76-82, 1989.

107) IZRAELI, S., ALCALAY, M., WALLACH, R., TOCHNER, Z. and AKSELROD, S., Pharmacological Modulation of Parasympathetic Cardiac Control: Dose-dependent Effect of Atropine of the Power Spectrum of the

Heart-Rate Fluctuations, Proceedings of Computers in Cardiology, IEEE 0276-6574/90/0000/0057, 57-60, 1989.

108) ABI-SAMRA, F.M., FOUAD, F.M., BRAVO, E.L., MALONEY, J.D. and CASTLE, L.W., Vasovagal Syncope: Vagal Overtone or Lack of Sympathetic Stimulation?, Abstracts: Circulation, Vol. 74, Supp II, II-182, October 1986.

109) KAMATH, M.V., GHISTA, D.N., FALLEN, E.L., FITCHETT, D., MILLER, D. and MCKELVIE, R., Heart Rate Variability Power Spectrogram as a Potential Noninvasive Signature of Cardiac Regulatory System Response, Mechanisms, and Disorders, Heart Vessels, 3:33-41, 1987.

110) BINKLEY, P.F., NUNZIATA, E., HAAS, G.J., NELSON, S.D. and CODY, R.J., ParaSympathetic Withdrawal Is an Integral Component of Autonomic Imbalance in Congestive Heart Failure: Demonstration In Human Subjects and Verification in a Paced Canine Model of Ventricular Failure, J. Am. Coll. Cardiol., 18:464-74, 1991.

111) BURKE, D., SUNDLOF, G. and WALLIN B.G., Postural effects on muscle Sympathetic Activity in Man. J. Physiol. Lond. 272:399-414, 1977.

112) MADWED, JB, SANDS, KEF, SAUL, JP and COHEN, RJ, Spectral Analysis of beat-to-beat Variability in Heart Rate and Arterial Blood Pressure during Haemorrhage and Aortic Constriction, In *Neural Mechanisms and Cardiovascular Disease*, Lown B, Malliani A, Prosdocimi M (eds), Fidia Research Series, vol. 5, Liviana Press, Padova, 1986.

113) FISER, B., HONZIKOVA, N. and PENAZ, J., Power Spectra of Spontaneous Variations of Indirectly Recorded Blood Pressure, Heart Rate and Arterial Blood Flow, Automedica, 2, 143-147, 1978.

114) BOUDREAU, G., Effect de la modification du contenu d'adrénaline du myocarde sur la libération d'adrénaline et de noradrénaline par les fibres sympathiques cardiaques chez le chien anesthésiés, Ph.D. dissertation, Université de Montréal, 1992.

115) LANGER, SZ. and ARBILLA S., Presynaptic Receptors on Peripheral Noradrenergic Neurons, Presynaptic Receptors and the Question of Autoregulation of Neurotransmitter Release, edited by Kalsner, S. and Westfall, TC., Annals of the New York Academy of Sciences, volume 604:7-16, 1990.

116) LEVY, MN. and WARNER MR., Autonomic Interactions in Cardiac Control: Role of Neuropeptides, pp. 305-311, in Cardiac Electrophysiology, From Cell to Bedside, edited by Zipes, DP. and Jalife, J., W.B. Saunders Company, Harcourt Brace Jovanovich, Inc., 1990.

Appendix A Spectral Analysis Guide

The following sections present a step by step procedure to use our spectral analysis package (ref. Figure A.1). This package requires an IMB PC, PS/2 or compatible with DOS version 2.0 or higher, graphic card (supporting CGA, EGA or VGA and Hercules), hard disk with 5 MB free space. The data acquisition program also requires a computer equipped with an A/D card (Data Translation, model DT2801).

1. Acquisition of the signals

The acquisition program can be accessed from DOS by the ACQ8 command. This program will create a signal file (*.SIG). Subsequent programs will use it to produce graphs and results from spectral analysis.

This software allows acquisition of at most eight independent simultaneous signals. A maximum of four simultaneous signals will appear on screen. It is therefore important for the user to take note of additional signals if any. The program will ask the following information: (items in square brackets [] are optional)

1. patient name;
2. patient identification (reference code);
3. [a brief description of the patient];
4. [a brief description of the experiment];
5. the number of channels (corresponding to the number of signals);
6. name of signal on each channel (ECG, PRES, RESP, DP/DT...) (order corresponds to hardware connection 0-7);

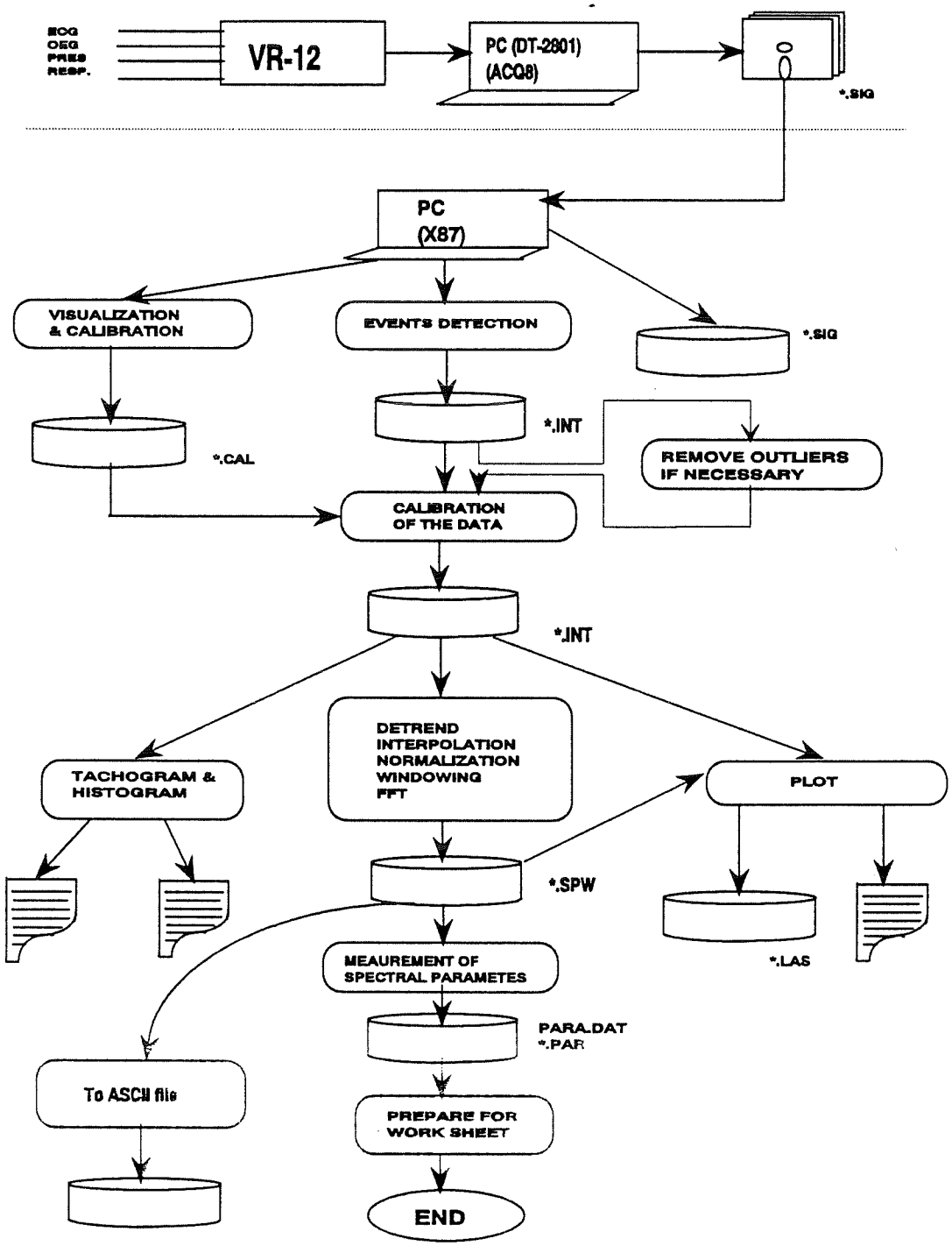

Figure A.1 Flowchart of the data processing procedure

7. the recording gain, 2 for humans and dogs;
8. sampling frequency (used as: dogs=500, humans=250);
9. recording duration (seconds) (calculated to include at least 532 heart beats);
10. a letter to identify recording sequence in the experiment for a given patient.

Then a file *.SIG (filename is generated Automatically as NNNMMDDL.SIG, where NNN are the first three letters of patient name, MM and DD are the month and date when the experiment is conducted, L is the recording sequence given in item 10) with a size required by the given duration will be created on the hard disk and filled up with zeroes. This reduces the disk access time during recording because the linkage of sectors has been established. After this initiation step, signals will be displayed. Recording will be started once key S is pressed. The recording will stop when the duration given in item 9 has elapsed or key Q is pressed.

It is important to make sure that none of the signals saturates the screen. It is equally important that the amplitude of the signal occupies approximately 75% of the dynamic range of the A/D converter. Adjusting the gain at the source of the signal or choosing the appropriate gain of the A/D board (in item 7) will insure that the signal is within acceptable limits.

2. Recording the calibration signal for the blood pressure

The blood pressure signal needs calibration information to convert the unit voltages into mmHg. The calibration signal should be generated and stored to a file before recording blood pressure signals. The calibration signal should give levels of 0 mmHg and 100 mmHg. Calibration signal recording is performed the same way

as presented in section 1.

3. Extraction of the calibration information

The calibration signal cannot be used directly to calibrate the blood pressure. A program has been written to read the calibration signal and to give: 1) factor, number of A/D conversion unit for 1 mmHg; 2) offset of the 0 mmHg level in mmHg. It is designed this way because the calibration procedure may vary from one laboratory to another.

This program will run with the Hercule Graphics Mode (see your graphic adaptor manual for the command to switch between display modes). The program is invoked by typing VIEWCALI /h<RETURN>, where /h forces the program run in Hercule mode. The program will ask for the type of acquisition card, the current type is a 12 bit card. The next step is to select item 1: view a file on screen. The filename is then entered and the file is viewed frame by frame, not continuously.

At this stage signals appear on the screen as well as a menu bar at the top of the screen. Menu items can be accessed using the space bar or by typing the capitalized letter in each menu item. On screen, cursors appear once the cursor keys are pressed, their locations are then controlled by the left and right cursor keys. An arrow indicates the cursor currently under control, the cursors are numbered from right to left (1,2 and 3). Control is passed from one cursor to another by typing the corresponding number.

Commands and their corresponding functions are:

1. Begin: returns on screen viewing to the beginning of the file;
2. Exit: return to DOS;
3. Next: view next frame;
4. Prec: returns the on screen viewing to the previous frame;
5. Calib: calibrate the signal
    1. cursor 1 must be at the minimum and cursor 2 at the maximum;
    2. calculate values once at least three positions are taken;
    3. exit to viewing mode.
6. Zoom: change the time window for viewing.

The program will create a calibration file with a CAL extension using the same format as the SIG files. Since one calibration file might apply to more than one signal (SIG) file, it is the user's responsibility to note which SIG files are associated with a given calibration (CAL) file.

4. Detection of events

This section of the package is accessed from DOS using the DETHUM command for humans, the DETRAT command for rats or the DETDOG command for dogs. These programs differ only in their output and not in the manner that they are used. The command line arguments are filename (*.SIG) [\t] [\v] (wildcards are accepted), the arguments in brackets being optional. The second argument allows the user to specify the time (in seconds) at which he or she wishes to begin the detection. The third argument specifies on screen viewing.

The first menu to appear allows to choose the graphic adaptor and the pointing

device. It can be accepted without modification since the program detect automatically the type of graphic card on the machine where the program is running. The second menu allows the user to specify which file is to be analyzed. One last menu updates default information regarding the detection itself, the default values for the channels and their corresponding signals are usually the only values that need modifications.

The detection of events is achieved by placing markers at R waves of the ECG signal. When the program runs in supervised mode, signals and markers will be displayed. Several beats will appear on screen, if all the events in the frame are correctly identified, the PAGE UP key calls the next frame in the time window. The PAGE DOWN key allows to return to the previous frame, while the HOME and END keys set on screen viewing to the beginning and end of the time window respectively. If the events in all the frames of a given window are correctly identified then the N key calls the next time window (important: once the next time window is accessed it is impossible to return to a previous window to make cursor editing). If the program seems to be finding all the events in several consecutive windows, the C key allows the program to work unsupervised. Once 532 R waves have been detected or the end of file has been reached the program terminates Automatically and creates a new file *.INT.

The program will usually correctly identify all events in the signal, but errors do occur in noisy signals. There are two kinds of errors:

1. The program incorrectly places the cursor.

Solution: -visually position the cursor at the incorrectly marked R wave and press the delete key to remove the false event;

-place visually the cursor at the correct position and press the insert key to add an event.

2. An error message appears on screen.

Solution: -it is best to go to the end of the time window (END key). Proceeding backwards delete any misplaced cursors or insert any missing cursors. This procedure often avoids time consuming fatal errors.

Summary of key functions:

Note: A time window corresponds to a certain duration of signals to be processed each time. A frame is part of the time window to be displayed on the screen, which varies according to the resolution of the graphic adaptor used.

1. Cursor keys: position cursor;
2. INSERT key: insert an event;
3. DELETE key: delete an event;
4. PAGE UP key: next frame in time window;
5. PAGE DOWN key: previous frame;
6. N key: go to next time window;
7. C key: allow program to work unsupervised (Automatic mode);
8. E key: exit before 532 events detected.

Note: 1) Once a time window is left it is impossible to return to it. Errors can no longer be corrected except by restarting the detection over again.

2) Another version of this detection program, which detects events in a file

until the end of file has been reached instead of a maximum of 532 R waves, is also available. But the output of this program cannot be processed further with this package directly (revised for another project).

5. Elimination of extrasystoles or outlier

There are two programs used to accomplish this task. One program is applied to *.EXT files and the other to *.INT files. In DOS, the files are processed by typing EXTRASYS filename.EXT or EXTRAINT filename.INT. The differences between *.EXT files and *.INT file are the number of events, the former contains 532 events but the latter contains 512 events. The program EXTRASYS reads *.EXT file and generates *.INT files. The *.EXT files can not be used directly for spectral analysis with this package since a 512 point limit was imposed

*.INT files are used to produce tachograms and are further processed for spectral analysis.

This procedure can be repeated several times if necessary. Usually, we can check the tachogram if there are any extrasystoles or outlier (with appearance of big sudden changes) and then decide if the procedure is needed.

6. Calibration of a signal

The *.CAL files, created in step 3, are used to calibrate the *.INT files (blood pressure signal only). In DOS this is done by typing:

PRESCALI filename.INT filename.CAL

Note: any *.CAL file will work with any INT file, any error will not be noticed by the program. The *.INT file is modified and cannot be recovered.

7. Creation of the spectral analysis files

Spectral estimation is applied on a *.INT file and the resulting spectra is stored in a *.SPW file. The *.SPW file is created by typing SPNORMAL filename.INT for dogs and humans and SPRAT filename.INT for rats.

8. Extraction of spectral parameters

SPPA1 filename.SPW [\v] <RETURN> (for human and dogs)

When parameter \v is omitted, the spectral parameters will be measured without the user's supervision. When \v is applied, first the spectrum of respiration signal will be displayed with a horizontal bar marking the HF band which was defined according to the criteria given in chapter 2. This band can be modified by repositioning the limits. Type key E to accept the HF band, which can also be modified in other spectra (RR, SYS,..). Then a menu appears to allow user to select a spectrum to visualize. The spectrum is plotted with three bars to mark the three bands (VLF, LF and HF). Parameters of each peak are also displayed at the right top corner. The program allows the user to position a cursor on a spectral peak and to modify band limits. Once a band is changed, it will be applied for all spectra to calculate the areas in the band. This procedures is at the user's discretion and may be repeated many times. The program appends the spectral parameters and recording identification in an ASCII file, PARAS.DAT.

9. Utilities

a) Display of tachograms

Type TACHO [*.INT] is to specify on screen viewing of tachograms.

The user will be asked to enter a filename (wildcards accepted). Choices will appear on screen to allow user to select the tachogram to visualize.

b) Printing of tachograms and spectra

DOS: WORKHP8H (filename)****.INT (or *.SPW)

The user will be prompted for information concerning the format of output. The user can modify scales and the order of appearance of the possible graphs. A LAS extension file is created by the program for every INT or SPW file. **.LAS files which is also in HPGL, can be sent to the HP laser printer for printing.